

**CYTOPROTECTIVE EFFECTS OF LITHIUM ON ENDOTHELIAL INTEGRITY  
AND IMMUNE PROFILES INDUCED BY RIFT VALLEY FEVER VIRUS ON  
HUVEC AND RAW 264.7 CELLS**

by

**RAYMOND TSHEPISO MAKOLA**

**THESIS**

submitted in fulfilment of the requirements for the degree of

**DOCTOR OF PHILOSOPHY**

in

**Biochemistry**

in the Faculty of

**SCIENCE AND AGRICULTURE**

at the University of Limpopo, South Africa

**SUPERVISOR: PROF T. M. MATSEBATLELA**

**CO-SUPERVISORS: PROF J. T. PAWESKA**

**DR PETRUS. JANSEN VAN VUREN**

**2021**

**DECLARATION**

I declare that the thesis hereby submitted to the University of Limpopo, for the degree of Doctor of Philosophy in Biochemistry has not previously been submitted by me for a degree at this or any other university; that it is my work in design and in execution, and that all materials contained herein have been duly acknowledged.



---

Mr RT Makola

05/ 02/ 2021

---

Date

## DEDICATION

I dedicate this work to my mother Mamoshiane Linah Makola and my late father Kgalagadishe Solomon Makola, as well as my uncle Rex Maloke Mashabela for their great support and motivation to work hard.

My parents had a dream of education and a better life. Kgalagadishe dedicated his life to make sure everybody around him live that dream, his efforts went beyond the family boundaries to the rest of the village. Unfortunately, he couldn't see the fruits of his hard work. His efforts will always be valued and celebrated. We miss you so much Thakgetse, Mphele wa Nape le Hunadi.

I appreciate my mother's efforts to make us live the family dream of education and self-empowerment. She has always advised me to look full into Christ's wonderful face and respect church days. Thanks so much Nareadi wa Hulabela le Modirwadi.

## ACKNOWLEDGEMENTS

The list below represents people who contributed in one way or another towards the success of this work/ project.

1. Prof Thabe M Matsebatlela, Prof Janusz T Paweska, Dr Joe Kgaladi, Dr Petrus Jansen van Vuren and Prof Matlou P Mokgotho, for dedicating their time and resources to make this project a success.
2. My academic fellows, Dr Nadia Storm, Dr Gaby Moteiro for their endless support, as well as Mrs Miranda Tshabalala, Nondumiso Mpuhlu, Busisiwe Mogodi, Phumza Ohaebosim, Elliot Motaung and Robert Nkwana for the constant support and love.
3. I also appreciate help from Dr Monica Birkhead, Dr Nazneen Moola and Dr Jacqueline Weyer with my lab work.
4. The Poliomyelitis Research foundation and National Research Foundation for financial support.
5. My parents, relatives and siblings for their constant support
6. My lovely fiancé Kholofelo Matshego Seloga and my little princess Nareadi Naledi Mamoshiane Makola for their continued support, courage and love.

Above all I thank the God of Mount Zion

## TABLE OF CONTENT

Title page.....	i
Declaration.....	ii
Dedication.....	iii
Acknowledgements.....	iv
List of figures.....	vi
List of tables.....	vii
List of abbreviations.....	viii
Publications.....	ix
Abstract.....	x
 CHAPTER 1: Literature review.....	 1
 CHAPTER 2: Lithium Lowers Rift Valley Fever Virus Replication In Raw 264.7 Macrophages Through Induction of Programmed Cell Death	 32
Death.....	32
Abstract.....	32
Introduction.....	33
Material and Methods.....	36
Results.....	42
Discussion.....	53
Conclusion.....	57
 CHAPTER 3: Lithium inhibits NF- $\kappa$ B nuclear translocation and modulate inflammation profiles in Rift Valley fever Virus-infected Raw 264.7 macrophages	 58
.....	58
Abstract.....	58
Introduction.....	59
Material and Methods.....	62
Results.....	68
Discussion.....	82
Conclusion.....	86
 CHAPTER 4: Effects of lithium-treated and RVFV inoculated Raw 264.7 macrophage cells supernatant on endothelial monolayer integrity co-inoculation	 88
.....	88
Abstract.....	88
Introduction.....	89

	Material and Methods.....	92
	Results.....	97
	Discussion.....	105
	Conclusion.....	109
CHAPTER 5:	Overall Conclusion.....	110
	Future work.....	111
REFERENCE	.....	112

## LIST OF FIGURES

Figure 1: Geographic distribution of the outbreaks and transition mechanism of the RVFV .....	2
Figure 2: Determination of the mechanism of viral attachment and replication in a cell host as well as viral budding .....	4
Figure 3: Depiction of RVFV structure and the genome segments.....	5
Figure 2.1: Depiction of the difference between the morphological alterations of cells undergoing apoptosis and normal cells.....	38
Figure 2.2: determination of the xcelligence cell analyser system.....	39
Figure 2.3: Determination of the cytotoxic effects of lithium on Raw 264.7 macrophage cell after inoculation with RVFV .....	43
Figure 2.4: Determination of the cytotoxic effects of lithium on MNA control cell after inoculation with RVFV .....	44
Figure 2.6: Determination of mode of cell death after RVFV inoculation and influence of lithium ions on MNA and Raw 264.7 macrophage cells .....	479
Figure 2.7: Determination of mode of cell death induced by Rift Valley Fiver Virus through molecular expression of Bax/Bcl-2 .....	49
Figure 2.9: Examination of the effects of lithium on RVFV replication on Raw 264.7 macrophage cells .....	512
Figure 3.1: Depiction of NF- $\kappa$ B location during viral activation and on a resting cells .....	65
Figure 3.2: Determination of the effects lithium on TNF- $\alpha$ production after inoculation with the RVFV .....	69
Figure 3.3: Determination of the effects of lithium on oxidative burst after Raw 264.7 cell are challenged with RVFV and expression of levels of antioxidant enzyme.....	73
Figure 3.4: Determination of the effects of lithium on production of inflammatory reactive nitrogen species 24 hrs post RVFV inoculation and expression levels of the NOS enzyme .....	75
Figure 3.5: Effects of lithium on translocation of NF- $\kappa$ B between the cytoplasm and nucleus, and expression levels of I $\kappa$ B.....	78
Figure 3.6: Determination of the canonical NF- $\kappa$ B and IRF3/7 signalling pathways and the effects of lithium post RVFV infection .....	80
Figure 4.1: Depiction of the transwell plate and mechanisms used by this assay to measure monolayer integrity.....	94
Figure 4.2: Examination of the effects of macrophage supernatant on endothelial cell integrity and the influence of lithium .....	98
Figure 4.3: The Permeability effects of lithium on the endothelial cells (Huvec cells) after exposure to supernatant of pre-treated and pre inoculated Raw 264.7 macrophage cells .....	100

Figure 4.4: Effects of lithium pre-treated Raw 264.7 macrophage cells supernatant on Adherence junction gene expression profiles using Huvec cells as the model for endothelial cells monolayer .....104

**LIST OF TABLES**

Table 4.1 Adherence junction gene table. Accession numbers of the gene primer used in the Profiler Real Time PCR array assay on Raw 264.7 macrophage cells lithium-treated and RVFV inoculated supernatant endothelial cells co-inoculation ..... 96



## LIST OF ABBREVIATIONS

DAF-2DA:	5,6-Diaminofluorescein diacetate
Dapi	4',6-diamidino-2-phenylindole
FBS:	Fetal bovine serum
FDA:	US Food and Drug Administration
FITC:	Fluorescein isothiocyanate
GSK-3:	Glycogen synthase kinase-3
H <sub>2</sub> DCF-DA:	2',7'-dichlorodihydrofluorescein diacetate
HO:	Haem oxygenase
IFNs:	Interferons
IL-6:	Interleukin-6
iNOS:	Inducible nitric oxide synthase
IPS-1:	IFN- $\beta$ promoter stimulator-1
IRF:	Interferon regulatory factor
I $\kappa$ B- $\alpha$ :	Inhibitor of kappaB kinase alpha
LiCl	Lithium chloride
LPS:	Lipopolysaccharide
MTT:	3-(4,5-dimethylthiazol-2-yl)-2,5 diphenyltetrazolium bromide
MyD88:	Myeloid differentiation factor 88
NaCl	Sodium chloride
NF- $\kappa$ B:	Nuclear factor associated kappa B
NSs:	78-kDa non-structural protein
PI:	Propidium iodide
RANTES	Regulated on Activation, Normal T Cell Expressed and Secreted
RANTES:	Regulated on activation, normal T cell expressed and secreted
RIG-1:	Retinoic acid-inducible gene 1
RNS	Reactive nitrogen species
RNS:	Reactive nitrogen species
ROS:	Reactive oxygen species
ROS:	Reactive oxygen species
RTCA:	Real time cell analyser system
RTCA:	Real time cell analyser
RVFV:	Rift valley fever virus

Tak1:	Transforming growth factor- $\beta$ activated kinase-1
TBK:	TANK-binding kinase 1
Tcf-Lef:	T-cell factor- lymphoid enhancing factor
TCID <sub>50</sub>	Fifty-percent tissue culture infectious dose
Tirap:	TIR domain containing adaptor protein
TLR:	Toll like receptors
TNF- $\alpha$ :	Tumour necrosis alpha
Tollip:	Toll interacting protein
Traf:	TNF receptor-associated factor
TRAF3:	TNF receptor-associated factor 3
TRIF:	TIR-domain-containing adaptor protein-inducing IFN- $\beta$
$\gamma$ -GCS:	$\gamma$ - glutamylcysteine synthetase

## LIST OF PUBLICATIONS

### PUBLISHED

1. **Makola R. T.**, Mbazima V. G., Mokgotho M. P. and Matsebatlela TM (2020) The effect of lithium on inflammation-associated genes in lipopolysaccharide-activated Raw 264.7 macrophages, International Journal of Inflammation, vol. 2020, Article ID 8340195, <https://doi.org/10.1155/2020/8340195>
2. **Raymond Tshepiso Makola**, Joe Kgaladi, Garland Kgosi More, Petrus Jansen van Vuren, Janusz Tadeusz Paweska, and Thabe Moses Matsebatlela Lithium inhibits NF- $\kappa$ B nuclear translocation and modulate inflammation profiles in Rift valley fever virus-infected Raw 264.7 macrophages. Virol J. 2021; 18: 116. PMID: 34088327, doi: 10.1186/s12985-021-01579-z

### SUBMITTED FOR PUBLICATION

1. **Makola R.T.**, Kgaladi J., Mbita Z., More G. K., Jansen van Vuren P., Paweska J. T. and Matsebatlela T. M. (2021). Lithium inhibits NF- $\kappa$ B nuclear translocation and modulate inflammation profiles in Rift Valley Fever Virus-infected Raw 264.7 macrophages. Viruses 2021, 13, x. <https://doi.org/10.3390/xxxxx>
2. **Makola R.T.**, More G. K., Jansen van Vuren P., Paweska J. T. and Matsebatlela T. M. (2021). Effects of lithium-treated and rvfv inoculated raw 264.7 macrophage cells supernatant on endothelial monolayer integrity co-inoculation. Viruses 2021, 13, x. <https://doi.org/10.3390/xxxxx>

### PUBLICATIONS WITH CONTRIBUTION FROM CURRENT WORK

1. Garland More, **Raymond Makola**, and Gerhard Prinsloo (2021). In vitro evaluation of anti-Rift Valley fever virus, antioxidant and anti-inflammatory activity of South African Medicinal Plant extracts. Viruses, 2021(13) 221. DOI: 10.3390/v13020221.
2. More G.K and **Makola RT** (2020) In-vitro analysis of free radical scavenging activities and suppression of LPS-induced ROS production in macrophage cells by *Solanum sisymbriifolium* extracts. Nature: Scientific Reports, 10: 6493 DOI: 10.1038/s41598-020-63491-w

## ABSTRACT

**Introduction:** Rift Valley fever virus (RVFV) is an arthropod-borne RNA zoonotic virus causing Rift Valley fever (RVF) disease. RVFV is prevalent across sub-Saharan Africa and the Arabian Peninsula with no existing effective and approved antiviral remedies for humans or animals. RVFV has developed mechanisms to hide from immune recognition and induce anti-apoptosis processes to keep the infected host cells viable in an attempt to advance their viral progeny. RVFV is a single-stranded enveloped RNA genome virus composed of 3 segments; the L, M and S segments. The S segment is known to encode a non-structural protein (NSs) identified to be the main virulence factor promoting viral replication through immune suppression. RVFV elicits a set of diverse symptoms ranging from a febrile illness to more severe symptoms that usually culminate in life-threatening haemorrhagic fever with high fatality rates. Thus, this study was designed to investigate the efficacy of lithium as a potential drug for reduction of RVFV load and amelioration of imbalanced and dysregulated inflammatory responses observed in Huvec and Raw 264.7 macrophages infected with this virus.

**Methods and results:** The MTT and Cyquant viability assays were used to demonstrate that lithium exerts no cytotoxic effects on non-infected Raw 264.7 macrophage cells but rather promotes cell growth and proliferation. Conversely, lithium was shown to significantly induce cell death in RVFV-infected Raw 264.7 macrophages. The Annexin-V/PI apoptosis assay was employed to demonstrate that RVFV induces apoptosis as a mode of cell death on Raw 264.7 cells. RVFV-induced apoptosis was accompanied by antagonistic Bax/Bcl-2 protein expression ratios. RVFV-infected cells treated with lithium resulted in higher levels of apoptosis signals compared to untreated RVFV-infected cells. Analysis of apoptosis stages using the real-time cell analyser (RTCA) also revealed that lithium induced early forms of apoptosis in RVFV-infected cells. Interestingly, induction of early apoptosis in these cells corresponds with lower viral load, probably as a result of early inhibition of viral progeny replication, as determined using viral titration assay.

Immune response profiles elicited in Raw 264.7 macrophages infected with RVFV and treated with lithium were monitored. An ELISA assay was used to determine the effect of lithium on cytokines and chemokine production in this cell model. The results obtained showed that lithium significantly stimulated production of IFN- $\gamma$  as RVFV-infected lithium-treated cells produced high levels of IFN- $\gamma$  compared to lithium-free

RVFV-infected control cells. Furthermore, in the same setting, the secondary pro-inflammatory cytokine, IL-6, and chemokine, RANTES, were stimulated by lithium 12 hrs post-infection (pi). Lithium was shown to significantly stimulate TNF- $\alpha$  production as early as 3 hrs pi. In addition to TNF- $\alpha$  expression, the expression of the regulatory cytokine, IL-10, was significantly stimulated by lithium with the highest expression peak at 12 hrs pi. As determined using the H<sub>2</sub>DCF-DA and DAF-2 DA fluorogenic assays, reduced production of the ROS and RNS was observed in RVFV-infected lithium-treated cells as opposed to untreated RVFV-infected controls. This was further supported by the Western blot assay results that showed low expression of the iNOS while upregulating expression of heme oxygenase and I $\kappa$ B in RVFV-infected lithium-treated cells. Results from immunocytochemistry and Western blot assays revealed that lithium inhibits NF- $\kappa$ B nuclear translocation in RVFV-infected cells compared to lithium-free RVFV-infected cells and 5 mg/ml LPS controls.

This study hypothesises persistent and deregulated inflammation as the central phenomenon responsible for endothelial damage and haemorrhagic fever in RVFV pathogenesis. Supernatants were collected from RVFV-infected macrophage cells treated with lithium and their effects on the integrity of endothelial cells were evaluated. The xcelligence real-time cell analyser system (RTCA) and transwell assay that measure endothelial monolayer integrity were used to demonstrate that lithium protects endothelial cells from RVFV-induced cellular damage. Moreover, lithium was shown to upregulate expression of cytoplasmic molecules such as  $\alpha$  and  $\beta$ -catenins involved in attaching the cadherin molecules to the actin cytoskeleton on the endothelial cell. Expression of  $\alpha$ -catenins, talins, zyxins and vinculins that attach integrins to the extracellular matrix and to other cells were observed to be upregulated by supernatants from RVFV-infected Raw 264.7 macrophage cells treated with lithium. Endothelial cell monolayer exposed to supernatants from RVFV-infected lithium-treated Raw 264.7 cells displayed upregulated expression of transmembrane molecules such as E-cadherins and N-cadherins. However, expression of VE-cadherins was observed to be lower compared to those treated with supernatants from lithium-free RVFV-infected Raw 264.7 control cells.

**Conclusion:** These findings propose that lithium limits viral replication and viral load in macrophages by inducing early apoptosis in RVFV-infected cells. Since lithium was shown to promote Raw 264.7 macrophage proliferation, it is thus suggested that the use of lithium as an RVFV antiviral drug is less likely to elicit leukocytopenia. Lithium seems to regulate excessive inflammation in RVFV-infected Raw 264.7 macrophages

by modulating the NF- $\kappa$ B signalling pathway. The endothelial integrity observed in the permeability assays has been supported by the expression of the molecules involved in keeping the cell to cell adhesion intact. This study links endothelial integrity patterns exerted by lithium with lowered production of inflammatory mediators such as ROS and RNS as these molecules are involved in destabilisation of cell junctions. Results from this study point towards the use of lithium as a potential treatment for RVFV infections by limiting viral replication, restricting viral spread and restoring the inflammation-regulating machinery.

Key words. Lithium, Rift Valley fever virus, NF- $\kappa$ B, endothelial integrity, inflammation and apoptosis

## CHAPTER 1: LITERATURE REVIEW

### 1.1. Rift valley fever virus background

Rift Valley fever virus (RVFV) is an arthropod-borne life-threatening pathogen that belongs to the Bunyavirales order, *Phenuiviridae* family and *Phlebovirus* genus (Ngoshe *et al.*, 2020). It is endemic to sub-Saharan African countries that include Tanzania, Kenya, Somalia, South Africa, Sudan, Uganda, Mauritania, Madagascar and Senegal (Harmon *et al.*, 2012), without exclusion of North African countries such as Egypt, and beyond in Yemen as well as Saudi Arabia (Nfon *et al.*, 2012). The Rift Valley fever (RVF)-like disease was first described in 1913 by Stordy at Kabete (Veterinary Research Laboratory) in Kenya. Later in the 1930s, Daubrey and colleagues, in the same veterinary laboratory in Kenya, characterised RVFV as a highly fatal disease in the Rift Valley on a wool sheep farm (Davies *et al.*, 2010).

RVFV was first identified in South Africa in 1951 after the febrile illness of people who were exposed to infected dead animals. In 1977, an outbreak occurred in Egypt resulting in 20 – 40 000 infections and 600 deaths. The epizootics in West African countries and Egypt were characterised by haemorrhagic fever that was accompanied by elevated mortality. In 2000, RVFV outbreak was first reported outside Africa, in Saudi Arabia (Davies *et al.*, 2010). RVFV is the causative agent of human and veterinary RVF disease with both mild and clinical symptoms that include a self-limiting febrile illness, retinal vasculitis, meningoencephalitis, renal failure, fatal hepatitis, hemorrhagic fever, encephalitis and long-term sequelae (Bird and McElroy, 2016).

Seasonal occurrences and transmission mechanisms of this life threatening zoonotic viral infection makes it a worldwide concern (Bird and McElroy, 2016; Islam *et al.*, 2018). RVFV is transmitted amongst humans and animals by more than 30 species of *Aedes* and *Culex* mosquitoes as well as contact with virus-contaminated livestock tissues and body fluids. Moreover, RVFV is transmitted possibly by aerosols, and hence considered a potential biological weapon. In support to aerosol transmission findings, Gaudreault and colleagues observed replication of this virus on various lung cell line models (Gaudreault *et al.*, 2015; Habjan *et al.*, 2009). Transmission between adult animals is postulated to occur through direct contact with infected body tissues or fluids (Mansfield *et al.*, 2015).

In addition, adult animals may possibly pass the infection to the young ones through lactation (Mansfield *et al.*, 2015). The infection cycle among infected adult mosquitoes to offspring is sustained by trans-ovarian transmission of the virus (Gaudreault *et al.*, 2015). In some reported outbreaks, this viral infection has resulted in more than 30% deaths of infected humans with clinical symptoms. Other severe outcomes include permanent vision impairment in some infected survivors (Islam *et al.*, 2018). Infection of domestic ruminants with RVFV results in high abortion rate in pregnant animals and more than 90% death rate in newborns. RVFV outbreaks harm trade and agricultural activities, resulting in severe socio-economic losses and trade restrictions (Islam *et al.*, 2018). This virus has been reported to survive for years in mosquito eggs and reappear during rainy seasons after the eggs had hatched (Le May *et al.*, 2004). These findings correspond with the studies that link the RVFV outbreak with heavy rainfall and elevated temperatures (Mosomtai *et al.*, 2016). Heavy rainfall leads to floods, and this is suggested to enhance vegetation growth and breeding of RVFV mosquito vectors (Mosomtai *et al.*, 2016).

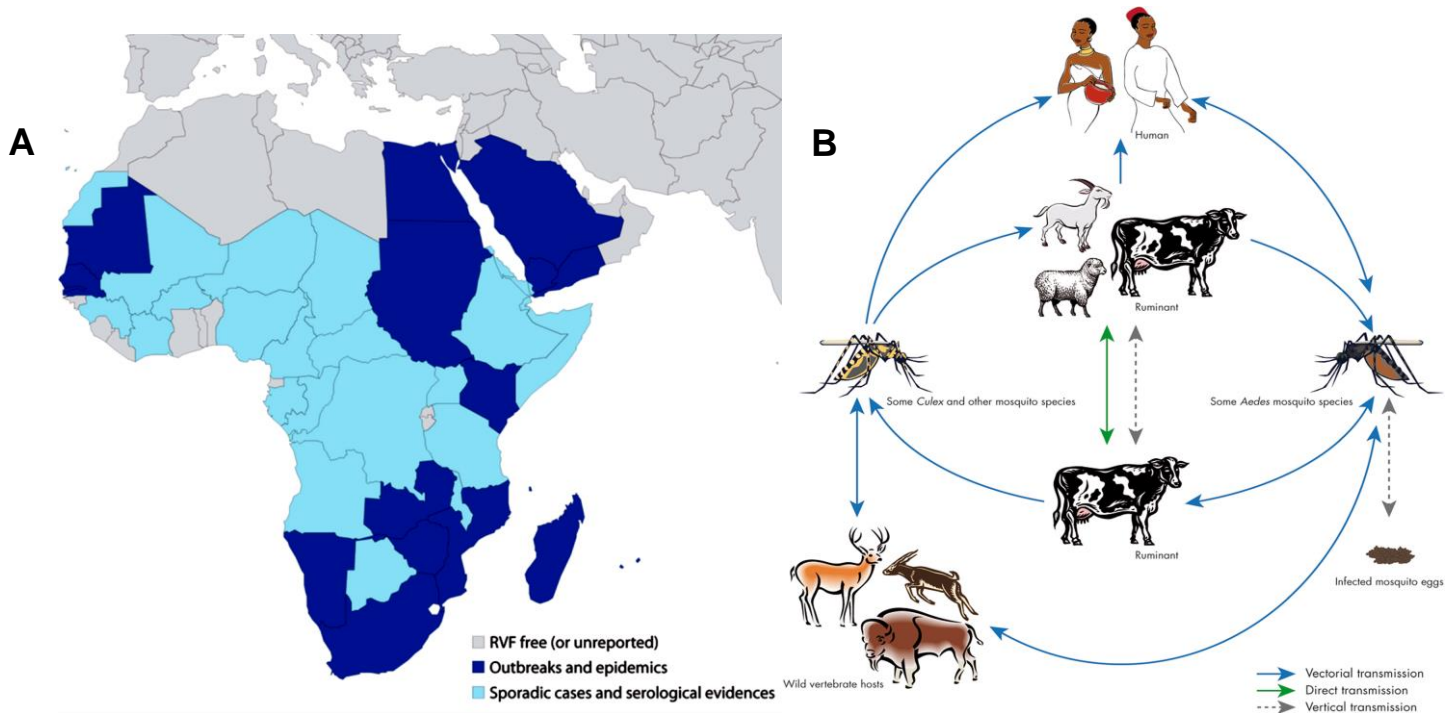


**Figure 1: Geographic distribution of RVF outbreaks and RVFV transmission mechanism.** Picture (B) depicts the epidemiologic transmission mechanism of RVFV from reservoir mosquito eggs all the way to humans. Mosquitos remain central to this viral transmission, as they can transmit the viral infection to both humans and animals. Picture (A) depicts the RVFV free countries and endemic countries in Africa and beyond African borders. This image shows the occurrence and outbreaks of this virus and spreading trends to other parts of the world (Balenghien *et al.*, 2013).



The RVFV enters host cells through endocytosis, a mechanism to internalise vital extracellular molecules such as hormones, nutrients and extracellular fluids (Harmon *et al.*, 2012). The RVFV fusion and entry relies on class II fusion mechanisms induced by a low pH. The fusion is executed via the involvement of glycoproteins, Gc and Gn (Filone *et al.*, 2006). The primary transcription commences after the release of the genome into the cytosol, followed by vRNA replication and viral assembly in the viral factories (rough endoplasmic reticulum). The virions are transported by vacuoles to the membrane where they fuse releasing the virus (Paweska and Jansen van Vuren, 2014).

Clathrin-mediated endocytosis (CME), caveola-mediated endocytosis (CavME), and macropinocytosis are the main endocytosis mechanisms used by cells to internalise extracellular molecules. Of the three mechanisms, the most explored and used by viruses for cell entry is the CME. CME uses clathrin proteins to coat the inner bilayer and form clathrin pits which induce internalisation, with cleavage by GTPase dynamin II to release the vesicles (Harmon *et al.*, 2012).

Caveola-mediated endocytosis is similar to CEM however, much slower and initiated through ligand-binding. Receptor-ligand complex resulting in engulfment of bacterial toxins and membrane components. This endocytosis process is dependent on dynamin II for cleaving of vesicles from the membrane. Caveolins are the main scaffolding structural proteins composed of the caveolae and interact with ganglioside, integrin and cholesterol on the inner layer of the lipid bilayer. Caveolae are lipid-rich rafts micro-domains rich in caveolin-1, cholesterol and sphingolipids (Harmon *et al.*, 2012). The Glycoproteins, Gn and Gc, are largely involved in cell fusion and internalisation, however, the structural properties that enable this fusion character are yet to be defined (Filone *et al.*, 2006). The host cell membrane molecules to which RVFV glycoproteins bind remain mysterious due to the diversity of cells that RVFV can fuse with to gain entry (Filone *et al.*, 2006).

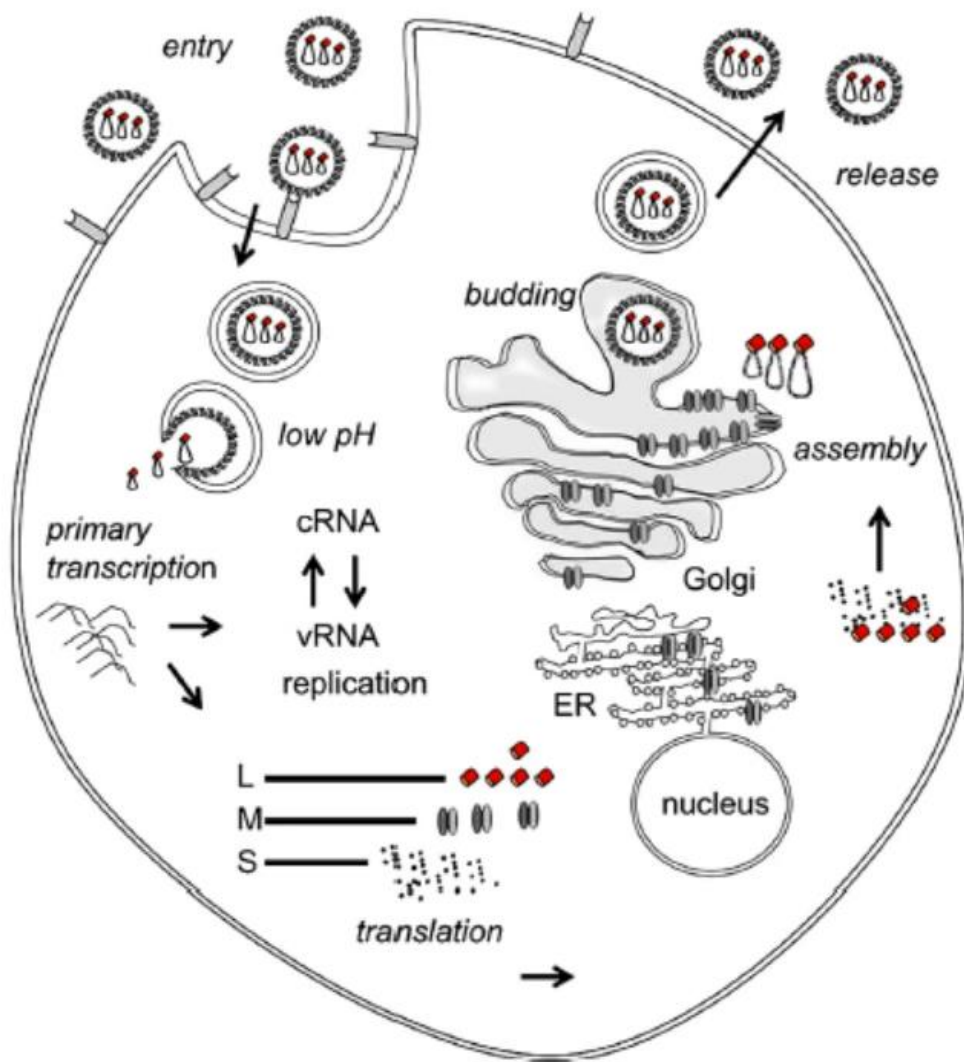


**Figure 2: The mechanism of viral attachment fusion and replication in a cell host as well as viral release.** The diagram illustrates the route taken by the RVFV from the point of entry into the infected cells until the budding off of the resulting virions (Paweska and Jansen van Vuren, 2014).

RVFV is an enveloped virus of 90-100 nm with a negative sense single-stranded RNA genome made up of 3 segments, namely, the L, M and S segments. The L segments encode viral RNA dependent RNA polymerase while the negative-sense M segments encode envelop glycoproteins (Gn and Gc), a 78 kDa protein and a 14 kDa non-structural protein (NSm). The S segment encodes the nucleoprotein (N) in the negative-sense and a non-structural protein (NSs) (Nfon *et al.*, 2012). The NSs has been shown to be the major virulence factor. This protein is a type I IFNs antagonist suggested to promote early viral replication and viremia (Nfon *et al.*, 2012). Le May and colleagues suggested that this type of interferon antagonistic role of the NSs

emanates from a total mRNA synthesis inhibition as a mechanism used by viruses to invade eukaryotic system (Le May *et al.*, 2004).

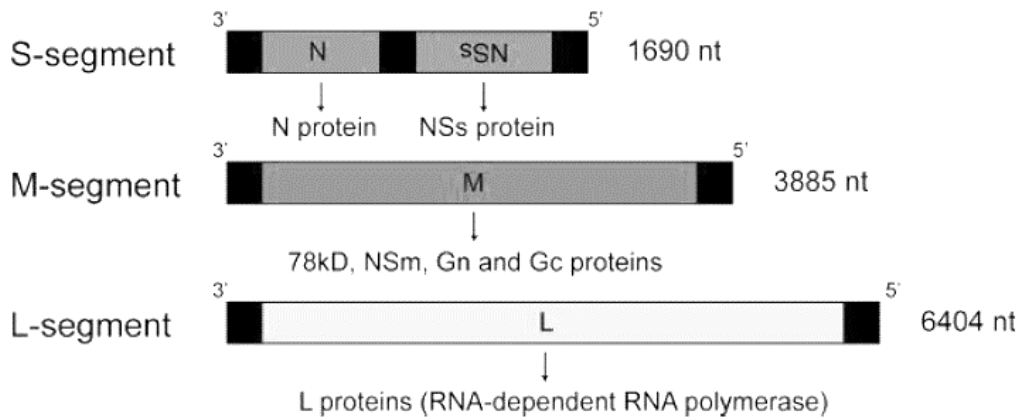


**Figure 3: Rift Valley Fever Virus genome structure.** The 3 segments of the genome structure of RVFV are depicted with components of each segment illustrated (Kalveram *et al.*, 2011).

Other RNA viruses such as poliovirus and vesicular stomatitis virus target the RNA polymerase II (Le May *et al.*, 2004). However, the RVFV NSs protein was shown to circumvent the innate immune response system through inhibition of type I IFN ( $\alpha$  &  $\beta$ ) (Nfon *et al.*, 2012). Other studies have shown that RVFV NSs proteins can induce suppression of the mRNA synthesis machinery (Le May *et al.*, 2004; Wood *et al.*, 2004). This virulent molecule has been shown to interact with p44 and XPD subunits of the TFIIF basal transcription factor. The NSs disturb the assembly of this basal transcription factor, suggesting the suppression of several gene expression mechanisms. The NSs aggregates with p44 and XPD and form nuclear filament-like structures that are thought to impair the transcription machinery (Le May *et al.*, 2004; Zachary *et al.*, 2004).

NSs is involved in the RVFV pathogenesis through a transcriptional shut down that leads to a weakened anti-viral IFNs response system. IFNs are important antiviral factors that activate antiviral molecules and recruit multiple immune cells to the inflamed site in order to limit viral spread. The type I IFNs have been shown to enhance constitutive expression of the protein kinase RNA activation (PKR) system. In addition to the IFNs system, the PKR expression is enhanced by dsRNA and ssRNA. The role of this serine threonine kinase is to phosphorylate eukaryotic translational inhibition factor 2 (eIF2), leading to translational arrest of both cellular

and viral mRNA. Thus, PKR has some inhibitory properties only in the absence of NSs protein since NSs was shown to directly degrade PKR (Habjan *et al.*, 2009).

Monkeys that have shown high expression of IFNs did not develop RVF disease after inoculation with RVFV. As a result, these cytokines were suggested to possess protective properties against RVFV. Animal model studies show selective inhibition of IFN- $\alpha$  since production of IFN- $\gamma$ , IL-6, IL-12, and IL-1  $\beta$  was observed without detectable levels of IFN- $\alpha$ . Interestingly, IFN- $\gamma$  and IL-12 have been suggested to lower viremia by stimulating NK cells and their cytotoxic activities. Interferon alpha is one of the important antiviral cytokines that has shown great potentials of stimulating production of antiviral molecules (i.e. nitric oxide NO) from a number of innate and adaptive immune cells (Nfon *et al.*, 2012)

The ability of NSs to antagonise the IFNs cytokines makes RVFV infection difficult to clear. Moreover, *ex vivo* studies demonstrated that this mosquito borne virus induce decline in the innate immune cells such as monocytes and dendritic cells which were reported to be the targeted cells (Nfon *et al.*, 2012). An *ex vivo* study conducted by Jansen van Vuren and colleagues on RVFV-induced inflammation did not yield changes suggested by Le May and colleagues (Le May *et al.*, 2004; Jansen van Vuren *et al.*, 2015). This study was conducted using samples of patients with RVFV symptoms during the South Africa RVFV outbreak of 2010/11. van Vuren and colleagues showed that inflammation is mounted to a more or less same extent in both the fatal cases and non-fatal cases (Jansen van Vuren *et al.*, 2015).

Immune response profiles were examined in both survivors and deceased patients who suffered RVFV infection. This study showed that serum samples from patients with early infection exhibited high levels of IL-8 and CCL-2/MCP-1 compared to uninfected controls. Interestingly, serum samples from fatal cases showed 10-fold increased levels of IL-6 (pro-inflammatory cytokine) than non-fatal case. The serum levels of IL-10 in both early and late samples of the fatal and non-fatal infections were not statistically different. This study pointed out that NSs did not induce total transcriptional shutdown as some genes are produced. Moreover, the fatality and survival rate of patients might not rely solely on the inflammatory response but rather on the extent of inflammatory response regulation (Jansen van Vuren *et al.*, 2015).

This immune regulatory evidence was supported other in other reports that highlighted the deleterious outcomes of under-regulated or persistent inflammation

(Reuter *et al.*, 2010). During inflammation, the innate immune cell produces an excess of toxic reactive oxygen/ nitrogen species in an attempt to degrade invading pathogens. Thus, persistent inflammation can expose biomolecules such as proteins, nucleic acids and lipids to these toxic molecules. Damage to these molecules change the cell functions and may lead to cell death (Makola, 2020). The uncontrolled production of these inflammatory molecules has been linked to pathogenesis of most of the chronic ailments such as neurodegeneration and cancer (Jope *et al.*, 2007). Furthermore, information from induced autoimmune encephalomyelitis studies showed that under-controlled inflammation weakens endothelial barrier leading to uncontrolled leukocyte extravasation (De Sarno *et al.*, 2008).

## 1.2 Programmed cell death

Programmed cell death or apoptosis plays a considerable pivotal role in maintaining proper normal cell turnover and physiological processes. Apoptosis has been known since the mid-nineteen centuries (Gewies, 2003) as a biological process involved in embryonic development, regulation of hematopoietic progenitor cells, management of cell proliferation and prevention of viral replication (Elmore, 2007). During development, cells are produced in excess and eventually undergo apoptosis in order to produce functional organs and tissues. For example, during brain development half of formed neuronal cells die in the later stage when the adult brain reaches complete development (Gewies, 2003).

Ninety-five percent of developing lymphocytes die either during genetic rearrangement events in the formation of antigen receptors in the thymus/bone marrow, or during negative selection, in an attempt to produce efficient and functional but not self-reactive immune cells (Gewies, 2003). Apoptosis remains one of the highly regulated processes since over- and under-regulation of this process elicits various human conditions that include cancer, neurodegeneration, ischemic damage and autoimmunity (Elmore, 2007). Apoptosis is executed in two pathways; the extrinsic and intrinsic pathway, depending on the apoptotic stimuli. The extrinsic apoptosis signalling pathway is induced by some external stimulus such as Fas-L and TNF- $\alpha$  which bind to their specific receptors, Fas-R and TNF-R1, respectively (Galluzzi *et al.*, 2008).

Apoptotic ligand-receptor complexes intracellularly recruit apoptosis adaptor molecules such as FADD and TRADD. These adaptor molecules facilitate

dimerisation of the death domains, leading to the formation of the death-inducing signalling complex (DISC) that in turn activate the caspase cascade (Elmore, 2007). On the other hand, the mitochondria-controlled intrinsic pathway is induced mostly by pro-apoptosis signals from other organelles within the cell, including some from the external environment. The intrinsic pro-apoptotic stimuli propagate various cell stress signals that lead to mitochondrial permeability. Intermembrane proteins such as cytochrome c, Smac as well as independent death effectors such as apoptosis inducing factor (AIF) get to be released from a permeable mitochondrial membrane (Galluzzi *et al.*, 2008). The released cytochrome-c binds and activate the Apaf-1 and caspase 9, forming an apoptosome. The other types of intramembrane proteins such as AIF and endonuclease G molecules translocate to the nucleus and induce cleavage of the DNA in a caspase-independent manner (Elmore, 2007). Activation of these proteolytic enzymes and nucleases by released intermembrane proteins facilitate fragmentation of both the nucleus and cytoplasmic contents leading to apoptosis morphological features and associated biochemical changes (Gewies, 2003). The mitochondrial apoptosis is regulated by the Bcl-2 family of proteins through controlling mitochondrial permeability. The Bcl-2 family is composed of both the pro and anti-apoptosis members (Elmore, 2007).

The reciprocal effects of the pro- and anti-apoptosis events were well defined in apoptotic and non-apoptotic cells. The expression of pro apoptotic proteins downregulates the anti-apoptotic counterparts and vice versa (Elmore, 2007). Morphological and biochemical features formed during apoptosis include loss of cell membrane integrity, nuclear shrinkage, nucleosomal DNA fragmentation, nuclear condensation, inward out-flipping and budding of plasma membrane, and formation of apoptotic bodies (Gewies, 2003). The apoptosis programmed processes are natural since their occurrences do not elicit immune response. Dead cells are removed by residential phagocytic cells (mainly macrophage) without triggering an immune response. This is as a result of steps that lead to cell demise without expose cell contents as compared to other modes of cell death (Elmore, 2007).

Viruses are among apoptotic stimuli previously thought to induce necrosis. They have evolved distinct mechanisms to evade host cell defenses in order to utilise the host replication machinery (Galluzzi *et al.*, 2008). Viruses produce pro- and anti-apoptosis proteins that aid in cell invasion and replication (Galluzzi *et al.*, 2008). The pro-apoptotic viral molecules are subdivided into direct and indirect apoptosis-inducing

proteins that aid in release of the viral progeny. Direct pro-apoptosis proteins induce apoptosis within the infected cell. Viruses such as human immunodeficiency virus (HIV) express pro-apoptotic viral proteins that directly induce cell death. The viral protein R (Vpr) aid in depletion of CD4 positive cells through interaction with the adenine nucleotide translocase and voltage-dependent anion channel (VDAC) (Galluzzi *et al.*, 2008).

Indirect pro-apoptosis proteins induce apoptosis indirectly on uninfected neighbouring cells. These viral proteins are thought to mimic the apoptosis ligands and bind apoptosis receptors such as TNF- $\alpha$ R (Galluzzi *et al.*, 2008). The indirect pro-apoptosis protein behaviour has been observed with HIV envelop glycol proteins (gp 140 and gp 41) (Galluzzi *et al.*, 2008). The HIV envelop glycol proteins are expressed by infected cells that coagulate the neighbouring cells by binding the receptors and co-receptors (CD4 and CCR5) (Galluzzi *et al.*, 2008). This cell aggregation is then followed by mitochondrial permeability and then apoptosis.

Apoptosis is induced by a sequence of events and activation of cyclin-dependent kinase 1 (Cdk1) that target the p38 and p53 dependent activation of Puma and Bax. (Galluzzi *et al.*, 2008). It has been recognised that most of the RNA genome viruses induce apoptosis as opposed to DNA genome viruses (Koyama *et al.*, 1998). The virally induced apoptosis has some biological importance. The host cells undergo apoptosis as a defense mechanism to avoid viral multiplication by aborting viral progeny replication. However, this host defense mechanism can lead to a disease condition in some viral infections such as HIV (Koyama *et al.*, 1998).

However, the host apoptosis defense mechanism can trigger induced fulminant hepatitis resulting in loss of a number of hepatocytes (Koyama *et al.*, 1998). Virus-induced apoptosis is detrimental to host cell populations but can lead to lowered viremia through abortion of viral replication in infected cells via apoptosis. Thus, viruses produce anti-apoptosis proteins to delay apoptosis of infected cells and sustain viral replication. DNA viruses such as poxvirus and herpesviruses delay apoptosis in infected cells by some encoded antiviral proteins that are then synthesised through the host protein translation machinery (Koyama *et al.*, 1998). Those encoded anti-apoptosis molecules possess the Bcl-2 homology domain. This domain is encoded by adenovirus anti-apoptosis protein E1B-19K (encoded by E1B gene) (Galluzzi *et al.*, 2008).

The E1B-19K viral proteins inhibit host cell apoptosis induced by virus independent stimulus such as growth factor deprivation, ligation of the TNFR, Fas and TRAIL, and Bax expression. These viral proteins have been shown to be located around the mitochondria removing multiple pro-apoptotic proteins (Galluzzi *et al.*, 2008). The cytomegalovirus (CMV) UL-36 genes encode an inhibitor of pro-domains of caspase-8 (vICA), facilitating inhibition of Fas/CD95-mediated apoptosis (Galluzzi *et al.*, 2008). Moreover, studies show that other viruses such as the vesicular stomatitis virus (VSV) circumvent apoptosis as a host defense mechanism through rapid multiplication of the virus before the cell undergoes apoptosis to overcome abortion of the progeny (Galluzzi *et al.*, 2008 and Koyama *et al.*, 1998). Most of the small genome RNA viruses have been observed to use this mechanism (Koyama *et al.*, 1998).

Tumour necrosis factor alpha (TNF- $\alpha$ ) and type 1 and 2 interferons have shown some antiviral activity when the vesicular stomatitis virus (VSV) model was used. This model uses VSV as a small genome that escapes the host viral defense mechanism by rapid multiplication. Thus, cells pre-treated with TNF- $\alpha$  and thereafter infected with the virus showed low progeny. This then suggested that these cytokines stimulate early apoptosis that lower viral multiplication (Koyama *et al.*, 1998). In addition to their antiviral properties, TNF- $\alpha$  and the IFNs have been observed to activate natural killer cells and recruit various immune cells to the inflamed site (Elmore, 2007).

The adaptive immune response has been seen to be recruited by IFN  $\alpha$  and  $\beta$ , through modulation of the MHC class I and II that in turn modulate the cytotoxic T-cells. These cytokines were identified more than 6 decades ago and recognised for their ability to inhibit replication of the influenza virus. These IFNs cytokines are classified into class I which include IFN  $\alpha$  and  $\beta$  (produced by leukocytes and fibroblast cells) while class II IFN cytokines like IFN  $\gamma$  are known to be produced by TH-1 lymphocytes and NK cells. Production of these molecules is induced by factors such as viruses, dsRNA through interferon-regulatory factor (IRF-3), NF- $\kappa$ B and the dsRNA through the dependent protein kinase (Elmore, 2007).

### **1.2.1 RVFV apoptosis invasion mechanisms**

Viruses have developed mechanisms to manipulate host cells regulatory machinery in an order to support viral replication. This machinery includes p53, a tumour suppressor protein shown to be involved in regulating genome stability, cell stress



and apoptosis (Lazo and Santos, 2011). The p53 protein has been shown to be the most mutated gene in a number of human cancers leading to under-regulated cell proliferation (Pietsch *et al.*, 2009). This molecule is known to be involved in a number of biological processes and is said to influence these processes both as a transcription factor and through protein-protein interactions (Austin *et al.*, 2012).

A number of viral infections target this molecule both directly and indirectly in an attempt to perpetuate viral progeny (Austin *et al.*, 2012). Viral proteins such as HPV E6 protein from the Human papilloma virus (HPV) and HTLV-1 tax protein from the human T-cells leukaemia virus 1 inactivate p53 in an attempt to inhibit apoptosis for the benefit of completion of viral replication (Austin *et al.*, 2012). However, other viruses enhance p53 activity which aid in their viral progeny release and dissemination. West Nile Virus (WNV) capsid protein induces accumulation of the p53 and its stability by inhibiting its interaction with MDM-2. During the WNV infection, the upregulated p53 would stimulate transcription of the pro-apoptotic protein Bax that induces apoptosis (Austin *et al.*, 2012).

In p53 null cells, apoptosis and viral replication of the WNV were observed to be lowered, showing that p53 promotes WNV propagation and release (Austin *et al.*, 2012). The p53 protein is phosphorylated on various target serine residues and is composed of the amino-terminal transactivation domain (TAD), which is involved in transcriptional regulation. The p53 protein is phosphorylated on Ser 9, 15, 20 and 37 to activate its stability. The p53 carboxyl-terminal possesses DNA binding domain (DBD) which directs DNA binding specificity while its C-terminal constitutes the oligomerisation domain (OD) (Austin *et al.*, 2012; Pietsch *et al.*, 2009).

Austin and colleagues suggested that RVFV requires p53 to induce cell death and viremia. RVFV also induced p53 phosphorylation at Ser 46 suggested to be involved in apoptosis. These serine residues were phosphorylated 48 hrs post infection. Serine 46 phosphorylation and p53 stability that stimulate apoptosis are linked to molecular translocation of the filamentous NSs which is thought to induce DNA damage response (DDR) protein kinases such as Ataxia-Telangiectasia Mutated (ATM). On the other hand, NSm is known to possess anti-apoptosis properties used to delay apoptosis. This molecule is suggested to balance the p53 modulated apoptosis so as to accommodate completion of viral replication (Austin *et al.*, 2012). Won and colleagues (2007) reported that NSm is used to delay apoptosis in order to produce a complete viral replication. This study reported delayed apoptosis of the RVFV wild

type as compared to arMP-12de121/384 strain that lack the NSm and 78 kDa proteins (Won *et al.*, 2007).

### **1.3 Endothelial integrity**

#### **1.3.1 Junctional organelles involved in endothelial integrity**

The integrity of a thin layer of squamous endothelial cell integrity is regulated by structural organisation that constitutes a regulatory blood and tissue barrier (Niessen, 2007). This barrier regulates passage of plasma macromolecules and circulating leukocytes and maintains homeostasis. The endothelial structural assembly and regulatory passage of molecules through endothelial cells lining/monolayer is controlled by junctional organelles. Organelles are structural molecules that ensure endothelial integrity and selective barrier. Four junctional organelles are well defined and these are the tight junctions, gap junctions, syndesmos junctions, and adherens junctions (Dejana *et al.*, 1995). These organelles are composed of a network of intracellular and transmembrane proteins which are permissible of rearrangement and passage of a macromolecule or circulating leukocytes (Dejana *et al.*, 1995).

Junctional integrity is altered in response to inflammatory mediators such as inadequate levels of NO (Habib and Baig, 2007) and cytokines that bind to the membrane ligands and induce rearrangement of the intracellular components of the junction that will allow opening of endothelial junctions. The degree of junctional complexity varies along the vascular tree depending on the requirements of a tissue. The junctional organisation in blood brain is well organised with a number of tight junctions as per tight control on permeability required by brain. However, the tight junction structure is not well organised on the postcapillary venules and allow trafficking of circulating cells and plasma proteins (Bazzoni and Dejana, 2004).

Syndesmos junctions have been shown to strengthen the cell to cell adhesion of adjacent endothelial cells (Dejana *et al.*, 1995). A host of adherens junctions are involved in the control of paracellular permeability to circulating leukocytes and solutes. These junctional organelles play a distinctive role during new vessels organisation (angiogenesis) (Bazzoni and Dejana, 2004). Gap junctions are involved in control of adjacent cell communications as opposed to adhesion and passage of small molecules through endothelial cells. They are composed of transmembrane adhesive molecules (Connexins family of proteins). These molecules form a channel

for passage of ions and small molecular weight molecules (Bazzoni and Dejana, 2004).

Syndesomes, also known as complexus adherents, are junctional molecules that mediate a strong junctional integrity accomplished by transmembrane glycoprotein molecules from desnoglins and desmocolins. These transmembrane molecules interact with intracellular keratin microfilaments. There is no evidence of keratin expression in endothelial cells and multiple experimental indications have only documented this type of junction in epithelial cells (Bazzoni and Dejana, 2004). Adherens junctions also known as zonula adherences are localised below tight junctions in the epithelial cell whereas in the endothelial cells were found to intermingle with tight junctions. Adherence junctions initiate and maintain cell to cell contact. In addition, adherence junctions are known to regulate the actin cytoskeleton, intracellular signalling and transcriptional regulation (Hartsock and Nelson, 2008).

Adherence junctions are composed of two fundamental complexes; the nectin-afadin and classical cadherin-catenin complexes. These complex molecules are involved in initiation and maintenance of a strong adherence junction. The nectin are a family of IgG like receptors adhesion molecules consisting of 4 nectin molecules. They are known to be dimeric molecules with an extracellular domain that is composed of three loops that bind using both heterophilic and homophilic adhesions. The intracellular domain c-terminal has PDZ domain like cadherins. The nectin molecules form a complex with afadin (Af-6) that link nectin molecules to the actin cytoskeleton. On the other hand, the transmembrane adhesive glycoprotein molecules named type 1 classical cadherin family of proteins interact with catenin ( $\beta$ -catenin and p120 catenin) (Bazzoni and Dejana, 2004; Niessen, 2007).

The catenin proteins are composed of the armadillo repeats with triple  $\alpha$ -helices that bind the c-terminal of the cytosolic domains of cadherin molecules (Hartsock and Nelson, 2008). Beta-catenin and p120 interact directly with cadherin proteins via armadillo repeats while  $\alpha$ -catenin (actin linker) connect via  $\beta$ -catenin (Niessen, 2007). Cadherins are composed of a conserved cytoplasmic entity and a  $\text{Ca}^{++}$  dependent extracellular domain involved in cell to cell adhesion. These molecules are known to be involved in homophilic cell to cell adhesion and can organise a complex structure at the cell boarder (Bazzoni and Dejana, 2004).

Vascular endothelial cadherin (VE-cadherin) assembly at cell boarder is tension dependent. The activated non-muscle myosin II binds and slides the anti-parallel actin filaments thereby generating tension which  $\alpha$ -catenin simultaneously bind the  $\beta$ -catenin and actin cytoskeleton. Adherence junctions induce tension and clustering of the VE-cadherin molecules followed by assembly at the cell boarder. VE-cadherins utilises the conserved Trp 2 and 4 to encourage moieties to partner with the ectodomain in order to form the trans dimerisation of the VE-cadherin molecules (Komarova *et al.*, 2017). There are a number of cadherin molecules known to be either specific or non-specific to endothelial cells (Bazzoni and Dejana, 2004).

Epithelial-cadherin (E-cadherin) is an epithelial cell specific cadherin and has been shown to play an extensive role in initiation of transmembrane contact via trans-pairing of cadherin molecules on adjacent cells (Niessen, 2007). E-cadherin is a transmembrane protein forming homophilic interaction with the neighbouring cell in a  $Ca^{++}$  dependent manner. This molecule has been observed to be involved in the early endothelial cell developments (Hyenne *et al.*, 2005). VE-cadherins are endothelial cells-specific cadherins located at the intercellular junctions. Other cadherin molecules such as placental, T and Neural-cadherins (N-cadherins) have been identified in neuronal, muscle and endothelial cells (Bazzoni and Dejana, 2004). The N-cadherins have been shown to be involved in recruitment of pericytes and AJ assembly. The T-cadherin lacks both the transmembrane and cytosolic region and is not involved in association of the cadherin to the actin cytoskeleton, however, it is anchored to the lipids rafts and involved in cell signalling and also as the LDL receptor (Komarova *et al.*, 2017).

VE-cadherins elicit critical primary adhesion events during vascular development (Komarova *et al.*, 2017). The carboxy-terminal of VE-cadherin complexes with cytoplasmic  $\beta$ -catenin and plakoglobin which are linked to an anchor molecule,  $\alpha$ -catenin. The  $\alpha$ -catenin connect the cadherin,  $\beta$ -catenin and plakoglobin complex with actin filaments. Other extensively studied adhesive molecules have been recognised outside the adherence junction and tight junction regions and include platelet and endothelial cells adhesion molecule 1 (PECAM). This molecule is a transmembrane adhesive protein that has been found at the intercellular contact and is expressed by leukocytes and platelets (Bazzoni and Dejana, 2004).

Several *in vitro* and *in vivo* studies have reported the involvement of this molecule in leukocyte extravasation. Thus, extensive expression of this molecule promote homo

and heterophilic adhesion to heterophilic ligands which include  $\alpha\beta$ -integrins that promote leukocyte extravasation. Intracellularly, PECAM interacts with SHP-2 and  $\beta$ -catenin to accomplish cell to cell adhesive activities like any cadherin and it is also involved in leukocyte extravasation (Bazzoni and Dejana, 2004). S-endo 1 is another molecule recognised between cell to cell borders that was originally identified as a melanoma marker. It is an immunoglobulin molecule that is expressed in endothelial cells and smooth muscle cells and not in any blood cells or hematopoietic stem cells (Bazzoni and Dejana, 2004).

Adherens junctions are well documented to play an important role in endothelial contact inhibition which is influenced by the interaction of VE-cadherin and cytoplasmic  $\beta$ -catenin that in turn bind to  $\alpha$ -catenin. Beta-catenin has a transcriptional role enabling it to stabilise the Tcf-Lef transcription factor in the Wnt signalling pathway. The contact inhibition role is executed by interaction of  $\beta$ -catenin with cadherin molecules thereby strengthening endothelial cell to cell contact while limiting cytoplasmic  $\beta$ -catenins that modulate transcription and promotion of cell growth and proliferation via the Akt signalling pathway (Bazzoni and Dejana, 2004). The affinity of  $\beta$ -catenin to cadherins is modulated by phosphorylation of specific Serine residues; the S-684, S-692 and S-686. However, dissociation of  $\beta$ -catenin from cadherin complex is achieved through phosphorylation of Tyr-654 and 489, resulting in alteration of cadherin binding affinity (Hartsock and Nelson, 2008).

Moreover, phosphorylation of Y142 weakens binding of  $\alpha$ -catenin to  $\beta$ -catenin. Thus, released  $\beta$ -catenin is sequestered in the nucleus for gene expression (Bazzoni and Dejana, 2004). Kinases that phosphorylate this catenin molecule include Src, Abl, EGF receptor and Fer kinase (Hartsock and Nelson, 2008). Other studies argue that the limitation in cytoplasmic  $\beta$ -catenin is due to its targeted degradation by proteases. However, experimental evidence points towards the involvement of BCL-9-2, a transcription factor that has been shown to induce functional switch in adhesive and transcriptional role of  $\beta$ -catenin (Hartsock and Nelson, 2008) This switch was postulated to occur via phosphorylation of tyrosine (Y142) which allow binding of BCL-9-2 and then translocation into the nucleus (Hartsock and Nelson, 2008). It has been noted that  $\beta$ -catenin is not the only cadherin intracellular partner that mediate Wnt signalling transcriptional activity since it was reported that plakoglobine and p120 are involved in transcriptional regulation of Wnt signalling (Niessen, 2007).

Thus, deleted VE-cadherins might increase  $\beta$ -catenin and induce cell growth resulting in transformation. VE-cadherin clustering at the cell boarder enables VEGF activation of the Akt/ PI3K survival pathway. Subsequently, changes in cadherin cell boarder clustering alter the Akt phosphorylation by VEGF and this leads to apoptosis. It is suggested that perhaps VE-cadherin associates with some growth factor receptors such as growth epidermal factor (EGF) receptor. Vascular endothelial-cadherin permeability impact is dependent on the tissue and the tight junction organisation. In well organised tight junction tissues such as brain, skin and muscles permeability is not affected or altered (Hartsock and Nelson, 2008).

The integrity can be altered by various factors such VEGF, it induces phosphorylation of VE-cadherin and catenin complex, which increases junctional phosphorylation. VEGF endothelial permeability is reported to be linked to VE-cadherin  $\beta$ -arrestin-dependent endocytosis (Gavard and Gutkind, 2006). Moreover, inflammatory mediators such as TNF- $\alpha$ , histamine and platelet activating factor (PAF) have been observed to alter VE-cadherin assembly to the adherence junction via phosphorylation of the VE-cadherin and p120-catenin resulting in phosphorylation of the  $\beta$ -catenin at Tyr654 and Tyr489 by c-Src. This phosphorylation lowers  $\beta$ -catenin affinity to the VE-cadherin and destabilisation of the adherence junction (Komarova *et al.*, 2016). Endothelial nitric oxide synthase (eNOS) produce adequate level of NO involved in maintenance of endothelial integrity (Komarova *et al.*, 2016).

Furthermore, elevated production of this molecule is linked to stimulation of eNOS by the VEGF and platelet-activating factor (PAF) leading to endothelial instability and leakage. The elevated levels of NO elicits protein S-nitrosylation (a covalent link between the NO group and cysteine thiol). S-nitrosylation of  $\beta$ -catenin occurs on the Cys619, p120-catenin, Cys579, Cys429, Cys450, Cys618 and Cys692, while VE-cadherin occurs at Cys579. The S-nitrosylation lowers affinity of  $\alpha$ -catenin to  $\beta$ -catenin and p120-catenin, destabilising the catenin VE-cadherin complex and endothelial integrity (Komarova *et al.*, 2016)

Molecules that do not belong to any of the junctions such as PECAM can be altered by the permeability increasing agents such as VEGF and shear stress, and have been shown to be displaced by inflammatory cytokines. PECAM-null mice show increased permeability only in pathologic conditions. Tight junction serves as the main regulatory barrier that is responsible for paracellular permeability and polarity. Tight

junction is composed of two transmembrane proteins, occludin and claudin, which control permeability and polarity. At resting state, occludin is localised in the cytoplasmic vesicles and is sequestered to the tight junction after phosphorylation of Threonine, Serine and Tyrosine (Niessen, 2007).

Occludin is a tetrameric molecule with two extracellular domains that are known to regulate cell to cell polarity. Claudin is another pivotal tight junction molecule which is known to regulate the paracellular tight junction channel (PTJC). Claudin consists of 24 members of 20-27 kDa. These molecules have a conserved Tyrosine and Valine dipeptide which is used to bind to the PDZ domain grooves of ZO-1, 2 and 3 (Niessen, 2007). These molecules are well organised in large arteries than in veins. In the same manner organisation of tight junction has been observed to be well organised in small vessels as opposed to postcapillary venules. To a large extent the organisation of tight junction is tissue dependent (Niessen, 2007).

The tight junction intracellular molecules zonula occludin-1 (ZO-1) was identified in 1986. It belongs to MAGKUK family and has binding domains to adherence, tight junctions and the actin cytoskeleton. This family of proteins is characterised by domains used in binding to transmembrane proteins that include PDZ, SH3 and guanylate kinase domain (Niessen, 2007). Later in 1993 the transmembrane molecule occludin was recognised. Other transmembrane proteins in addition to occludin include claudin-1 and Junctional adhesion molecules (JAMs). The tight junction transmembrane protein, occludin, uses carboxy-terminal domains to interact directly with three ZO molecules which contain coiled-coil motif, the region that include SH3 and Guanylate kinase domain of the ZO-1 (Bazzoni and Dejana, 2004).

Zonula Occludin serves as a linker between the transmembrane molecules (occludin, claudins and JAMs) and the actin cytoskeleton. These cytoplasmic molecules interact with the N-terminal PDZ while the C-terminal interacts with the actin filaments (Niessen, 2007). Zonula occludin-1 interacts with actin fibres indirectly via ZO-2 and ZO-3; however, reports show that ZO-1 and ZO-2 are crucial for clustering of claudin molecules and barrier function. The claudin is a 24 membered group that induce  $\text{Ca}^{2+}$  independent cell to cell adhesion and formation of tight junction fibres (Niessen, 2007). These molecules are known to interact both directly and indirectly with ZO-1 to 3. The JAMs have consensus motifs that bind the type II PDZ domain containing intracellular molecules such as ZO-1, AF-6/ Afadin, PAR-3/ ASIP, CASK/ Lin-2 and

Mupp-1. The PDZ molecules, especially ZOs, are anchors of JAMs to F-actin (Bazzoni and Dejana, 2004).

These molecules consist of the JAM A-C that are closely related and a distant JAM-4. The JAM molecules are not only found in endo and epithelial cell only, but also leukocytes. They are intensely involved in heterophilic and homophilic adhesion and aid in leukocyte transmigration (Niessen, 2007).

### **1.3.2 Movement of cells through endothelial walls (Diapedesis)**

Transmigration of circulating leukocyte cells to the inflamed tissue is an essential process during inflammation and elimination of invading agents. Differentiated residential cells recruit other immune cells to the inflamed site by producing a number of inflammatory mediators. The inflammatory mediators stimulate not only the circulating leukocytes but the endothelial cells to allow diapedesis of the leukocyte cells. Diapedesis is a process where white blood cells squeeze between endothelial cells borders in an amoeba-like fashion upon immunologic stimulation and expression of some integrin and endothelial adhesive molecules. The passage of molecules across the endothelial lining is accomplished by two defined pathways; the transcellular and paracellular passage (Bazzoni and Dejana, 2004).

The paracellular passages allow movement of molecules between cell to cell gates or junctions, by rearrangement of junctional structures and endothelial openings. The transcellular pathway supports movement of molecules through a cell with the aid of vacuoles (Bazzoni and Dejana, 2004; Wahl-Jensen *et al.*, 2005). The paracellular mechanism of cell passages was thought to be the only mode of extravasation as 90% of migrating cells use this mode. The transcellular mode of extravasation occurs at blood brain barrier (BBB) regions where the junctions are very tight. Diapedesis is a tightly regulated process that involves cytoplasmic and transmembrane receptors or adhesive molecules and integrin (Wahl-Jensen *et al.*, 2005).

The under-controlled passage of the monocytes-macrophages phenomenon is linked to encephalomyelitis aggravation leading to axonal loss, astrogliosis and neurodegenerative disorders (Vogel *et al.*, 2015). The TNF- $\alpha$ , and other acute inflammatory molecules such as histamine, chemokines and cytokines play a central role during diapedesis. These molecules activate the translocation of P-selectin molecule from the Weibel-Palade bodies to the endothelial cell surface where they interact with stimulated rolling leukocyte cells that have expressed and activated the



P-selectin ligands such as P-selectin glycoprotein 1. This allows slow rolling in order to increase the chance of leukocyte adherence to the luminal surface of the endothelial lining (Muller, 2013).

The selectin molecules are thought to stimulate firm leukocyte adhesion to the endothelial cells through partial activation of integrin molecules on the leukocyte (i.e. LFA-1, Mac-1 and VA-4) that interact with intercellular adhesion molecules (ICAM-1 and ICAM-2) on the endothelial cells (Kamei and Charman, 2010). Integrins are heterodimeric adhesion molecules composed of both the  $\alpha$  and  $\beta$  chains which remain inactive in resting cells. Chemokine activation of the integrin proteins result in conformational change making this molecule adhesive to its ligands. Diapedesis is the sequential process that include rolling, activation, adhesion and squeezing of cells to borders for extravasation (Muller, 2013).

Squeezing of cells between endothelial borders is supported by leukocyte integrin and endothelial cell adhesion molecules. Leukocytes Mac-1 interacts with ICAM-1 while monocytes LFA-1 interacts with endothelial ICAM-2 (Muller, 2013). A Study by Kamei and charman reported that a cup-like structure enriched with E-selectin, ICAM-1, actin, VCAM-1 and ezrin, radixin and moesin proteins (ERM proteins), the cytoskeletal adapter molecules, strengthen leukocyte adhesion and diapedesis (Kamei and Charman 2010). In other studies, it was illustrated that tetraspanin CD151 and CD9 in association with endothelial adhesion molecules such as ICAM and VCAM, without exclusion of other endothelial adhesive proteins, form a tetraspanin microdomain that is postulated to enhance adhesion molecules binding affinity to the leukocytes integrin molecules (Barreiro *et al.*, 2005).

The tetraspanin microdomains are suggested to be a coalescence of clustered endothelial adhesion molecules, actin, ERM and tetraspanin pockets with a sole function of enhancing efficiency of leukocyte adhesion and migration. Tetraspanins are transmembrane low molecular-weight polypeptides (30-33 amino acids) that do not function as receptors although hepatitis C virus protein E2 binds to them (Barreiro *et al.*, 2005; Hemler, 2008). Experimental evidence show that tetraspanins interact with membrane receptors via their cytoplasmic domains (Barreiro *et al.*, 2005). In addition to these integrin molecules, there is PECAM-1, a cytoplasmic molecule expressed by both the leukocytes and endothelial cells at the borders (Kamei and Charman 2010).

PECAM-1 was the first to be demonstrated to take part in leukocytes extravasation in both *in vivo* and *in vitro* assays. The JAM-like protein from a family of JAMs, with an exception of being expressed exclusively by leukocytes, was found to execute leukocyte adhesion in a Very Late Antigen-4 (VLA-4) dependent manner (Muller, 2013). VLA-4, also known as Integrin alpha4beta1, facilitates JAM-L dimerisation and enhances its endothelial adhesion molecules binding affinity (Kamei and Charman 2010). Experimental evidence has shown inhibition of extravasation without interfering with other diapedesis steps. Molecules known to play a significant role in diapedesis include ICAM-1, ICAM-2, PECAM, JAM A and C, CD99 and CD 99L2, and VCAM-1. However, PECAM and CD99 are the only molecules not involved in precursor steps or the extravasation step. VE-cadherin is a junctional molecule that downregulates diapedesis in order to sustain endothelial integrity (Muller, 2013).

Inhibition of VE-cadherin allows early transmigration of leukocyte cells through the endothelial cell borders. Both *in vivo* and *in vitro* studies reported partial removal of the VE-cadherin upon transmigration of cells through the endothelial cell borders (Muller, 2013). VE-cadherin is one of the adhesion junction proteins that keep junctional organelles intact. Thus, inactivation of this adherence junction protein is very crucial for junctional instability so as to promote diapedesis. In addition to adhesion of leukocytes to the endothelial cells by clustered ICAM-1 and VCAM-1, this clustering favours stimulation of intercellular endothelial kinases such as myosin light chain kinase (MLCK). The MLCK is stimulated by free calcium as accumulated by clustered ICAM-1 and VCAM-1. In turn, MLCK stimulate contraction of the actin-myosin fibers and endothelial permeability. The clustering is known to stimulate the accumulation of free cytoplasmic calcium that activate MLCK (Muller, 2013).

The vascular endothelial protein, tyrosin phosphate (VE-PTP), interact with the VE-cadherin in resting cells and is only dislocated during cytokine endothelial cell stimulation that favour clustering of ICAM-1 and VCAM-1. Destabilisation of VE-PTP expose the VE-cadherin to phosphorylation by Src and Pyk2 kinase at the p120 and  $\beta$ -catenin binding sites (tyrosin residue 658 and 731). This phosphorylation inhibits binding of p120 and  $\beta$ -catenin and the stability of the VE-cadherin that leads to junction instability. Reactive oxygen species were shown to stimulate permeability of the endothelial cells. Production of these small species is stimulated by the VCAM-1 cross-linking with subsequent activation of the Rac-1. Moreover, activated Rac-1 is

known to phosphorylate and inhibit VE-cadherin at serine residue 662 and then its clathrin-dependent internalisation (Muller, 2013).

Endothelial cells integrity is as important as movement of the leukocytes through the endothelial lining. However, under-regulated movement of leukocytes is very dangerous. The under-regulation of inflammation jeopardises endothelial cell integrity. Innate immune cells such as macrophages are the first cells to interact with invading agents. They produce a plethora of cytokines and chemokines (McElroy and Nichol, 2012) which in large amounts, weaken the endothelial lining. Subsequently, loss of the endothelial integrity observed through leukocytes infiltration that leads to ineffective immune networking and maintenance of homeostasis resulting in irregular fluid circulation and severe haemorrhagic fever (Wahl-Jensen *et al.*, 2005). The viruses from families such as *Filoviridae* and *Phenuiviridae* elicit haemorrhagic fever by disrupting the endothelial integrity (Wahl-Jensen *et al.*, 2005).

Other studies argue that, in addition to cytopathic properties evoked by this family of viruses, pro-inflammatory cytokines such as TNF- $\alpha$  are directly associated with promotion of endothelial cell permeability (Gupta *et al.*, 2001; Wahl-Jensen *et al.*, 2005). Vogel and colleagues illustrate that granulocyte macrophage colony stimulating factor (GM-CSF) increase inflammatory demyelination of axons on neuronal cells during pathogenesis of multiple sclerosis (MS) in a TNF- $\alpha$  dependent manner. Animal models of the MS were used to demonstrate that GM-CSF stimulate production of TNF- $\alpha$  by residential microglia and macrophage. Moreover, the TNF- $\alpha$  cytokines perpetuate the extravasation of GM-CSF stimulated circulating macrophage-monocytes (Vogel *et al.*, 2015). The TNF- $\alpha$  cytokine is well documented to weaken endothelial integrity and activate integrins in leukocytes and endothelial adhesion molecules (Wahl-Jensen *et al.*, 2005).

### **1.3.3 Molecules influencing junctions and endothelial integrity**

Nitric oxide (NO) is lipophilic free radical with physiological and pathological functions (Soufli *et al.*, 2016). It is one of the highly volatile free radicals with a half-life of only five seconds (Clancy *et al.*, 1998). Nitric oxide is metabolised to nitrate and nitrite in the presence of oxygen, these molecules are the stable forms of NO (Clancy *et al.*, 1998). Nitric oxide is produced from oxidation of L-arginine to give NO and L-citrulline using either a calcium dependent constitutively expressed endothelial nitric oxide synthase (eNOS) and neuronal nitric oxide synthase (nNOS) or a calcium

independent inducible nitric oxide synthase (iNOS) (Clancy *et al.*, 1998). Endothelial nitric oxide synthase is localised in the caveolae in the cell membrane. Pico-molar amounts of produced NO diffuse to the vessels and adjacent smooth muscles and induce vasodilation (Habib and Baig, 2007).

Large amounts of iNOS isoforms are produced and contribute enormously during innate immunity and inflammation (Soufli *et al.*, 2016). Nitric oxide has been shown to play a dual role as an anti- and pro-inflammatory molecule, a phenomenon known as the nitric oxide paradox. It has shown contradictory outcomes as it can be both protective and destructive. The amount of NO produced determines the extent to which it can elicit an immune response in a certain location (Clancy *et al.*, 1998). Furthermore, the effects of this molecule have been reported to depend on the location of production, duration and concentration (Soufli *et al.*, 2016). The low NO concentrations produced by calcium dependent constitutively expressed isoform of nitric oxide synthase have demonstrated its regulatory functions such as neurotransmission and regulation of blood vessel tone (Soufli *et al.*, 2016).

The eNOS derived NO is known to prevent processes that elicits atherosclerotic plaque. These processes include leukocyte adhesion and extravasation, low density lipoprotein (LDL) oxidation, smooth muscles (SMC) proliferation as well as platelets function regulation (Habib and Baig, 2007). At low levels, NO shows protective properties on endothelial cell integrity wherein damage to endothelial cells is one of the main pathological features of early atherosclerosis (Clancy *et al.*, 1998). Low levels of NO benefit not only the endothelial cells but was also shown to stimulate lymphocyte activation and proliferation (Clancy *et al.*, 1998). Thus, inadequate levels of NO lead to endothelial cell damage, resulting in onset of atherosclerosis (Habib and Baig, 2007).

The onsets of diseases like atherosclerosis is accompanied by low levels of NO which mostly is characteristic of excessive reactive oxygen species or free radicals such as super oxide anion, leading to leukocytes diapedesis and exposure of LDLs to oxidation. This perpetuates smooth muscles proliferation and platelet aggregation resulting in thrombosis (Habib and Baig, 2007). Increase in levels of free radicals or oxidative stress diminish the NO levels. These NO molecules react with super oxide anions to produce a very reactive molecule, peroxynitrite (Habib and Baig, 2007). These reactive free radicals are known to exacerbate atherosclerosis by oxidising LDL and inactivating eNOS by targeting endothelial cells. Damage to endothelial cells

leads to vascular inflammation which promote iNOS activation (Habib and Baig, 2007).

Activation of iNOS enzymes lead to elevated levels of peroxynitrite and tissue damage that are perpetuated by the cytotoxicity of peroxynitrite (Habib and Baig, 2007). Production of NO is also known to be involved in the maintenance of persistent inflammation observed in inflammatory bowel disease (IBD). A study by Soufli has reported the link between the disturbed balance between pro-inflammatory cytokines (TNF- $\alpha$ , IL-1 $\beta$ , IL-8 and IL-17A), anti-inflammatory cytokines (IL-4 and IL-13), regulatory cytokines (IL-10 and transforming growth factor  $\beta$ ) and elevated production of NO (Soufli *et al.*, 2016).

Elevated levels of NO have been reported in most of the inflammatory conditions such as sepsis, ulcerative colitis, psoriasis, arthritis and multiple sclerosis. Thus, high levels of NO are pro-inflammatory and result in damage to the host cells. It has been extensively demonstrated that NO possess some antimicrobial activity to bacteria, viruses and parasites. Although NO forms part of be first line of defense, its cytotoxicity is not specific to the invading microbes (Clancy *at al.*, 1998). The elevated concentrations of NO are stimulated by various factors such as infections which stimulate iNOS and increase in production of NO as part of first line of defense reactions (Lamping, 2007).

The high concentration of these pro-inflammatory cytokines elicits endothelial dysfunction leading to leukocyte infiltration and smooth muscle infiltration that evoke atherosclerotic lesions. Hyperlipidaemia, hyperglycaemia and aging are some of the contributing factors to release of cytokines, reactive oxygen species and other inflammatory molecules from endothelial lining, vascular muscles and infiltrating leukocytes. These situations inactivate the endothelial cell-derived NO and perpetuate the endothelial damage. Hence, the use of circulating endothelial progenitor cells to ameliorate endothelial damage and atherosclerotic lesions was previously proposed (Lamping, 2007)

#### **1.4 Cytokine and chemokines involved in RVFV infection**

The innate immune system constitutes the first line of defense and its efficacy relies on presence of inflammatory mediators that include the complement system components, lipid mediators, reactive oxygen and nitrogen species (free radicals) as well as soluble molecules such as cytokines. The latter are small polypeptides known

to play a central role in regulation of both the innate and adaptive immune system (Roitt *et al.*, 1998). Cytokines are described as hormone like signalling polypeptides that originate from a nucleated cell source. However, these molecules are predominantly produced by helper T cells and monocytes. Previously, cytokines were named after the cell that was discovered to produce that cytokine; such include lymphokines originating from lymphocytes, monokines from monocytes, chemokines and to induced chemotactic activity and interleukins since they are produced by one lymphocyte to activate neighbouring lymphocytes (Nedoshztko *et al.*., 2014; Zhang, and An, 2007).

These soluble polypeptide molecules were thought to be produced exclusively by lymphocytes and monocytes, however, they were found to be produced by many other cells types. Cytokines are not stored in the cells rather produced *de novo* upon cell stimulation. Cytokines are known to be involved in various cell processes such as regulation of cell trafficking, initiation, maintenance and termination of inflammation and cell infiltration (Nedoshztko *et al.*, 2014). Cytokines are receptor-specific molecules that operate mostly through autocrine and paracrine networking system and are found in plasma using paracrine systems in incidences of persistent inflammation-inducing agents (Nedoshztko *et al.*, 2014; Zhang and An, 2007).

These molecules have been shown to exhibit pleiotropy (numerous biological effects) and redundancy (shared biological effects) due to their structural similarity. Moreover, some may have synergistic effects while others may act antagonistically (Nedoshztko *et al.*, 2014; Zhang and An, 2007). Cytokines are involved in regulation of both the cell and humoral-based immune response. They induce differentiation, proliferation and activation of B and T lymphocytes, NK cells, monocytes/ macrophages, granulocytes and keratinocyte. Cytokines are signalling molecules that influence the function and migration of mature cells such as neutrophils, mast cells, basophils and eosinophils through activation of adhesion molecules and activation of synthesis of chemotactic factors (Nedoshztko *et al.*, 2014).

Cytokines are subdivided in to various categories based on their function. Among other functions, cytokines can be pro-inflammatory, anti-inflammatory, mitogenic (regulation of cell growth and proliferation), hematopoietic or chemotactic (chemokines). Pro-inflammatory cytokines are sub-divided into primary and secondary cytokines wherein primary cytokines include IL-1 and TNF- $\alpha$  which are produced during the early cell response as a result of inflammatory stimulus. The

primary pro-inflammatory cytokines stimulate production of secondary pro-inflammatory cytokines such as IL-6, IL-8, IL-12, IL-15 and IL-17. The pro-inflammatory cytokines include molecules from other groups such as IFN- $\gamma$ , oncostatin-M (OSM), GM-CSF and M-CSF. Cytokines can also have antagonistic properties wherein anti-inflammatory cytokines such as IL-4, IL-10, IL-11, IL-13 and TNF- $\beta$ , inhibit production of pro-inflammatory cytokines and subsequent inflammatory responses (Nedosztko *et al.*, 2014).

The growth and proliferation regulatory factors include IL-2, IL-4, IL-12, PDGF, VEGF, FGF, and TGF- $\beta$ . The hematopoietic cytokines include GM-CSF, M-CSF, G-CSF, SCF, haemopoietin and IL-6. Chemotactic cytokines create a chemical gradient for leukocytes to follow to an inflamed site and these molecules include IL-8, RANTES and monocytes chemotactic protein (MCP-1). The chemokines have the principal function of serving as chemo-attractants for white blood cells trafficking to aid in mounting immune response. Chemokines are a type of cytokines that are classified by the cysteine location on the polypeptide chain; C, CC, CXC and CX3C. These molecules are involved in other multiple biological processes such as angiogenesis apart from inflammation and immune response (Nedosztko *et al.*, 2014).

Cytokines are grouped as constitutive (homeostatic) and inducible (inflammation) molecules. Constitutive chemokines are involved in maturation, differentiation and activation of the lymphocytes and dendritic cells (CCL-19 and 21). The inducible molecules are inflammatory chemokines such as RANTES, CCL-5, MCP-1, CCL-2 and eotaxin CCL-11. These molecules are produced in response to the primary pro-inflammatory cytokines (Nedosztko *et al.*, 2014). Despite the tightly regulated immune response, viruses have developed several mechanisms aiming to alter and invade this well-structured immune surveillance system (Ghaemi-Bafghi and Haghparast, 2013; Le May *et al.*, 2004).

Viruses inhibit production of cytokines, resulting in a weakened immune system networking and low viral elimination (Ghaemi-Bafghi and Haghparast, 2013). Other viruses produce virokines and viroceptors which are virally synthesised cytokines and receptors that mimic the host cytokine-receptor system. This is another mechanism utilised by viruses to alter immune system efficacy in order to maximise viral replication (Ghaemi-Bafghi and Haghparast, 2013). Antigen variation is the most utilised viral strategy which is as a result of low viral RNA replication fidelity which lead to viral genomic instability and polypeptide modification. Altered polypeptides

may translate in to a new antigen, making humoral immunity to have a short half-life. The short memory from antigens shortens the relevance of the newly developed vaccine (Roitt *et al.*, 1998).

The modified polypeptide might as well not bind to the MHC (Ghaemi-Bafghi and Haghparast, 2013). Similarly, adenoviruses encode a protein that inhibits translocation of the class I MHC (Roitt *et al.*, 1998). A number of viral pathogens attenuate production and function of the Interferons as their mechanism to disturb and circumvent the immune system (Ghaemi-Bafghi and Haghparast, 2013). The RVFV uses its non-structural molecule (NSs) to inhibit production of the IFNs (Nfon *et al.*, 2012). Other viral pathogens produce viral interferon that bind to the interferon receptors and inhibit the IFNs induced signalling pathway and expression of the IFN-stimulated genes (ISGs). Other viruses inhibit IFNs at the transcription level by obstructing the transcriptional process of the ISGs, thus shutting down the antiviral state (Ghaemi-Bafghi and Haghparast, 2013).

Parainfluenza virus is thought to inhibit IFN signalling through induced degradation of the STAT-1 by the cellular proteases. The RVFV NSs induce suppressor of cytokines signalling 1 (SOCS-1) to block the IFN signalling. The PKR is one of the viral targets and this molecule is activated by the viral double stranded RNA to phosphorylate eukaryotic translation initiation factor-2a (eIF2a) followed by inhibition of both the host and viral protein synthesis (McElroy and Nichol, 2012; Ghaemi-Bafghi and Haghparast, 2013). The African swine fever virus produces the I $\kappa$ B homology protein that inhibits NF- $\kappa$ B and nuclear factor activated T cells (NFAT) and the cytokines thereof. The cytokines play a significant role in immune response and this makes them a target for most of the viral pathogens (Ghaemi-Bafghi and Haghparast, 2013).

The type I and II IFNs are involved in immunomodulation, while type I induce antiviral activity through stimulation of the ISGs, a molecule predominantly produced by T-cells and NK cells. Expression of these molecules follow a signalling cascade that include the recognition of replicating viruses by pathogen recognition receptors (PRRs) such as retinoic acid-inducible gene-I (RIG-1), melanoma differentiation associated genes (MDAS) and Toll-like receptors. These receptors activate the mitochondrial antiviral signalling (MAVS) protein which activates TBK1. Activated TBK1 induce dimerisation and translocation of the IRF-3, NF- $\kappa$ B and AP-1 transcription factors (Ly and Ikegami, 2016).



RVFV NSs is shown to silence the production of type I IFN beyond the transcription factors dimerisation and translocation (IRF-3, NF- $\kappa$ B and AP-1) through dislocation of some subunits of the TFIID basal transcription factors that lead to silenced host RNA synthesis while the RVFV replicates in the cytoplasm (Le may *et al.*, 2004; Ly and Ikegami, 2016). Other studies showed that inhibition of transcription factor YY1 and SAP30 by the NSs lead to silencing of the IFN- $\beta$  promoter resulting in inhibition of IFN- $\beta$  (McElroy and Nichol, 2012).

TFIID is a multi-subunit basal Pol II transcription initiation factor that is composed of nine subunits (between 34 – 89 kDa). This molecule is involved in the preinitiation complex at a promoter that involve TFIIE and Pol II. The preinitiation complex is followed by opening of a promoter since the TFIID is composed of some DNA-dependent ATPase DNA helicase (XPB, XPD). In addition to the involvement of TFIID in transcription of the protein encoding genes, DNA repair (nucleotide excision repair) and cell cycle are some of the important biological process this molecule is involved in (Iben *et al.*, 2002). TFIID is divided into two sub-complexes: core complex that includes subunits such as XPB, XPD, TTD-A/P8, p62, p44, p34 and cyclin-dependent kinase (CDK), and an activating kinase (CAK) complex. The CAK is composed of the CDK7, cyclin-H and MAT1/p32 (Mydlikova *et al.*, 2010).

Interference of the NSs with the p44 subunit of the TFIID dismantle the transcription initiation function of the TFIID and lead to type I IFN and total RNA synthesis inhibition (Le may *et al.*, 2004). Interestingly, the NSs was shown to support the viral protein translation and viral replication while silencing the host transcription machinery through interference with the basal transcription factor TFIID. Moreover, NSs target the PKR and induce its degradation leading to blocking of the PKR mediated eukaryotic initiation factor-2 (eIF-2 $\alpha$ ) phosphorylation and degradation (Ly and Ikegami, 2016). RVFV-influenced inflammatory response patterns have been of great interest in order to delineate the pathogenesis elicited by this virus. The non-structural molecule NSs inhibitory role has been at the centre of these investigations.

Studies have linked RVFV pathogenesis with weakened immune response due to the role of NSs as an antagonist of IFNs production and total shut down of the host translation as it tampers with basal transcription factor, TFIID (Nfon *et al.*, 2012; Le May *et al.*, 2004; Wood *et al.*, 2004). Study by Nfon *et al.*, (2012) in goat animal model linked pro-inflammation with animal survival as IL-12, IFN- $\gamma$ , IL-6 and IL-1 $\beta$  have been expressed from serum of surviving infected goats as compared to fatal goats.

Interleukin-12 and IFN- $\gamma$  production amongst other factors have been suggested to play a role in lowering viral load and survival of the infected goats. Interleukin-12 stimulates NK to activate production of the IFN- $\gamma$  which then activate the cytotoxicity function of the NK cells. In addition to the NK cells activation role played by the IFN- $\gamma$ , this molecule was shown to stimulate down-stream adaptive response and inhibition of viral replication. (Nfon *et al.*, 2012).

Most interestingly other studies have linked RVFV pathogenesis and lethality with under-controlled pro-inflammation. Caroline *et al.*, (2016) have labelled MCP-1, RANTES and Gro/KC as biomarkers, since these molecules have been elevated in an animal model system while other cytokines such as IL-12, IL-10, IL-6, IFN- $\gamma$  and TNF- $\alpha$  remain unchanged. This study used an aerosol viral inoculation method to determine the contributing factors that lead to diverse pathological symptoms behind this viral infection. The use of this method has resulted in high viremia in the brain compared to peripheral tissues (Caroline *et al.*, 2016; Jansen van Vuren *et al.*, 2015; Gray *et al.*, 2012). The NSs inhibitory role has stimulated interest in understanding the inflammatory patterns behind RVFV. Both the wildtype RVFV and  $\Delta$ NSs RVFV (MP-12) strains have shown to mount immune response upon infection with these viruses (Gray *et al.*, 2012).

A number of cytokine and chemokines expression has been noticed with wildtype RVFV as compared to the vaccine strain (MP-12). These findings hypothesise a very strong immune response, linking pathogenicity with pro-inflammation. Moreover, elevated expression of IL-6, GCSF and MCP-1 is suggested to contribute to endothelial leakage. The NSs-inhibited IFN- $\beta$  was shown to be stimulated 2-4 fold in the spleen and liver in wildtype virus as compared to vaccine virus (Gray *et al.*, 2012). The study by Jansen van Vuren and colleagues outlined pro-inflammatory responses in both fatal and non-fatal cases, suggesting that the balance and level of inflammation could be the determining factor between survival and fatal cases (Jansen van Vuren *et al.*, 2015).

Samples from infected patients during the 2011 RVFV outbreak in South Africa, link pro-inflammation to fatal outcomes. Pro-inflammatory cytokines such as IL-8, CCL2/MCP-1 and IL-6 are, nonetheless, expressed to the same degree in both the fatal and non-fatal cases (Jansen van Vuren *et al.*, 2015). This work has shown lowered levels of RANTES in fatal cases compared to survivors; however, there was increased level of IL-10 in the fatal than non-fatal cases. These findings show that

most of the fatal cases have shown dysregulation in cytokine production (Jansen van Vuren *et al.*, 2015). There was a clear evidence of immune response in both the survivors and fatal cases; however, the balance and levels of cytokine production determined survival or death (Jansen van Vuren *et al.*, 2015).

This study reported that most of the fatal cases displayed dysregulations in cytokine production. The production of IL-10 was observed to be higher in some tested patients and, this was related to imbalances in cytokine production. In addition, RANTES, a chemokine known to activate and induce proliferation of the T-cells, was shown to be associated with immune response against Ebola virus. Elevated levels of RANTES were reported in Ebola survivors since this is an important mechanism that strengthens regulation and activation of humoral immunity (McElroy *et al.*, 2014). The extent of viral load was also suggested to be the most determining factor, Jansen van Vuren showed some possible links between the liver damage and fatality to viral load (Jansen van Vuren *et al.*, 2015).

### **1.5 Lithium background and molecular involvement**

Lithium was medically established in 1949 (Cade, 1949) and used as a prominent psychiatric disease prophylaxis with remarkable clinical outcomes for the past 7 decades. Lithium has reduced the need for hospitalisation through prevention of manic episodes such as depression, cyclothymic and schizophrenia in bipolar disorder patients (Birch *et al.*, 1993). More profoundly, lithium treatment has reduced suicidal deaths in bipolar patients (Nassar *et al.*, 2014) despite lithium's obscure therapeutic mode of action underlying its anti-depressant properties (De Sarno *et al.*, 2008). However, lithium remains a preferred first line therapeutic drug for treatment of bipolar disorders (Plotnikov *et al.*, 2014).

Lithium is known to be involved in haematopoiesis (Barr and Galbraith, 1983) and exert biological activities such as proliferative, anti-apoptotic and neuroprotective properties. Experimental evidence suggested that lithium stimulate TNF- $\alpha$  production in macrophages which in turn stimulate production of GM-CSF from the endothelial cells, a growth factor involved in stimulation of haematopoiesis (Kleinerman *et al.*, 1989). At molecular level, neuroprotective properties of lithium are suggested to be linked to activation of c-Jun N-terminal kinase (JNK), PI3K/Akt and Wnt anti-apoptotic signalling pathways (Candé *et al.*, 2002; Sinha *et al.*, 2004; Yeste-velasco *et al.*,

2008). Other studies reported that lithium induces minimal side effects and significant increment of white blood cell count (Li *et al.*, 2010; Lenox and Wang, 2003).

Chronic treatment of bipolar disorders with lithium results in nephrotoxicity that leads to terminal renal failure in 2% of aged proportion of patients (Plotnikov *et al.*, 2014). Lithium is a monovalent alkali metal and trace element whose reactivity is thought to emanate from its valence electron (Strunecká *et al.*, 2005). Lithium is well elucidated to inhibit glycogen synthase kinase-3 (GSK-3) both directly and indirectly. This inhibitory phenomenon was thought to be the mechanism which lithium utilises to lower manic episodes and reduce the need for hospitalisation of bipolar patients (Plotnikov *et al.*, 2014).

This serine threonine kinase, GSK-3, is involved in a number of signalling pathways that include glycogen metabolism, cell proliferation, neuronal function, oncogenesis, and the innate immune response. In the regulation of immune response, it was shown to modulate pro- and anti-inflammatory cytokines that regulate the extent of inflammation (Wang *et al.*, 2013). GSK3- $\beta$  is known to interact with TANK-binding kinase 1 (TBK1) in a viral load dependent manner, promoting TBK1 self-association and auto-phosphorylation and initiate IRF-3 activation leading to production of type I IFN (IFN- $\beta$ ). Lithium was also shown to promote inhibition of IFN- $\beta$  production. These inhibitory characteristics of lithium were demonstrated in lipopolysaccharide (LPS), polyinosinic-polycytidylic acid and viral RNA-stimulated *in vitro* settings (Wang *et al.*, 2013).

In the same *in vivo* setting, mice treated with lithium did not develop severe leukocyte extravasation and tissue damage as seen in the untreated control. These outcomes are suggested to be as a result of immune regulatory properties elicited by lithium (Wang *et al.*, 2013). In addition to altered immune response, lithium lowers replication of gram-negative bacteria and DNA viruses at 12 mM lithium concentration. Treatment with lithium (10-30 mM) has specifically inhibited replication of DNA viruses such as Herpes Simplex virus (HSV), pseudorabies and vaccinia viruses in infected Vero cells. This is thought to be due to the lithium ion influx that alter cellular concentration of other cations (Hartley *et al.*, 1993).

This inhibitory role of lithium did not hold in RNA viruses such as influenza and encephalomyocarditis viruses (Hartley *et al.*, 1993). Lithium has been show to ameliorate multiple sclerosis clinical symptoms (MS). Multiple sclerosis is a central

nervous system (CNS) inflammatory disease condition characterised by immunologically linked neuronal demyelination. Induced autoimmune encephalomyelitis elicit blood brain barrier impairment and uncontrolled extravasation of macrophages, dendritic cells and residential glial cells leading to elevated demyelination of neuronal cells (De Sarno *et al.*, 2008). Using animal model systems, it was shown that lithium ameliorates these MS conditions after induced animal autoimmune encephalomyelitis by myelin oligodendrocyte glycoprotein peptide (MOG35–55). The lowered microglial activity has been suggested to be the mechanism in which lithium reverses demyelination since active microglia result in oxidative burst that is responsible for the demise of neuronal cells. In addition to oxidative radicals that weaken the endothelial lining, the excessive production of cytokines such as TNF- $\alpha$  facilitate leukocyte extravasation (Wahl-Jensen *et al.*, 2005).

Moreover, lithium lowers production of pro-inflammatory cytokines such as IFN- $\gamma$ , IL-6 and IL-17 without altering NK cell numbers, which is a significant observation since NK cells play a pivotal role in removing the virally infected cells from viral extrusions. Lithium was also showed to be highly involved in a plethora of therapeutics such as diabetes, experimental autoimmune encephalomyelitis, Alzheimer diseases and several neurologic defects (Wang *et al.*, 2013). It is these observed lithium actions on immune profiles in various immunological reactions towards virus infected cell systems that make a compelling argument for its possible involvement in management of similar immune profiles observed in patients infected with RVFV. The ability of lithium to modulate endothelial and macrophage activities necessitates an investigation on how lithium may affect activities of these cells in an RVFV-infection setting in an attempt to protect patients against RFV clinical manifestations.

## CHAPTER 2:

### LITHIUM LOWERS RIFT VALLEY FEVER VIRUS REPLICATION IN RAW 264.7 MACROPHAGES THROUGH INDUCTION OF PROGRAMMED CELL DEATH

---

#### **Abstract**

Rift Valley fever virus (RVFV) is a mosquito-borne zoonotic viral infection resulting in periodic outbreaks in domestic and wild ruminants causing high mortality and abortion rates. Survival and replication of RVFV relies on the induction of anti-apoptosis processes to keep the infected host cells viable in order to allow viral replication. This study investigated the efficacy of lithium as a potential drug to reduce RVF-viral load via induction of apoptosis in infected Raw 264.7 macrophages. The MTT viability assay was used to demonstrate that lithium has no cytotoxic effects on non-infected Raw 264.7 cells. Lithium stimulated growth and proliferation (1.5 fold) of Raw 264.7 macrophages while inducing death in RVFV-infected cells. Using the Annexin-V/propidium iodide (PI) apoptosis assay, RVFV was shown to induce apoptosis in Raw 264.7 and control MNA cells. RVFV-induced apoptosis was accompanied by a higher Bax to Bcl-2 protein expression ratio in lithium treated cells. Analysis of apoptosis stages using the real time cell analyser (RTCA) revealed that lithium induced early forms of apoptosis 10 hrs post infection (pi) in RVFV-infected cells compared to untreated RVFV-infected cells whose cell death induction only became apparent 44 hrs pi. Interestingly, induction of early apoptosis in these cells corresponds with a lower viral load, most probably as a result of early abortion of viral progeny replication, as determined using the viral titration assays (TCID<sub>50</sub>). These findings suggest that lithium limits viral replication and viral spread in Raw 264.7 cells via induction of early apoptosis. Since lithium is shown to enhance proliferation of macrophages, it is proposed that the use of lithium as an antiviral drug may not elicit leukocytopenia or compromised immunity in RVFV-infected patients but rather protect them from systemic infection via induction of early apoptosis in infected cells.

**Keywords:** Lithium; apoptosis; Rift Valley fever virus and cell proliferation

## **Introduction**

The Rift Valley fever virus (RVFV) belongs to the order Bunyavirales, Phenuiviridae family and is endemic to sub-Saharan African countries (Goshe *et al.* 2020; Harmon *et al.*, 2012). Other findings reported that it is widespread beyond African borders (Filone *et al.*, 2006). RVFV is disseminated among humans and animals by more than 30 species of *Aedes* and *Culex* mosquitoes as well as contact with virus-contaminated livestock tissues and body fluids. Transmission between adult animals may occur through direct contact with infected tissues or body fluids, while adult animals may possibly pass the disease to their young ones through lactation (Mansfield *et al.*, 2015). Moreover, RVFV was shown to be transmitted by aerosols; a phenomenon that led to its classification as a biological weapon (Islam *et al.*, 2018).

RVFV is the causative agent of human and veterinary Rift Valley Fever diseases, which manifest as fibril illness. While in some instances, Rift Valley Fever progresses to a more severe haemorrhagic fever condition. Some outbreaks have reported more than 30 % death of infected humans after developing clinical symptoms (Islam *et al.*, 2018; Nfon *et al.*, 2012). Other severe outcomes include permanent vision impairment, haemorrhage, and encephalitis in some infected survivors (Islam *et al.*, 2018). RVFV outbreaks resulted in abortion storms in pregnant animals and more than 90 % death rates in young animals leading to socioeconomic difficulties (Islam *et al.*, 2018). The seasonal occurrences and transmission mechanisms of this life-threatening zoonotic viral infection make RVFV infection a worldwide public concern (Bird *et al.*, 2016; Islam *et al.*, 2018).

RVFV is a negative sense single-stranded RNA genome made up of 3 segments: the L, M and S segments. The L segments encode the viral RNA-dependent RNA polymerase while the negative-sense M segments encode the envelop glycoproteins (Gn and Gc), a 78 kDa protein and a 14 kDa non-structural protein (NSm). The S segments encode the nucleoprotein (N) in the negative-sense and a non-structural protein (NSs) in the genomic direction (Won *et al.*, 2007; Nfon *et al.*, 2012). The non-structural protein, NSs, is the major virulence factor known to be an interferon antagonist and is suggested to aid in early viral replication and viremia (Nfon *et al.*, 2012).

The RVFV uses NSs molecules to invade host innate immune response while the non-structural molecule (NSm) delays apoptosis of infected cells in an attempt to

allow completion of viral replication (Won *et al.*, 2007; Nfon *et al.*, 2012). Previous studies have shown that most of the RNA genome viruses induce apoptosis as the mechanism of cell death compared to DNA genome viruses (Koyama *et al.*, 1998). Induced cell death in response to viral infection has been shown to have some significance in biological defense. The host cell undergoes apoptosis as a defense mechanism to avoid viral multiplication through abortion of viral progeny (Koyama *et al.*, 1998; Won *et al.*, 2007).

However, in some instances, apoptosis in defense of viral replication has resulted in diseases such as hepatitis, following the loss of hepatocytes (Koyama *et al.*, 1998). Studies highlighted that viruses, such as the vesicular stomatitis virus (VSV), circumvent apoptosis of virally-infected cells through rapid multiplication of the virus before the cell undergoes apoptosis in order to overcome abortion of the progeny (Galluzzi *et al.*, 2008; Koyama *et al.*, 1998). In addition to rapid replication, some viruses encode anti-apoptosis genes. The adenovirus genome encodes the E1B gene that produces the anti-apoptosis protein, E1B-19K, since these viral anti-apoptosis proteins possess the Bcl-2 domain (Galluzzi *et al.*, 2008).

RVFV encodes NSm, which has shown to delay apoptosis in Vero E6 cells infected with a recombinant MP-12 (arMP-12) vaccine candidate strain of RVFV as compared to NSm-null and 78-kDa-deleted RVFV viral strains (arMP-12-del21/384). NSm is thought to delay apoptosis in order to complete replication of the progeny. However, a study by Won and colleagues showed similar viral growth kinetics in both arMP-12 and arMP-12-del21/384 irrespective of variations in cell viability (Won *et al.*, 2007). Since the mid-nineteenth century, apoptosis was shown to play an important role in maintaining normal cell turnover and development of physiological processes which include embryonic development, regulation of hematopoietic progenitor cells, control of cell proliferation, and prevention of viral replication (Elmore *et al.*, 2007).

Apoptosis follows a series of morphological and biochemical modifications that result in cell death, without evoking any undesirable immune response (Gewies *et al.*, 2003). Apoptosis is a highly regulated process and its dysregulation may result in various undesirable conditions that include cancer, neurodegeneration, ischemic damage and autoimmunity (Elmore *et al.*, 2007). Apoptosis is modulated by various cell stress signals executed through intrinsic and extrinsic pathways (Galluzzi *et al.*, 2008). Mitochondria are a targeted organelle in the process of apoptosis as they release intermembrane proteins, such as Cytochrome-C, which stimulate the



downstream apoptosis pathway. The released Cytochrome-C activates caspase-9 and the executioner caspase-3 that execute apoptosis (Elmore *et al.*, 2007).

Mitochondria-based (intrinsic) apoptosis is regulated by the Bcl-2 family of proteins which serve as a regulatory machinery that maintain mitochondrial integrity. The Bcl-2 family is composed of both the pro- and anti-apoptosis constituents. The reciprocal expression pattern of pro- and anti-apoptosis proteins determine the mechanism of cell death (Elmore *et al.*, 2007). Small molecules and trace elements such as lithium have been proven to possess various biological properties such as neuroprotection, anti-inflammation and inhibition of oxidative stress. These biological properties of lithium have been linked to the activation of the c-Jun N-terminal kinase (JNK), PI3K/Akt and Wnt anti-apoptotic signalling pathways (Candé *et al.*, 2002; Sinha *et al.*, 2004; Yeste-velasco *et al.*, 2008).

Lithium is an FDA-approved drug used for the treatment and management of bipolar disorders since 1949 (Cade, 1949). Lithium has been utilised for more than 6 decades as a mood stabilizer and it has been shown to stimulates haematopoiesis and increment of white blood cells (Barr *et al.*, 1982; Plotnikov *et al.*, 2014). The putative mechanism behind haematopoiesis is suggested to involve lithium-stimulated production of TNF- $\alpha$  from macrophages. TNF- $\alpha$  then stimulates the production of the granulocyte-macrophage colony stimulating factor (GM-CSF) from endothelial cells; a growth factor involved in haematopoiesis (Kleinerman *et al.*, 1989).

In 1993, Hartley and colleagues observed the inhibition of a DNA viral replication and the inhibition of a gram-negative bacterial growth at 12 mM lithium concentration. The mechanism of inhibition of the viral replication was not well elucidated although there were suggestions that it could be the lithium ion influx that altered the cellular concentration of other cations (Hartley *et al.*, 1993). These findings were abandoned as a result of the controversial cytotoxic spectrum of lithium. Nevertheless, it was shown that this drug displayed selective anti-viral and anti-bacterial properties (Hartley *et al.*, 1993). The aim of this study was to evaluate the lithium-stimulated apoptosis in RVFV-infected cells and the relationship between apoptosis and viral replication. In addition to findings by Hartley and colleagues, our investigations are aimed at demonstrating a significant apoptotic influence of lithium on RVFV-infected cells and inhibition of the viral replication at low doses.

## **Material and Methods**

### *Cell Culture and Viral Propagation*

The RVFV AR 20368 strain was isolated in 1974 during the RVF outbreak in South Africa. The virus was propagated on Vero C1008 cells at the multiplicity of infection (MOI) of 0.2, followed by harvesting of the supernatant after extensive cytopathic effect (CPE). The supernatant was stored at -70°C after centrifugation at 3,000 xg for 30 minutes (Martín-Folgar *et al.*, 2010). The Raw 264.7 Murine macrophage cells were obtained from Prof Lyndy McGraw (University of Pretoria) and the MNA cells were obtained from Dr Kgaladi (NICD). The cells were maintained in cell culture flasks at 37°C, in a humidified 95% air and 5% CO<sub>2</sub> atmosphere. Raw 264.7 and MNA cells were propagated in Dulbecco Modified Eagle Medium (DMEM) supplemented with 10% fetal bovine serum (FBS), 2 mM L-glutamine and 1x penicillin-streptomycin. Vero C1008 cells were purchased from ATCC (USA) and propagated in Minimum Essential Medium (MEM), supplemented with 10 % FBS, 2 mM L-glutamine and 1x penicillin-streptomycin (Lonza). Trypan blue dye and haemocytometers were used to determine cell density (Matsebatlela *et al.*, 2012).

### *Cell treatment*

Lithium Chloride (LiCl) was purchased from Fluka (Chemika, Switzerland) and a 500 mM stock was prepared in sterile dH<sub>2</sub>O and stored at -20°C. Sodium Chloride was purchased from Sigma-Aldrich (USA) and the stock was prepared at 500 mM NaCl in sterile dH<sub>2</sub>O and stored at -20°C. The experiments were executed by seeding the Raw 264.7 and MNA cells at various densities depending on the experimental setting and then treated with lithium concentrations (LiCl 2.5, 1.25 and 0.625 mM) as well as NaCl (2.5 mM). The working concentrations have been motivated by the previous studies that confirmed the narrow spectrum of action/ activity shown by lithium at therapeutic concentrations (0.4–2.0mM LiCl), hence the use of these low doses in this study (Plotnikov *et al.*, 2014; Sproule, 2002).

#### *Determination of cell viability using MTT assay*

A water soluble 3-(4,5-Dimethylthiazol-2-yl)-2,5-Diphenyltetrazolium Bromide tetrazolium salt (MTT) that is reduced by mitochondrial enzyme succinate dehydrogenase to formazan was used as a measure of cell viability. This colorimetric assay measures the formazan optical density (OD) and relate it to cell viability. This assay was initiated by seeding Raw 264.7 cells in a 96 well culture plate at a density of  $3 \times 10^5$  cells/100  $\mu$ l for 3 hrs. Thereafter, cells were infected with RVFV at  $10^{3.8}$  TCID<sub>50</sub>/100  $\mu$ l. This was then followed by treating cells with LiCl as shown in the cell treatment section above for 3 days. Images were captured using the EVOS FL Colour imaging system (Life Technologies, USA). To each well, 5 mg/ml of MTT was added, followed by 1 hr incubation. Thereafter, the cell culture medium was aspirated, the insoluble formazan was dissolved with 100  $\mu$ l Dimethyl sulfoxide (DMSO) for 10 min and the OD was then measured at 490 nm with background reference at 630 nm using the ELx800 universal microplate reader (BioTek, USA).

#### *Determination of cell proliferation using Cyquant assay*

The Cyquant direct proliferation assay is a fluorogenic method that measures cell viability and proliferation based on the integrity of the nuclear DNA. It is composed of two reagents; the cell permeant nucleic acid binding green fluorescent dye and the fluorescence suppressor dye. Raw 264.7 cells were seeded at  $9 \times 10^5$  cell/100  $\mu$ l and  $6 \times 10^5$  cell/100  $\mu$ l for a 3 hrs. The cells were infected with RVFV at  $10^{3.8}$  viral titer/100  $\mu$ l and treated with LiCl (as outlined in cell treatment section) for 24 and 48 hrs. Curcumin (20  $\mu$ M) was used as a positive control. Cells were treated with curcumin for 24 hrs in all incubation times. Components A (Nucleic Acid Stain) and B (Background Suppressor) were diluted in a cell culture medium and 100  $\mu$ l of this mixture was added to cell cultures followed by incubation for 1 hr at 37°C. Fluorescence intensity was measured at Ex/Em 480/535 nm using a Fluoroskan Ascent FL (Thermo Fisher Scientific, USA).

*Evaluation of mode of cell death using Annexin-V FITC PI*

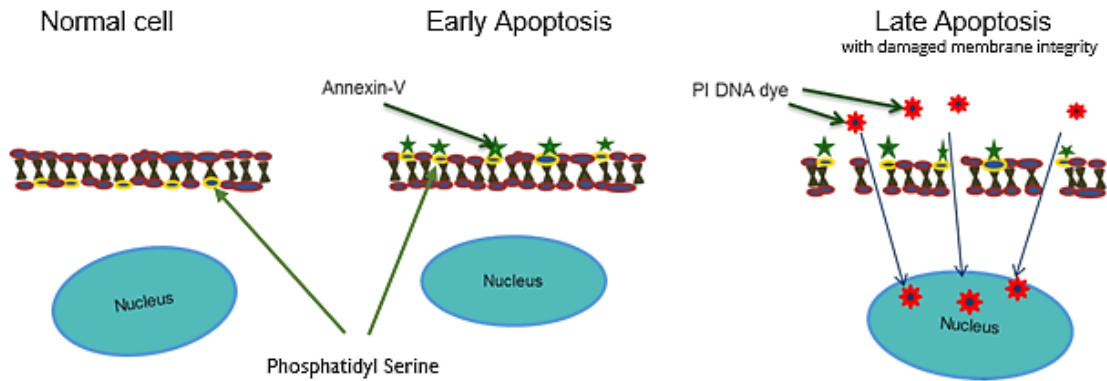


**Figure 2.1: Depiction of the difference between the morphological alterations of cells undergoing apoptosis and normal cells.** Early apoptosis is shown by flipping of lipid bilayer exposing phosphatidyl serine (yellow) found in the inner layer. Annexin-V conjugated by the FITC has high affinity to phosphatidyl serine therefore during apoptosis this annexin-V bind to exposed phosphatidyl serine. While late apoptosis is recognised by red DNA staining, the propidium iodide is membrane impermeable and only penetrate the membrane and stain the nucleus when the cell loss membrane integrity.

The mechanism and phase of cell death induced by RVFV was measured using the Annexin-V FITC PI apoptosis kit. This assay kit detects the flipping of the plasma membrane inward-out and membrane integrity. Raw 264.7 and MNA cells were seeded at  $2 \times 10^5$  cell/ 200  $\mu$ l and  $8 \times 10^4$  cell/ 200  $\mu$ l cell densities on coverslips in a 6-well plate for 3 hrs. Cells were then treated with lithium (as outlined in Cell treatment) and infected with RVFV at  $10^{3.8}$  and  $10^{0.8}$  viral titer/ 500  $\mu$ l for 3 days while positive control actinomycin-D 0.02 mg/ml was used for only 24 hrs. Thereafter, cells were washed with 1x PBS and stained with PI and Annexin-V for 20 min in the dark at room temperature (RT). Stained cells were fixed for 30 min with 4 % paraformaldehyde. Coverslips were then mounted with mounting medium on microscope slides and images were captured using the EVOS FL Colour imaging system (Life technologies, USA).

*Evaluation of real time cell proliferation using real time cell analyser system (RTCA) assay*

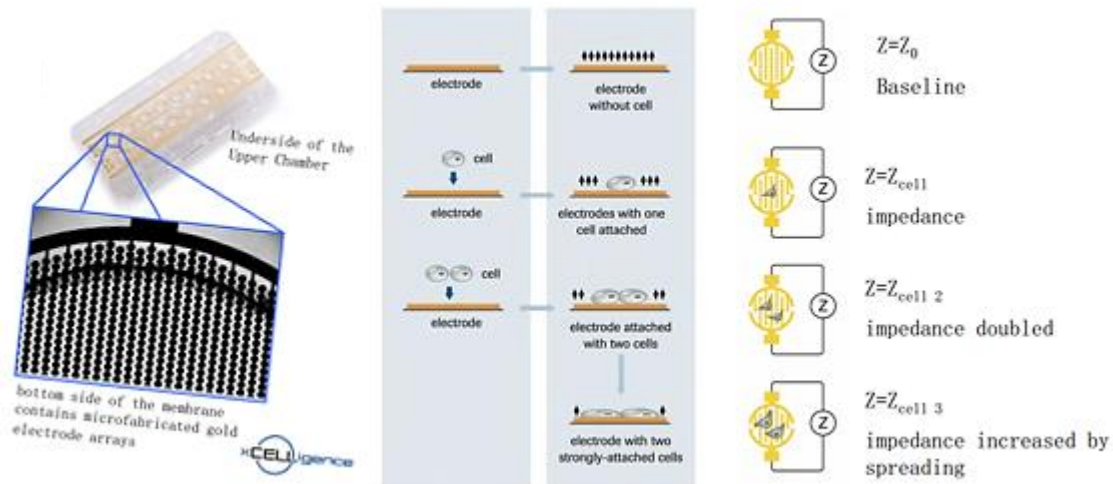


**Figure 2.2: determination of the xcelligence cell analyser system.** The xcelligence RTCA system measures cell index (cell number, adhesion and morphology) in real time as it relies on voltage impedance. This system uses plates embedded with gold electrode arrays that are highly sensitive to changes in cell index (Roche user manual)

The real time cell analyser system is a current impedance-based assay that relates electrical impedance to cell status/cell index as determined by cell morphology, cell adhesion and cell number. Thus, in order to measure the effects of lithium and RVFV on Raw 264.7 cell proliferation this system was set and initiated according to the manufacturer's protocol. The cells were seeded in the 16-E plates at a density of 40 000 cells/100  $\mu$ l for 3 hrs for cells to adapt and then connected to the equipment for 24 hrs. The cells were infected with RVFV at  $10^{3.8}$  viral titer/100  $\mu$ l and treated with lithium (as outlined in cell treatment above) for 72 hrs. The xCELLigence (Roche, USA) software was set to take readings at 15 minute intervals.

#### *Examination of apoptosis protein expression using Western blotting assay*

In order to examine the Bax and Bcl-2 protein expression ratio Raw 264.7 and MNA cells were seeded in T25 flasks for 3 hrs at a density of  $1 \times 10^6$  cell/ml and  $2 \times 10^5$  cells/ml, respectively. The cells were treated with lithium (as outlined in Cell treatment section) and infected for 3 days with RVFV  $10^{4.8}$  viral titer/ml and  $10^{1.8}$  viral titer/ml respectively. Cells were washed once with 1x PBS, thereafter cells lysis was accomplished with 500 $\mu$ l lysis buffer (10 mM Tris-HCl, pH 6.8, 1% SDS, 100 mM sodium chloride, 1 mM EDTA, 1% NP 40, protease inhibitor). The cells were vortexed for 10 seconds and incubated on ice for 30 minutes. The supernatant was collected

by centrifugation at 15 000 x g for 20 minutes at 4 °C and then protein concentration was determined using BCA protein assay at 562 nm. From the protein samples, 50µg was mixed with the sample buffer (1 mM Tris buffer pH 6.8, 20% SDS, 20% glycerol, 0.05% β-mercaptoethanol, 0.002% bromophenol blue), separated using 12% SDS-PAGE and then transferred to a polyvinylidene fluoride (PVDF) membrane using a semi-dry blotting system (Bio-Rad).

The membranes were blocked with tris buffered saline (TBS) (150 mM NaCl, 50 mM Tris, 0.1% Tween, pH 7.5) containing 3% fat free dried milk. The membranes were washed with wash buffer (0.05% TBS- Tween) and then incubated with anti-Bax, Bcl-2, or β actin primary antibodies (goat anti-mouse) at 1:500 dilutions for 1 hr at RT. After incubation, the membranes were washed 3 times with a wash buffer and corresponding peroxidase-conjugated secondary antibodies (rabbit-anti mouse) were added at 1:10 000 dilutions for 1hr at RT (Santa Cruz). The membranes were washed with a wash buffer and the immune-reactive proteins were detected using the super-signal west pico chemiluminescent substrate (Thermo Scientific, Rockford, USA) and thereafter visualised and photographed using the ChemiDoc XRS+ (Bio-RAD, USA).

#### *Determination of the infectious viral load using viral titration assay*

Tissue culture infectious dose of 50% (TCID<sub>50</sub>), is one of the method to determine viral titer that depends on Vero cell monolayer damage. In order to determine the TCID<sub>50</sub>, Raw 264.7 cells were seeded at 1 x 10<sup>6</sup> cells/ ml in a T 25 flask for 3 hrs. Cells were inoculated with 10<sup>4.8</sup> viral titer/ml RVFV for 1 hr and then the excess virus was discarded. Cells were then treated with lithium (as outlined in cell treatment section) and supernatants were collected in various time intervals (3, 6, 12, 24 and 48 hrs). Collected supernatants were titrated 10-fold in the Vero cells and the cytopathic effect (CPE) was measured. In order to measure virial load (TCID<sub>50</sub>) from lithium-treated and RVFV-infected Raw 264.7 cells, Vero cells were seeded at 2x10<sup>4</sup> cells/well and titrated with Raw 264.7 cells supernatant for seven days. The TCID<sub>50</sub> was then calculated after 7 days using Reed method (Reed and Muench, 1938).

#### *Determination of any direct effects of Lithium on RVFV titer*

The RVFV was diluted 1:10 and treated with 2.5, 1.25, 0.626 mM LiCl and 2.5 mM NaCl for various incubation time (3, 6, 12 and 24 hrs). The incubated virus with lithium was then stored at -20 °C for later use. The stored mixture of virus and lithium was titrated 10 fold in Vero cells and incubated for 7 days. The CPE was measured and the TCID<sub>50</sub> was calculated (Reed and Muench, 1938).

### *Statistical analyses*

All assays were performed 3 times in duplicates or triplicates and the error bars represent the degree of variance. Graph-Pad Prism 6 software was used to plot the graphs and statistical analysis was performed using GraphPad InStat 3 software. Duncan's multiple comparison *t*-test was used to determine significant differences between the means of treated and untreated groups. Differences were considered significant at \*  $p \leq 0.05$ ; \*\*  $p \leq 0.01$ , and \*\*\*  $p \leq 0.001$ .

## **Results**

### *Proliferative and growth effects of lithium post RVFV infection.*

Lithium did not induce any cytotoxic effects on Raw 264.7 cells but rather promoted their proliferation as illustrated using the MTT viability assay (Fig 2.3 A). Lithium improved proliferation of Raw 264.7 cells by about 1.5 fold compared to untreated control cells as well as 2.5 mM NaCl treated cells. On the contrary, RVFV-infected Raw 264.7 cells treated with lithium displayed a cell viability inhibition of 0.8 fold lower than that of RVFV-infected lithium-free control cells (Fig 2.3 A). Figure 2.3, B shows that Raw 264.7 cells treated with lithium retained their spindle shape morphology and increased in size as compared to lithium-free control cells. Cell density was comparable in both untreated and lithium-treated Raw 264.7 cells. The cell population size per field of focus remained unchanged even when Raw 264.7 cells were challenged with 0.625 – 2.5 mM lithium concentrations. The size of intercellular spaces between Raw 264.7 cells remained unchanged despite addition of various concentrations of lithium.

The RVFV-infected Raw 264.7 cells lost their spindle shape and most of them had already formed apoptotic bodies. The number of cells per field of focus decreased dramatically after infection of cells with RVFV. The cell size or cell volume and decreased significantly when Raw 264.7 cells were infected with RVFV. The intercellular spaces in Raw 264.7 cells infected with RVFV increased in size compared to uninfected cells. Cells were more sparsely distributed after infection with RVFV.

The Cyquant proliferation assay results supported the MTT assay findings, demonstrating that lithium concentrations stimulate cell proliferation with observed significant increase in cell proliferation after 48 hrs of treatment. Conversely, RVFV-infected cells treated with lithium showed a dramatic cell death. The positive control cells treated with 20  $\mu$ M curcumin displayed a low count of live cells resulting in viability of only 10% (Figure 2.4). The cell viability differences between RVFV-infected lithium-treated cells and lithium free RVFV-infected cells were not significant; and this could be attributed to assay sensitivity. The inhibition of cell viability in RVFV-infected cells by lithium on Raw cells was not concentration dependent.



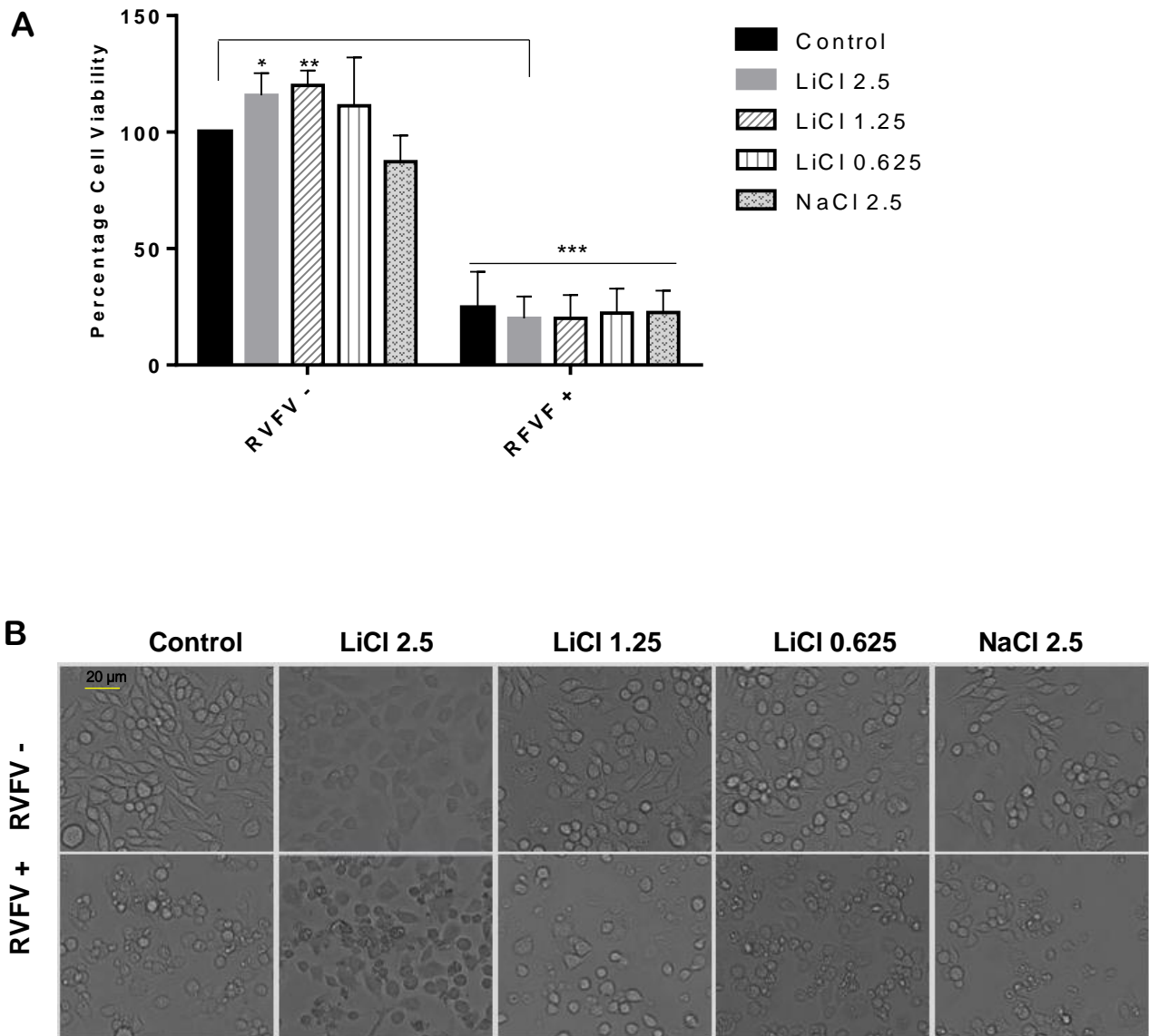


**Figure 2.3. Determination of the cytotoxic effects of lithium on Raw 264.7 macrophage cell after inoculation with RVFV.** Raw 264.7 cell were cultured at a density of  $1 \times 10^5$  cells/ml for 3 hrs and inoculated with  $10^{3.8}$  viral titer/100uL and treated with various doses of LiCl ranging between 2.5 mM and 0.624 mM including control 2.5 mM NaCl for 3 days. MTT was then added for 1 hr at 37 °C, followed by substitution of the medium with DMSO. OD was examined using the ELx800 universal microplate reader (BioTek, USA) [A]. The experiment was performed 3 times in triplicates to establish the error bars and then graphs were developed using the Graph Pad Prism-6 software. Statistical analysis was executed with GraphPad InStat-3 software, Duncan's multiple comparison *t*-test was used to determine significant differences between untreated control and other variants \*  $p \leq 0.05$ ; \*\*  $p \leq 0.01$ , and \*\*\*  $p \leq 0.001$ . The low OD represents cell death while high OD represents cell viability/ cell proliferation. Cell morphology in the wells was captured 20 x magnification using the EVOS FL Colour imaging system (Life technologies, USA) [B].

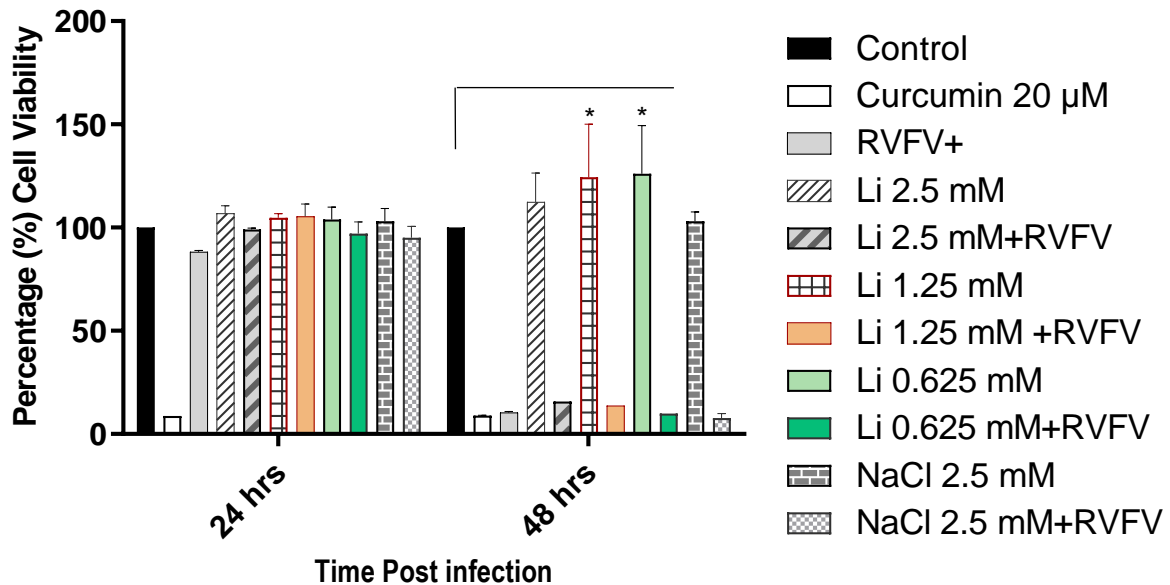


**Figure 2.4. Determination of cell viability using the Cyquant assay after Raw 264.7 cells were treated with lithium and inoculated with RVFV.** The above figure was accomplished by seeding cells at  $9 \times 10^5$  cell/well and  $6 \times 10^5$  cell/well for 3hrs. These cells were treated with 2.5, 1.25, and 0.625 mM LiCl as well as 2.5 mM NaCl, and then inoculated with  $10^{3.8}$  viral titer/100uL RVFV for 24 and 48 hrs. In both 24 and 48 hrs time post infection, the control 20 µM curcumin was added for 24 hrs. After every incubation time point the two components of Cyquant (nucleic acid binding stain and suppressor dye) were added for 60 min. The fluorescent reading was executed at 480/535 nm (excitation, emission), with Fluoroskan Ascent FL (Thermo Fisher Scientific, USA). The experiment was performed 3 times in triplicates to establish the error bars and then The graphs were developed with Graph Pad Prism-6 software and the statistical analysis was executed with GraphPad InStat-3 software. Duncan's multiple comparison *t*-test was used to determine significant differences between untreated control and other variants \*  $p \leq 0.05$ ; \*\*  $p \leq 0.01$ , and \*\*\*  $p \leq 0.001$ .

*Annexin-V PI, Mode of cell death*

The mechanism of cell death induced by RVFV and the influence that lithium has on Raw 264.7 cells were studied using the Annexin-V and PI apoptosis detection assay. Annexin-V has high affinity to phosphatidyl serine residues of the phospholipid bilayer. Phosphatidyl serine gets exposed on the extracellular side of the plasma membrane during the early phase of apoptosis as the membrane is flipped. Annexin-V is conjugated to FITC which then stains cells that are undergoing early apoptosis. Propidium iodide stains the nucleus orange-red only when cells have lost membrane integrity, indicative of the late phase of apoptosis. This assay showed that RVFV induces apoptosis as the mode of cell death, as positive staining with annexin-V and PI was observed in Raw 264.7 cells (Fig 2.5 A).

The cells that were infected with RVFV stained positive for Annexin-V (green staining). Amongst the green stained cells, an average of only 2 stained red per field of focus. Positive control Actinomycin-D showed similar staining patterns as in control RVFV but with estimated 5 cells per field stained red. It is worth noting that RVFV-infected Raw 264.7 cells treated with lithium exhibited an intense positive staining with both dyes. In 2.5 and 1.25 mM Lithium-treated and RVFV-infected cells displayed a more intense red stain with an average of 10 and 6 cells per field as compared to lithium-free RVFV-infected control cells and actinomycin-D treated cells (Fig 2.5 A). The Annexin-V and PI assay results suggest that lithium could be accelerating apoptosis in RVFV-infected Raw 264.7 cells.

The control MNA cells were used to examine if the RVFV induced apoptosis was cell specific. Thus, it has been observed that RVFV induce apoptosis in cells of different origins. Moreover, the MNA cells showed to be more sensitive to RVFV as most of the cells 3 days post exposure with RVFV were in late phase of apoptosis. The sensitivity of cells to RVFV exposure was more or less similar in all treatments regardless of increase in lithium concentration.

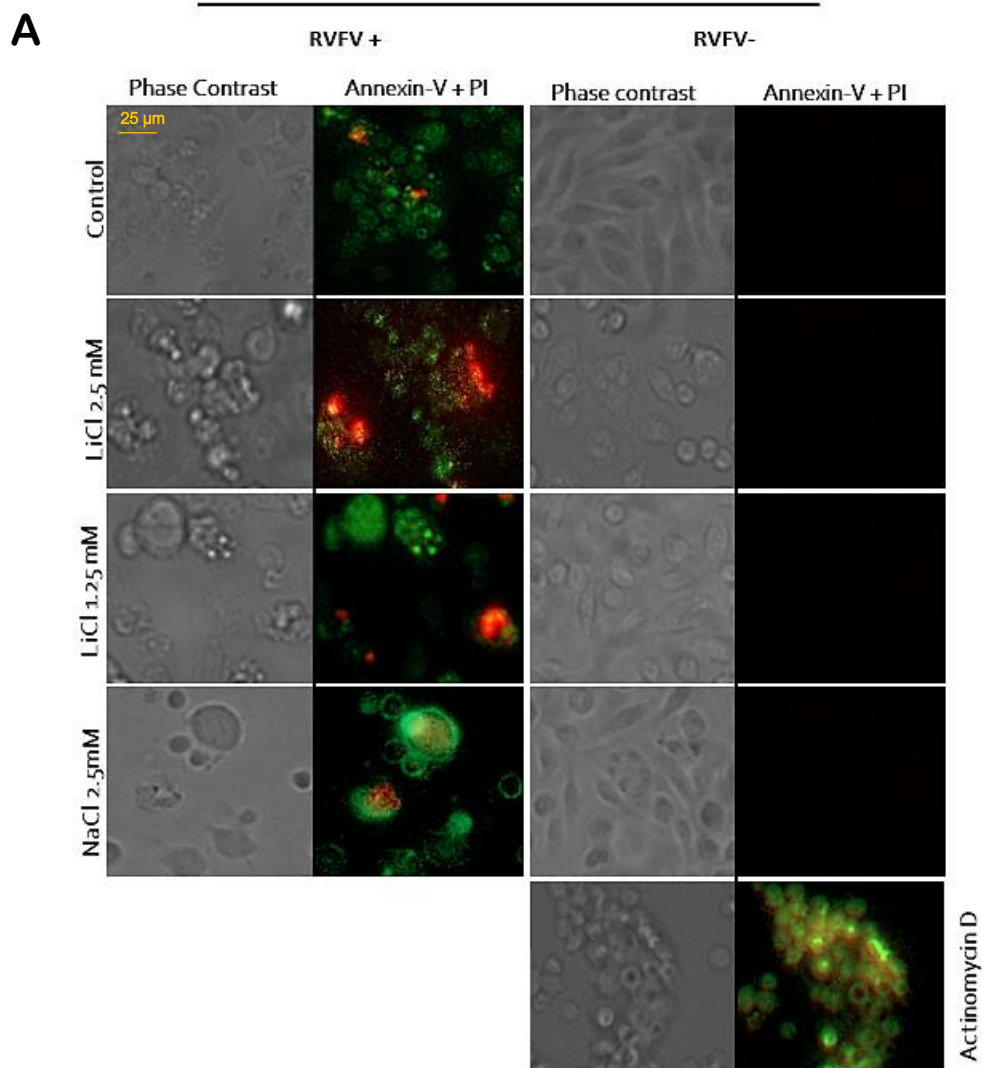


**Figure 2.5A. Determination of the mode of cell death after RVFV inoculation and influence of lithium ions on Raw 264.7 macrophage cells.** Raw 264.7 Cells were cultured at a density of  $2 \times 10^5$  cells/200  $\mu$ L on glass coverslips in a 6 well plate. This was followed by cell treatment with 2.5 mM lithium and 2.5 mM NaCl. Cells were inoculated with  $10^{3.8}$  viral titer/500uL for 3 days, while positive control actinomycin-D 0.02 mg/ml cells were treated for 24 hrs. Cells were stained with Annexin V/PI and fluorescence images were captured at 20x magnification with the EVOS FL Colour imaging system (Life technologies, USA). The Green fluorescence showed positive staining with Annexin-V that resemble apoptosis and Orange Red fluorescence showed positive staining with Propidium Iodide that resembles late phase of apoptosis. The experiments were executed three times and the best pictures were used above.

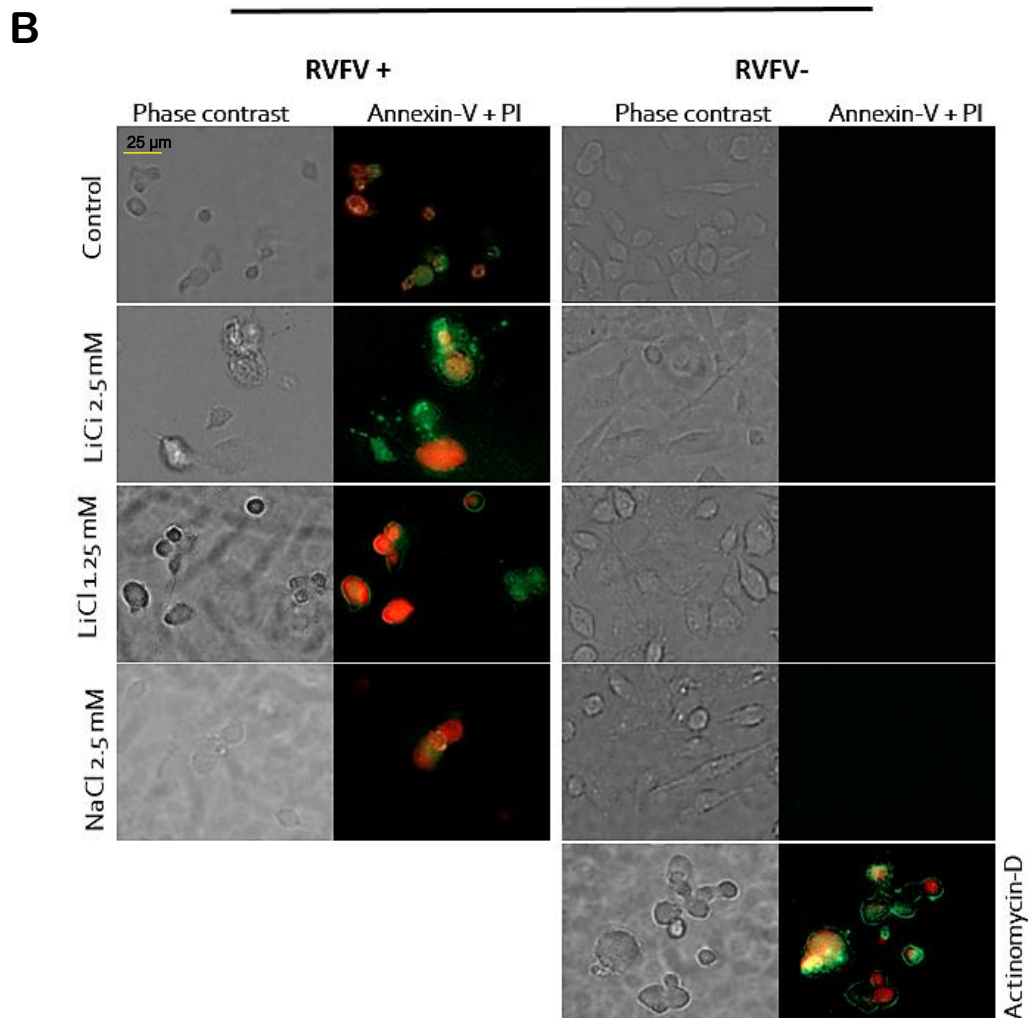


**Figure 2.5 B. Determination of the mode of cell death after RVFV inoculation and influence of lithium ions on MNA cells.** MNA Cells were cultured at a density of  $8 \times 10^4$  cell/200  $\mu$ L respectively on glass coverslips in a 6 well plate. This was followed by cell treatment with 2.5 mM lithium and 2.5 mM NaCl. Cells were then inoculated with  $10^{0.8}$  viral titer/500uL for 3 days, while actinomycin-D 0.02 mg/ml cells were treated for 24 hrs. Cells were stained with Annexin V/PI and fluorescence images were captured at 20x magnification with the EVOS FL Colour imaging system (Life technologies, USA). The Green fluorescence showed positive staining with Annexin-V that resemble apoptosis and Orange Red fluorescence showed positive staining with Propidium Iodide that resembles late phase of apoptosis. The experiments were conducted three times and best pictures was used above.

*Effects of lithium post RVFV infection on molecular expression of the apoptosis protein*

The Bax to Bcl-2 expression ratio is used as a measure of the extent and mode of cell death. Bax initiates apoptosis by inducing permeability of the mitochondria as a result of cell stress stimulus while the Bcl-2 counterpart antagonises that activity (Khodapasand *et al.*, 2015). Expression of one protein down-regulates the counterpart. A Bcl-2 protein expression higher than Bax represents cell viability whereas a Bax protein expression higher than Bcl-2 represents cell death. Therefore, the higher Bax to Bcl-2 ratio is indicative of cells most likely to undergo apoptosis. A down-regulated Bcl-2 protein expression and up-regulated Bax protein expression was observed in RVFV infected cells and positive control cells treated with curcumin (Fig 2.6). The Bax/Bcl-2 ratio in untreated control cells was 0.1 while the ratios in control RVFV and control curcumin were 1.4 and 9, respectively. The Bax/ Bcl-2 ratios in RVFV-infected cells treated with 1.25 and 2.5 mM LiCl were 3 and 4.15, respectively. The Bax/Bcl-2 ratios in RVFV-infected cells increased with increase in LiCl concentration.

The Bax/ Bcl-2 expression ratio which determines the mode of cell death was shown to be higher in lithium-treated and RVFV-infected cells. The protein band intensity of one protein over the other represents the rate of apoptosis in various treatments. The expression of the Bcl-2 anti-apoptotic protein was relatively found to be 2 folds lower in all RVFV-infected lithium-treated cells compared to the lithium-free control RVFV infected cells. This observation infers that RVFV induce apoptosis as a mode of cell death in Raw 264.7 cells. Moreover, the Bax pro-apoptotic protein showed to be highly expressed in cells treated with 2.5 mM lithium 1-fold more as compared to lithium-free RVFV infected control cells and the sensitivity was reduced with decreasing concentrations (Figure 2.6, B).

Interestingly the similar apoptotic patterns have been observed in control MNA cells. The Bax/ Bcl-2 ratio in untreated control was 0.2 while lithium-free RVFV infected control, NaCl 2.5 mM and 20  $\mu$ M curcumin ratio were 1, 4 and 3 respectively. The Bax/Bcl-2 ratio in Lithium 2.5, and 1.25 mM is 8 and 4 (Fig 2.6 C). These results agree with the results observed in Raw 264.7 cells (Fig 2.6 B).

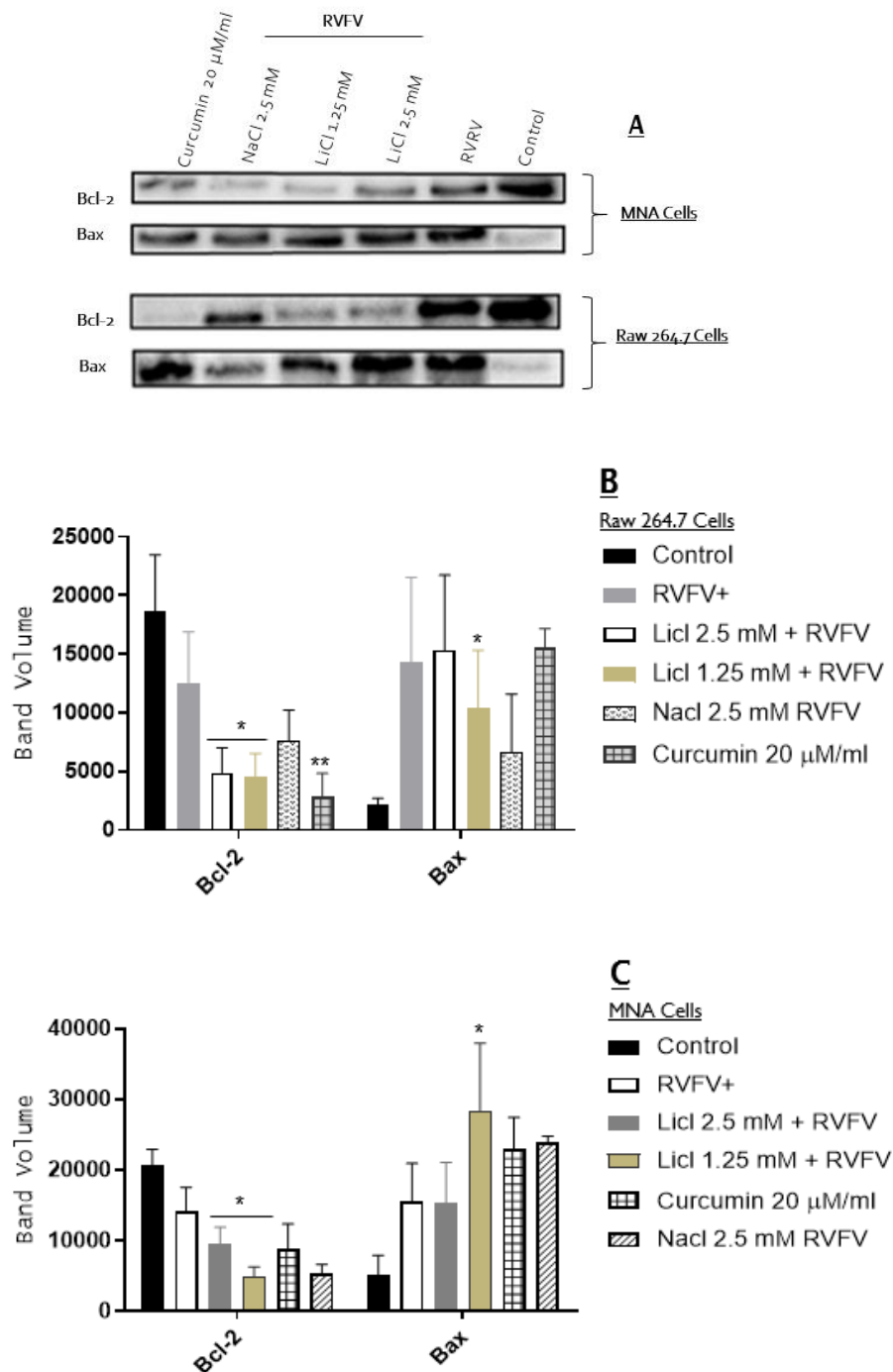


**Figure 2.6. Determination of mode of cell death induced by Rift Valley Fever Virus through molecular expression of Bax/Bcl-2.** Raw 264.7 and MNA cells were seeded at  $1 \times 10^6$  cell/ml and  $2 \times 10^5$  cells/ml for 3 hrs respectively. Cells were infected with  $10^{4.8}$  viral titer/mL and  $10^{1.8}$  viral titer/mL RVFV for 3 days. The control 20  $\mu$ M Curcumin was added for 24 hrs. This was then followed by isolation of proteins and the western blotting assay. The pictures were captured with ChemiDoc XRS+ (Bio-RAD, USA). The ChemiDoc XRS+ was used to capture blot images and measure band volume or intensity. The protein expression experiments were performed 3 times and the band volume were used to determine error bars. Plots were developed using a Graph Pad Prism-6 software to determine the expression differences of Bax and Bcl-2 in Raw 264.7 cells (B) and MNA cells (C). The statistical analysis was developed with the GraphPad InStat-3 software. Duncan's multiple comparison *t*-test was used to determine significant differences between control RVFV and other variants \*  $p \leq 0.05$ ; \*\*  $p \leq 0.01$ , and \*\*\*  $p \leq 0.001$ .

### Real time measurement of cell growth

The xCELLigence was used to monitor cell proliferation/growth in real time in an attempt to examine suspected lithium-accelerated apoptosis in RVFV-infected Raw 264.7 cells. The assay showed that as early as 10 hrs pi 2.5 [B] declined in cell viability as compared to untreated RVFV-infected control [E] and NaCl-treated RVFV-infected cells [D] (pointed out using a red dashed arrow). After 20 hrs pi lithium-treated RVFV-infected cells showed a complete switch from cell growth to cell death, at this point it is suggested that most of the cells got infected and the virus is replicating. The control RVFV-infected cells that were not exposed to lithium survived almost 2 days post RVFV infection before they underwent cell death (Fig 2.7).

The transition difference was almost 24 hrs as illustrated by the red solid horizontal line. The untreated and uninfected control cells showed an increase in growth until 90 hrs. These results support the previous cytotoxicity and apoptosis assays that showed the elevated cytotoxic and death signals in lithium-treated RVFV-infected cells compared to the control lithium-free RVFV-infected cells. Therefore, viral quantification remains necessary in an attempt to examine if lithium-accelerated apoptosis corresponds to altered viral replication.

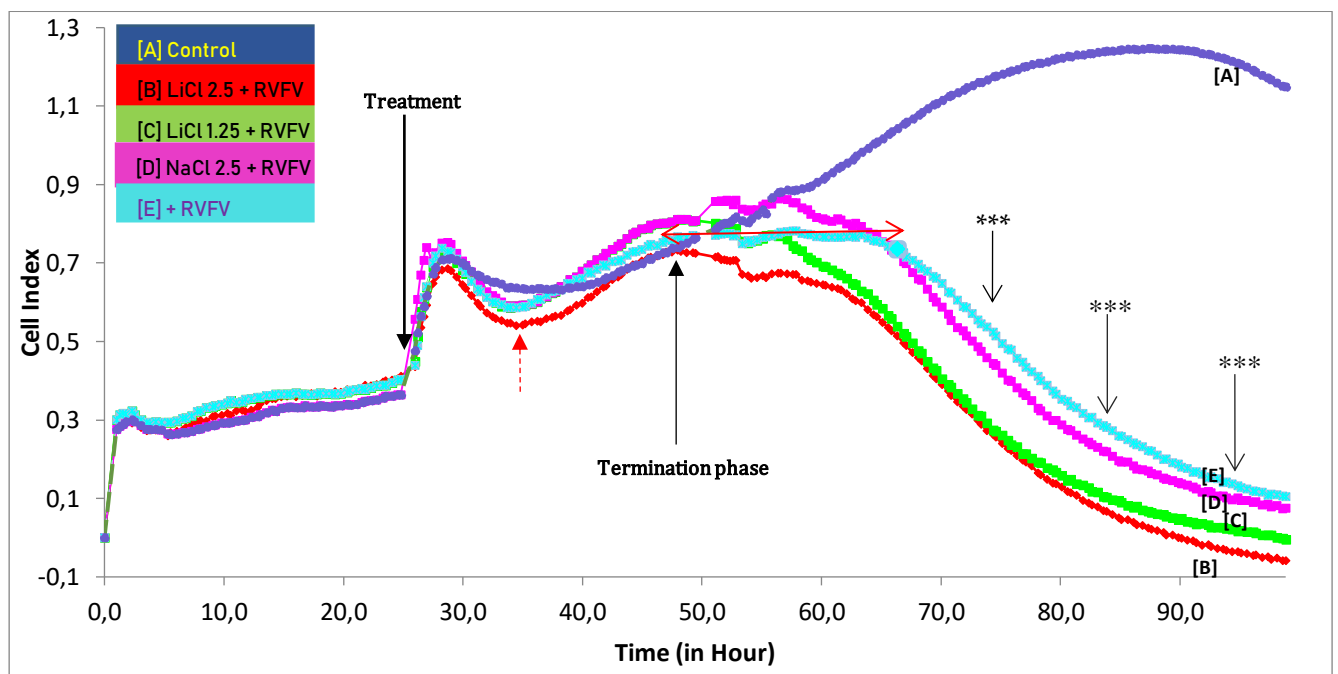


**Figure 2.7. Determination of the accelerated cell death induced by lithium in real time.** Cells were seeded at 40 000 cell/well for 3 hrs for cells to attach, therefore the cell behaviour was monitored with the xCELLigence detection system for 24 hrs, this was followed by treatment with LiCl (1.25 and 2.5 mM), NaCl 2.5 mM and  $10^{3.8}$  TCID<sub>50</sub>/100  $\mu$ L for 72 hrs. Cell viability was measured on real time using the xCELLigence real time and statistical analysis was done at 60, 70, 80 and 90 hrs time point with the GraphPad InStat-3 software. Student *t*-test was used to



determine significant differences between control RVFV and 1.25 mM LiCl+ RVFV \*  $p \leq 0.05$ ; \*\*  $p \leq 0.01$ , and \*\*\*  $p \leq 0.001$ .

#### Infectious viral titer

TCID<sub>50</sub> was used to measure the infectious viral titre at various time points so as to examine if the accelerated apoptosis corresponds with a lowered viral load. The RVFV infected lithium-treated cells showed lowered viral titre as compared to the lithium-free RVFV-infected control cells. Treatment of Raw 264.7 cells with lithium (2.5 and 1.25 mM) (Fig 2.8) significantly lowered the RVF viral titre as shown in various time points. Lowering of the viral titre started from 6 hrs time point. Corresponding with what has been observed in xCELLigence RTCA assay. This decline in cell viability was observed as early as 10 hrs pi. RVFV-infected Raw 264.7 cells that were treated with lithium show less viral load as compared to lithium-free RVFV-infected control cells.

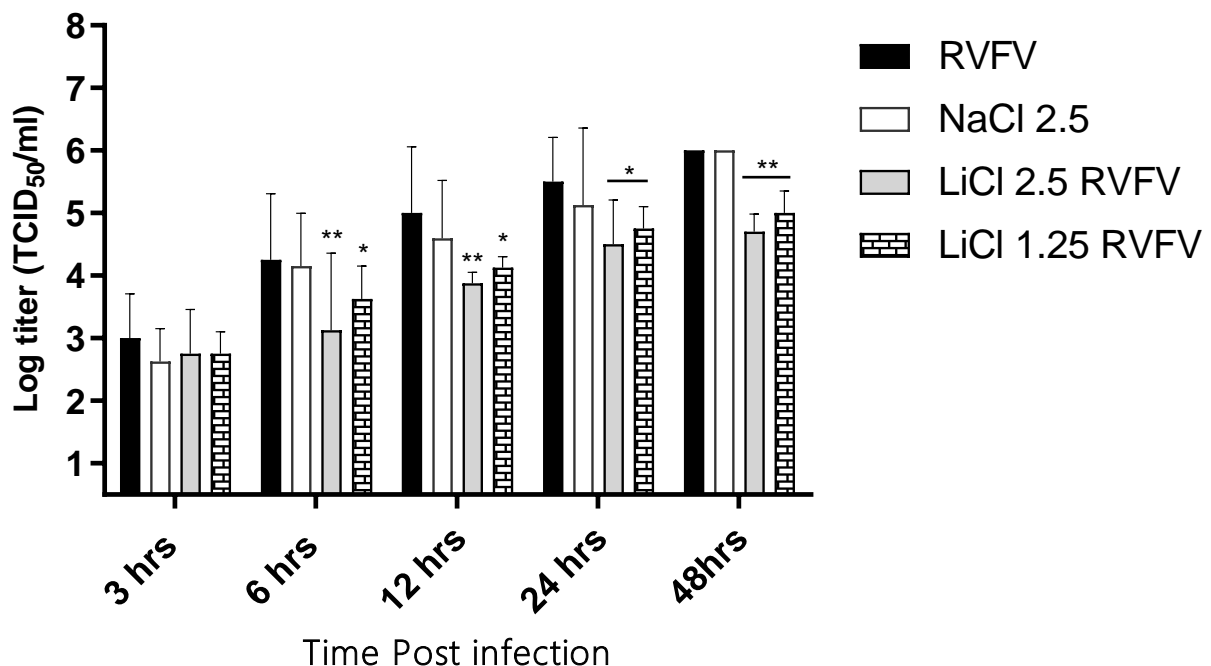


**Figure 2.8. Examination of the effects of lithium on Rift Valley Fever Virus replication on Raw 264.7 macrophage cells.** Vero cells were used to measure viral load of RVFV infected Raw 264.7 cells (TCID<sub>50</sub>). The cells were seeded at  $1 \times 10^6$  cells/ml for 3 hrs and then infected with  $10^{4.8}$  viral titer/mL RVFV for 1 hr. Thereafter the excess virus was removed. The cells were treated with 2.5 and 1.25 mM LiCl as well as 2.5 mM NaCl, and then the supernatants from those cells were collected after 3, 6, 12, 24 and 48 hrs and stored for later use at  $-20^\circ\text{C}$ . The viral titer on the collected supernatant was measured by the TCID<sub>50</sub> procedure on Vero cells seeded at  $2 \times 10^4$  Cells/well for seven days. The experiments were run 3 time in triplicates to develop the error bars. The plots were developed using Graph Pad Prism-6 software, while statistical analysis was executed with GraphPad InStat-3 software. Duncan's multiple comparison *t*-test was used to determine significant differences between control RVFV and other variants \*  $p \leq 0.05$ ; \*\*  $p \leq 0.01$ , and \*\*\*  $p \leq 0.001$ .

*Determination of Direct Effects of Lithium on RVFV.*

The lowered viral titre observed in figure 2.7 is suggested to be due to apoptosis and not the direct effects of lithium on the virus. Thus, the direct viral exposure to lithium show that lithium did not have any direct effects on the virus as viral titre was not different in lithium-RVFV compared to control RVFV (Fig 2.9). In figure 2.9 the viral titre was observed to be the same in all treatment.

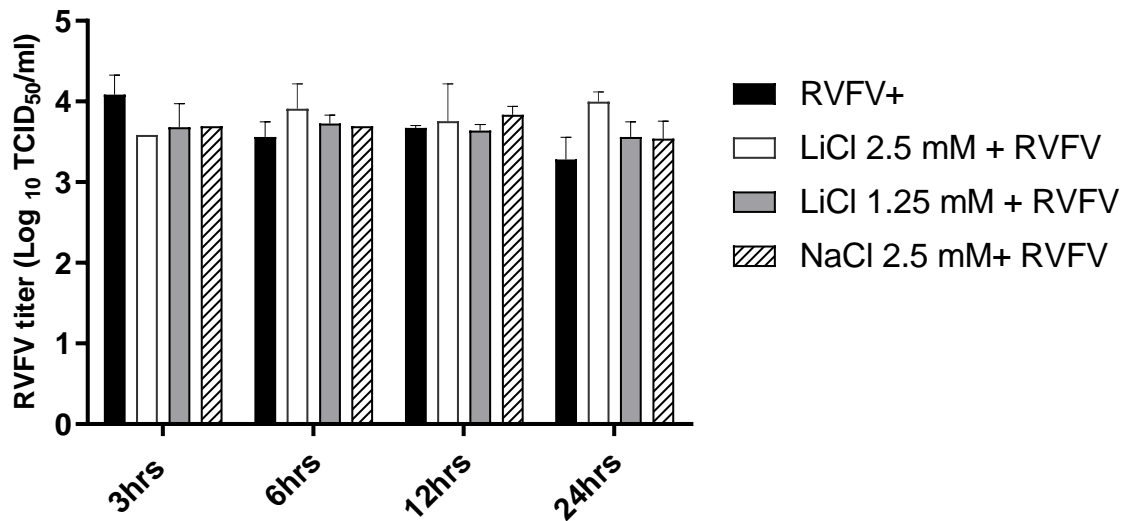


**Figure 2.9. Determination of the direct effect of lithium on RVFV integrity.** The virus was incubated with lithium chloride (2.5, 1.25 mM LiCl) and 2.5 mM NaCl at various time points that include 3, 6, 12 and 24 hrs. Thereafter, the virus was titrated on the Vero cells followed by measuring TCID<sub>50</sub>. The experiments were performed 3 time in triplicates to develop the error bars. The Graph was developed with Graph Pad Prism 6 and statistical analysis was executed with GraphPad InStat-3 software. Duncan's multiple comparison *t*-test was used to determine significant differences between control RVFV and other variants \*  $p \leq 0.05$ ; \*\*  $p \leq 0.01$ , and \*\*\*  $p \leq 0.001$ .

## **Discussion**

It has been more than eight decades since RVF viral infection came to recognition in the 1930s (Davies *et al.*, 2010) but an effective prophylaxis is yet to be established. This study examined the use of lithium as a possible treatment for this form of viral infection, focusing on the replication efficacy and haemorrhagic fever related morbidities. Although lithium has been medically used since 1949, as a preferred bipolar disorders remedy, this study examined its effects beyond its traditional use as a preferred treatment for bipolar (Cade, 1949). Lithium's mechanism of action underlying its role as a remedy for treatment of bipolar is poorly understood. However, its reactivity and its role in biological processes has been linked to its valance electrons (Strunecká, *et al.*, 2005).

This study showed that lithium is not cytotoxic to Raw 264.7 cells but significantly increases the proliferation of these immune macrophage cells (Fig 2.3 A and 2.4) as determined using the cell proliferation/ viability (Cyquant and MTT) assays. Our previous findings have demonstrated the safe use of lithium up to 20 mM on Raw 264.7 cells (Makola *et al.*, 2020). Despite lithium-induced cell proliferation, RVFV-infected lithium-treated cells were recorded to have the lowest viability in comparison to lithium-free RVFV-infected control cells (figure 2.3 A). Cells treated with lithium showed morphological growth as depicted in figure 2.3 B. This growth is suggested to occur during the preparatory phase of cell division; hence, the observed cell proliferation signal in viability assays (Fig 2.3 A).

The cell morphological growth observed in lithium-treated Raw 264.7 cells (Fig 2.3 B) is suggested to be due to high activity in the G2 phase of the cell cycle wherein cells prepare for mitosis (M phase) and subsequent duplication. López Cascales and Garda de la Torre, reported the influence of lithium on membrane fluidity. This work examined the behaviour of the lipid bilayer and the impact alkali metal ions such as lithium and sodium have on it. Lithium movement through the plasma membrane occurs through voltage-dependent Na<sup>+</sup> channels and it interacts with the charged phospholipids that constitute the lipid bilayer. Lithium ions induce order in the fatty acids, transforming the plasma membrane fluidity (López Cascales *et al.*, 1997). The combination of current results, along with López Cascales and Garda de la Torre's work, demonstrate the extended impact lithium has on the plasma cell membrane.

The proliferative properties of lithium observed in this study support the previous documentations that display the role of lithium in stimulating haematopoiesis (Barr *et al.*, 1983). Increment of white blood cell count was recorded as one of side effects in bipolar patients treated with lithium (Amitai *et al.*, 2014). In addition to cytotoxicity assays, this study examined the mode of cell death induced by RVFV. Nfon and colleagues reported a decline in the population of macrophage and dendritic cells post RVFV infection and suggested that the decline could be as a result of necrosis (Nfon *et al.*, 2012). Correspondingly, results from this study illustrate that RVFV induces apoptosis in Raw 264.7 macrophages.

Austin and colleagues have demonstrated a direct link between RVFV-induced apoptosis and activated p53 (Austin *et al.*, 2012). In the current study, cells infected with RVFV stained positive for Annexin-V FITC and a few of them stained positive for both Annexin-V and propidium iodide (PI) (Fig 2.5). This staining pattern is indicative of apoptosis as the mode of cell death. The RVFV-infected cells treated with lithium stained positive for both Annexin-V and PI and displayed a higher number of cells with an intense red staining (PI) compared to the lithium free RVFV-infected control cells and actinomycin-D control cells (Fig 2.5 A). These dual staining observations suggest that RVFV-infected cells treated with lithium were in the late phase of apoptosis. Figure 2.5 B depict similar staining patterns in control MNA cells. However, most cells were in late phase of apoptosis in all the treatments, suggesting sensitivity of these cells to the RVFV.

The Bax to Bcl-2 expression ratio was used as a molecular measure of the mechanism and extent of cell death (Elmore, 2007). It can be inferred from figure 2.6 A and B that cells infected with RVFV underwent apoptosis as a result of high Bax/Bcl-2 expression ratio in comparison to untreated control cells. These findings are in line with previous data, which suggest that RVFV induce apoptosis via the p53 signalling pathway as the p53 transcriptional target, Bax, is upregulated in the current apoptosis results (Austin *et al.*, 2012). Overall, the observed Bcl-2 expression in RVFV-infected lithium-treated cells was significantly less, as compared to lithium-free RVFV-infected control cells. In addition to lower Bcl-2 levels recorded in lithium-treated RVFV infected cells, higher levels of Bax expression and Bax/Bcl-2 ratio were observed in RVFV-infected lithium (2.5 and 1.25 mM) treated cells compared to control lithium-free RVFV-infected cells (Fig 2.6 A, B). Moreover, the MNA cells

showed that lithium-treated and RVFV-infected cells displayed high Bax/Bcl-2 ratio as compared to lithium-free RVFV-infected cells (Fig 2.6 C)

The combination of cytotoxicity and apoptosis assay results have shown elevated apoptosis signals in RVFV-infected cells treated with lithium. Thus, the xCELLigence system, which measures cell growth in real time, was employed to confirm that RVFV-infected lithium-treated cells undergo accelerated cell death. RVFV-infected lithium-treated cells displayed a decline in cell viability as early as 10 hrs pi and a complete viability transition was observed 20 hrs pi while lithium free RVFV infected control cells observed transition in cell viability almost 44 hrs later (Fig 2.7). These findings show that lithium induce accelerated apoptosis in RVFV-infected cells. A study by Koyama *et al* reported that virus-infected cells seem to undergo accelerated apoptosis as a defense mechanism in order to abort viral progeny, resulting in a reduced viral load (Koyama *et al.*, 1998).

Findings from this work provide a novel anti-viral approach using lithium as a source of treatment. Lithium lowers RVF viral titre at various concentrations (Fig 2.8). The suggested putative mechanism behind the lowered viral titre is ascertained to be through lithium-accelerated apoptosis in RVFV-infected cells, which in turn leads to abortion of viral progeny and disruption of viral replication. Accelerated apoptosis is suggested to be the mechanism behind lithium's anti-viral properties as the direct effects of lithium on the virus showed no differences in viral titre compared to control (Fig 2.9). Figure 2.8 displays the viral titration Log TCID<sub>50</sub> plot that shows a significantly lowered viral load in RVFV-infected lithium-treated cells compared to lithium-free RVFV-infected control cells. The xCELLigence assay show direct link between the lowered cell viability with reduced viral titre.

Viruses have various ways to manipulate the host cells so as to support viral replication (Galluzzi *et al.*, 2008). The RVFV encode NSm that delays apoptosis in favour of continual production of the viral progeny (Austin *et al.*, 2012; Won *et al.*, 2007). Previous work by Won and colleagues showed that the NSm mutant viral strain (arMP-12-del21/384) induce drastic cell death 48hrs pi in comparison to the recombinant vaccine candidate strain of RVFV (arMP-12). Similar observations have been reported by Austin and colleagues, showing that NSs activated p53 apoptosis occurs 48 hrs pi in the HSAEC cell (Austin *et al.*, 2012), this observations have motivated the choice of the RVFV incubation time intervals. These previous findings, alongside results from this study suggest that at 48 hrs RVFV incubation result in p53

expression which induces apoptosis, causing release of the viral progeny. However, treatment of RVFV-infected cells with lithium resulted in a decline in cell viability as early as 10 hrs pi and a massive decline 20 hrs pi (Fig 2.7), thereby aborting viral replication.

Since elevated white blood cell counts were reported in bipolar patients on lithium treatment, the use of lithium as an antiviral remedy *in vivo* could stimulate proliferation of virus-free immune cells while accelerating death in RVFV-infected cells. This phenomenon points towards protection of patients from leukocytopenia and compromised immune response. In 1993, Hartley and colleagues reported the selective replication inhibitory properties of high doses of lithium on DNA genome viruses and the growth of gram-negative bacteria with a poor understanding of its mechanism of action. Hartley and colleagues proposed lithium influx and altered cationic concentration in a cell. However, the current study links low lithium doses with altered viral replication as a result of accelerated apoptosis and viral progeny abortion (Hartley et al., 1993). Previous studies have confirmed the narrow spectrum of action/ activity shown by lithium at therapeutic concentrations (0.4–2.0mM LiCl), hence the use of these low doses in this study (Plotnikov *et al.*, 2014; Sproule, 2002).

Apoptosis of the virally infected antigen presenter cells (APC) and phagocytic innate immune cells such as macrophages is very crucial in limiting viral spread to target tissues. Owing to the role of macrophages as the first line of defence as well as their migration properties, they remain a preferred target for the viruses because they are used as vectors that transport viruses to target organs such as the liver and the brain. In addition to lithium accelerated apoptosis in virus-infected cells, in an *in vivo* system, the natural killer (NK) cells would increase the margin of cytotoxicity in infected host cells in order to reduce the migration of infected cells. Nfon and colleagues have shown that IFN- $\gamma$  and IL-12 expression stimulate NK cells and promote its cytotoxic role (Nfon *et al.*, 2012). This study suggests that lithium could be a potential treatment option for the RVF based viral haemorrhagic fevers and an ideal agent for combination therapy as it does not target the virus directly but targets the cells infected with the virus.

## **Conclusions**

Although the mechanism of action through which lithium induces suppression of manic and bipolar episodes remains an ongoing subject of interest, this study is the

first to link lithium-accelerated apoptosis to lowered viral load. Results from this work show that RVFV-infected cells treated with lithium undergo early apoptosis and this corresponds with lowered viral load. The lowered viral replication is postulated to be through abortion of the replicating viral progeny. In contrast, lithium stimulates proliferation of virus-free innate immune macrophage cells; a phenomenon that will help avoid leukocytopenia and a weakened immune system. Although further work is required to examine the effects of lithium against NSm, it has been shown that lithium lower viral load through accelerated apoptosis via expression of the p53 transcription target, the Bax pro-apoptotic protein. Furthermore, additional work is required to trace the exact signalling pathway that lithium uses to induce early apoptosis in RVFV-infected cells.

### CHAPTER 3

## LITHIUM INHIBITS NF- $\kappa$ B NUCLEAR TRANSLOCATION AND MODULATE INFLAMMATION PROFILES IN RIFT VALLEY FEVER VIRUS-INFECTED RAW 264.7 MACROPHAGES

---

### **Abstract**

Rift Valley fever virus (RVFV) is an emerging arbo virus endemic across sub-Saharan African countries and the Arabian Peninsula; with a growing panic of its spread to non-endemic regions. This viral infection triggers a wide spectrum of symptoms that span from fibril illnesses to more severe symptoms such as haemorrhagic fever and encephalitis. These severe symptoms have been associated with dysregulated immune response propagated by the virulence factor, non-structural protein (NSs). Thus, this study investigated the effects of lithium on NF- $\kappa$ B translocation and RVFV-induced inflammation in Raw 264.7 macrophages. The supernatant from lithium-treated RVFV-infected Raw 264.7 cells, was examined using an ELISA assay kit to measure levels of cytokines and chemokines. The H<sub>2</sub>DCF-DA and DAF-2 DA fluorogenic assays were used to determine the levels of ROS and RNS by measuring the cellular fluorescence intensity post RVFV-infection and lithium treatment. Western blot and immunocytochemistry assays were used to measure expression levels of the inflammatory proteins and cellular location of the NF- $\kappa$ B, respectively.

Lithium was shown to stimulate interferon-gamma (IFN- $\gamma$ ) production as early as 3 hrs pi. Production of interleukin-6 (IL-6) and regulated on activation normal T cell expressed and secreted (RANTES) cytokines was elevated by treatment of cells with lithium. The production of IL-6 pro-inflammatory cytokine and RANTES chemokine in Raw 264.7 cells was elevated as early as 12 hrs pi. Treatment with lithium stimulated increase of production of tumour necrosis factor-alpha (TNF- $\alpha$ ) and Interleukin -10 (IL-10) in RVFV-infected and uninfected macrophages as early as 3 hrs pi. The RVFV-infected cells treated with lithium displayed lower ROS and RNS production as opposed to lithium-free RVFV-infected controls. Western blot analyses demonstrated that lithium inhibited iNOS expression while stimulating expression of heme oxygenase (HO) and I $\kappa$ B in RVFV-infected Raw 264.7 macrophages. Results from immunocytochemistry and Western blot assays revealed that lithium inhibits NF- $\kappa$ B



nuclear translocation in RVFV-infected cells compared to lithium-free RVFV-infected cells and 5 mg/ml LPS controls. This study demonstrates that lithium inhibits NF- $\kappa$ B nuclear translocation and modulate inflammation profiles in RVFV-infected Raw 264.7 macrophage cells.

Keywords: Macrophages, Inflammation, RVFV and NF- $\kappa$ B

## **Introduction**

The immune system is the vertebrate-dependent phylogenetic defense mechanism against infectious agents such as toxins and microbes. It is classified into innate immune system and humoral immune system (Akira *et al.*, 2006; Xiao, 2017). Macrophages play a central role in the innate immune system and inflammation. These cells are antigen presenter cells (APC) located in various locations as tissue residential cells and also as circulating cells in the plasma (Plowden *et al.*, 2004). The innate immune system is not entirely non-specific since myeloid lineage cells such as dendritic and macrophages express the pathogen recognition receptors (PRR) that recognise microbial components termed pathogen-associated molecular patterns (PAMP) (Wang *et al.*, 2004).

Toll-like receptors (TLRs), Nucleotide-binding oligomerization domain-containing protein 1 (NOD1), NOD-2 and retinoic acid-inducible gene I (RIG-I)-like helicase receptors (RLRs) are PRR known to recognise microbial components and activate onset of various signalling pathways (Akira *et al.*, 2006; Wang *et al.*, 2013). Viral nucleic acids are recognised by a several receptors that include TLR-7 and 8 recognising viral single-stranded RNA (ssRNA), while RIG-I and TLR-3 recognise viral double stranded RNA (dsRNA). These molecules are expressed intracellularly on the endosome membrane. Viral glycol proteins are recognised by TLR 2 and 4, targeting mostly NF- $\kappa$ B linked inflammatory pathway and not the interferon regulatory transcription factor (IRF) 3 and 7. The IRF 3 and 7 are part of signalling pathway that produces anti-viral specific molecules such as type I IFN (Akira *et al.*, 2006).

The binding of viral ligands to the receptors recruit adaptor molecules such as myeloid differentiation primary response 88 (MyD88), Toll-interleukin 1 receptor domain-containing adapter protein (TIRAP) and TIR-domain-containing adapter-inducing interferon- $\beta$  (TRIF) to the cytoplasmic domain of the receptors (Akira *et al.*, 2006). Toll-like receptor-3 (TLR3) induce the production of IFN via MyD88-independent signalling pathway. TRIF is then recruited to dimerise with TLR-3 on the cytoplasmic

domain. The pathway culminates with activation of IRF-3 and IRF-7 which translocate into the nucleus and bind to the IFN-stimulated response elements (ISREs), resulting in the expression of IFN-inducible genes. Conversely, TLR 7 and 9 induce the production of IFN via the MyD88 signalling pathway (Akira *et al.*, 2006).

RIG-I is a cytoplasmic dsRNA detecting receptor which is not accessible to TLR-3. RIG-I interacts with IPS-1 through the CARD domain as its adaptor molecule. The resulting signalling cascade activates IRF-3 and IRF-7 in a similar manner used by TLR-3. The RIG-I detect the cytoplasmic replicating dsRNA while TLR-3 detect dsRNA in the apoptotic bodies of virally infected cells undergoing apoptosis (Akira *et al.*, 2006). Rift valley fever virus that causes Rift valley fever disease tri-segmented single stranded genome namely the L segments that encode viral RNA dependent RNA polymerase, the M segment that encode envelop glycoproteins (Gn and Gc) a 78 kDa protein and a 14 kDa non-structural protein (NSm) (Nfon *et al.*, 2012; Paweska and Jansen van Vuren, 2014).

Moreover, the S segments encode the nucleoprotein (N) in the negative-sense and a non-structural protein (NSs) in the genomic direction (Nfon *et al.*, 2012). The non-structural protein NSs was shown to be the main virulence molecule and this protein has innate immune suppressive properties that aid in the viral replication and viremia (Nfon *et al.*, 2012). RVFV NSs protein circumvents the innate immune system through inhibition of type I IFN ( $\alpha$  and  $\beta$ ) (Nfon *et al.*, 2012). Other studies linked the NSs with RVFV pathogenesis through transcriptional shut down that lead to a weakened anti-viral response and IFNs production system (Le May *et al.*, 2004; Wood *et al.*, 2004).

IFNs are important antiviral factors that stimulate antiviral molecules and recruit other immune cells to the inflamed site in order to limit viral spread. The type I IFNs have been shown to enhance the expression of protein kinase RNA-activation (PKR). In addition to the IFNs system, the PKR expression can be enhanced by dsRNA and ssRNA. The role of this serine threonine kinase is to phosphorylate eukaryotic translational inhibition factor 2 (eIF2), leading to the translational arrest of both cellular and viral mRNAs (Habjan *et al.*, 2009). The PKR has shown some activity in the absence of NSs protein since NSs was shown to directly degrade PKR (Habjan *et al.*, 2009).

Monkeys that have shown high expression of IFNs cytokines have not developed RVF disease after exposure to RVFV. As a result, these cytokines were suggested

to have the protective properties against RVFV. Animal model studies showed selective inhibition of the IFN- $\alpha$  since the production of IFN- $\gamma$ , TNF- $\alpha$ , IL-6, IL-12, and IL-1  $\beta$  was observed without detectable levels of IFN- $\alpha$ . Interestingly, IFN- $\gamma$  and IL-12 have been suggested to lower viremia by stimulating natural killer cells (NK) cells and its cytotoxic role (Nfon *et al.*, 2012). The evidence that NSs antagonise the IFNs cytokines makes RVFV infection difficult to clear. An *in vitro* study conducted by Jansen van Vuren and colleagues showed contradictory findings with those that postulate that NSs result in a transcriptional shut-down and weakened inflammatory response (Jansen van Vuren *et al.*, 2015, Le May *et al.*, 2004).

The work by Jansen van Vuren *et al* showed that immune response was mounted to a more or less similar extent in both the fatal cases and non-fatal cases. This study showed that early infection samples have high levels of IL-8 and CCL-2/MCP-1 in serum as compared to sera from uninfected controls. Interestingly, fatal case serum has shown 10-fold increased levels of IL-6 (a pro-inflammatory cytokine) than non-fatal cases. The serum level of IL-10 in both early and late samples of the fatal and non-fatal cases were statistically not different. This study demonstrated that the fatality and survival of patients might rely on the extent and regulation of inflammatory responses (Jansen van Vuren *et al.*, 2015).

This immune deregulatory evidence reported by Jansen van Vuren and other studies show severe outcomes that are linked to under-regulated and persistent inflammation (Reuter *et al.*, 2010). The uncontrolled production of these inflammatory molecules has been linked to the pathogenicity of most of the chronic ailments such as neurodegeneration and cancer (Jope *et al.*, 2007). Wang and colleagues have linked the West Nile virus (WNV) infection consequences to elevated inflammation and damage to the endothelial integrity. This led to leukocyte extravasation, encephalitis and death (Wang *et al.*, 2004). It is, therefore the aim of the study to examine the regulatory properties of lithium on inflammation and NF- $\kappa$ B nuclear translocation in Raw 264.7 macrophages exposed to Rift valley fever virus.

## **Materials and Methods**

### *Cell Culture and Viral Propagation*

The RVFV AR 20368 strain was isolated in 1974 during the RVF outbreak in South Africa. The virus was propagated on Vero C1008 cells at an MOI of 0.2, followed by harvesting the monolayer after extensive cytopathic effect (CPE) was observed. The supernatant was stored at -70°C after centrifugation at 3,000 xg for 30 minutes (Martín-Folgar *et al.*, 2010). The Raw 264.7 macrophage cells were obtained from Prof Lyndy McGraw (University of Pretoria). The cells were maintained in cell culture flasks at 37°C, in a humidified 95% air and 5% CO<sub>2</sub> atmosphere. Raw 264.7 cells were propagated in Dulbecco Modified Eagle Medium (DMEM) supplemented with 10% Fetal Bovine Serum (FBS), 2 mM L-glutamine and 1x penicillin-streptomycin. Vero C1008 cells were purchased from ATCC and propagated in Minimum Essential Medium (MEM), supplemented with 10 % FBS, 2 mM L-glutamine and 1x penicillin-streptomycin (Lonza). Trypan blue dye and haemocytometer were used to determine cell density (Matsebatlela *et al.*, 2012).

### *Cell treatment*

Lithium Chloride (LiCl) was purchased from Fluka (Chemika, Switzerland) and 500 mM stock was prepared in sterile dH<sub>2</sub>O and stored at -20°C. Sodium Chloride was purchased from Sigma-Aldrich (USA) and the stock was prepared at 500 mM NaCl in sterile dH<sub>2</sub>O and stored at -20°C. The experiments were executed by seeding the Raw 264.7 cells at various densities depending on the experimental setting and then treated with these lithium concentrations (LiCl 2.5, 1.25 and 0.625 mM) as well as NaCl (2.5 mM).

### *Determination of the cytokines expression pattern using ELISA*

In an attempt to measure the production of the cytokines and chemokines, Raw 264.7 cell were seeded at 2.4 X10<sup>6</sup> cells/ml in the T25 flasks and after 3 hrs cell adaptation, the cells were inoculated with 10<sup>4.8</sup> viral titre/mL for 1 hr. After 1 hr of inoculation the supernatant was removed and the cells were treated with lithium concentrations (as outlined in cell treatment section) and LPS (5 mg/ml) for 24 hrs while the supernatant

was collected in 3, 6, 12 and 24 hrs time intervals. The collected supernatant was frozen at  $-20^{\circ}\text{C}$  for later use. Enzyme-linked immunosorbent assay (ELISA) was executed according to the manufacturer's protocol (Preprotech, USA). The capture antibody (for IL-10, IL-6, TNF- $\alpha$ , IFN- $\gamma$  and RANTES) was diluted with PBS to 0.5  $\mu\text{g}/\text{ml}$  and 100 $\mu\text{L}$  was added to each well in a 96 well plate and incubated at room temperature (RT) overnight. The unbound excess capture antibody was aspirated and plates were washed with 300 $\mu\text{L}$  wash buffer (0.05 % tween-20 in 1x PBS) per well using ELx 405 auto plate washer (Bio-TEK instruments-Inc).

The standard was serially diluted 2 fold and 100 $\mu\text{L}$  was added in triplicates followed by addition of samples for 2 hrs. The added samples were aspirated and washed 4 times with wash buffer. The detection antibody was diluted in diluent to 0.5 $\mu\text{g}/\text{mL}$  and 100  $\mu\text{L}$  was added in each well for 2 hrs at RT. This was then followed by aspiration of excess detection antibody and plates were washed 4 times with wash buffer. The 5.5 $\mu\text{L}$  avian peroxidase was then diluted 1: 2000 in 11 ml diluent, thereafter 100  $\mu\text{L}$  of this diluted avian peroxidase was added to each well and incubated for 30 min at RT. This solution was aspirated and wells were washed 4 x with wash buffer. After blotting of wells, 100  $\mu\text{L}$  of ABTS substrates solution was added to each well and the plates were incubated for colour development. Thereafter the colour was measured by reading the OD at 405 nm with ELx 802 universal microplate reader (Bio-TEK instruments-Inc)

#### *Determination of the production of reactive oxygen species (ROS)*

The 2',7'-Dichlorofluorescein diacetate ( $\text{H}_2\text{DCF-DA}$ ) is a cell-permeable reactive oxygen species (ROS) non-fluorescent probe. This molecule is deacetylated by cellular esterases and react with ROS to form a highly fluorescent 2',7'-dichlorofluorescein. The Raw 264.7 cells were seeded at  $4 \times 10^5$  cells/200 $\mu\text{L}$  in a 6 well plate for 3 hrs and inoculation with RVFV at  $1 \times 10^{4.8}$  viral titre/ml for 1 hr. This was followed by discarding excess virus and cell treatment for 24 hrs with lithium concentrations (as outlined in cell treatment) and LPS (5 mg/ml) followed. After 24 hrs of inoculation and lithium treatment, cells were stained with permeant  $\text{H}_2\text{DCF-DA}$  at RT for 30 min in the dark and fixed with 3.7% paraformaldehyde for an hour. The fluorescent images were captured at 480 and 535 nm (Ex/Em) with EVOS FL Colour imaging system (Life technologies, USA).

Moreover, the ROS production was measured quantitatively by seeding Raw 264.7 cells at  $5 \times 10^5$  cells/well in a 96 well plate for 3 hrs. This was followed by inoculation of cells with RVFV at  $1 \times 10^{3.8}$  viral titre/ 100 $\mu$ l for 1 hr. After 1 hrs of cell inoculation excess virus was removed and treatment of cells with lithium was executed as above for 12 and 24 hrs. After the 24 hrs incubation time H<sub>2</sub>DCF-DA was added for 30 min and then fluorescence intensity was measured at ex/em 480/535 nm using a Fluoroskan Ascent FL (Thermo Fisher Scientific, USA).

*Determination of the production of the reactive nitrogen species (RNS)*

The 5,6-Diaminofluorescein diacetate (DAF-2 Da) is a cell permeant NO indicator that is deacetylated by intracellular esterase to DAF-2 that react with NO to yield a highly fluorescent triazolofluorescein (DAF-2T). The Raw 264.7 cells were seeded at  $4 \times 10^5$  cells/well in a 6 well plate for 3 hrs and inoculation with RVFV at  $1 \times 10^{4.8}$  viral titer /ml for 1 hr. The excess viral inoculum was replaced with lithium treatment (as outlined in cell treatment) and LPS (5 mg/ml) for 24 hrs. After 24 hrs of inoculation, cells were stained with DAF-2 DA at RT for 30 min in the dark then cell were fixed with 3.7% paraformaldehyde for an hour.

There after the pictures were captured with EVOS FL Colour imaging system (Life technologies, USA) at 480 and 535 nm (Ex/Em). For quantitative measure of NO, Raw 264.7 cells were seeded at  $5 \times 10^5$  cells/well in a 96 well plate for 3 hrs and then inoculated with RVFV at  $1 \times 10^{3.8}$  viral titre/ 100 $\mu$ l for 1 hr. And then excess virus was removed and treatment of cells with lithium was executed as above for 12 and 24 hrs. After the incubation time, DAF-2 Da was added for 30 min and then fluorescence intensity was measured at ex/em 480/535 nm using a Fluoroskan Ascent FL (Thermo Fisher Scientific, USA).

### NF- $\kappa$ B translocation immunofluorescence assay

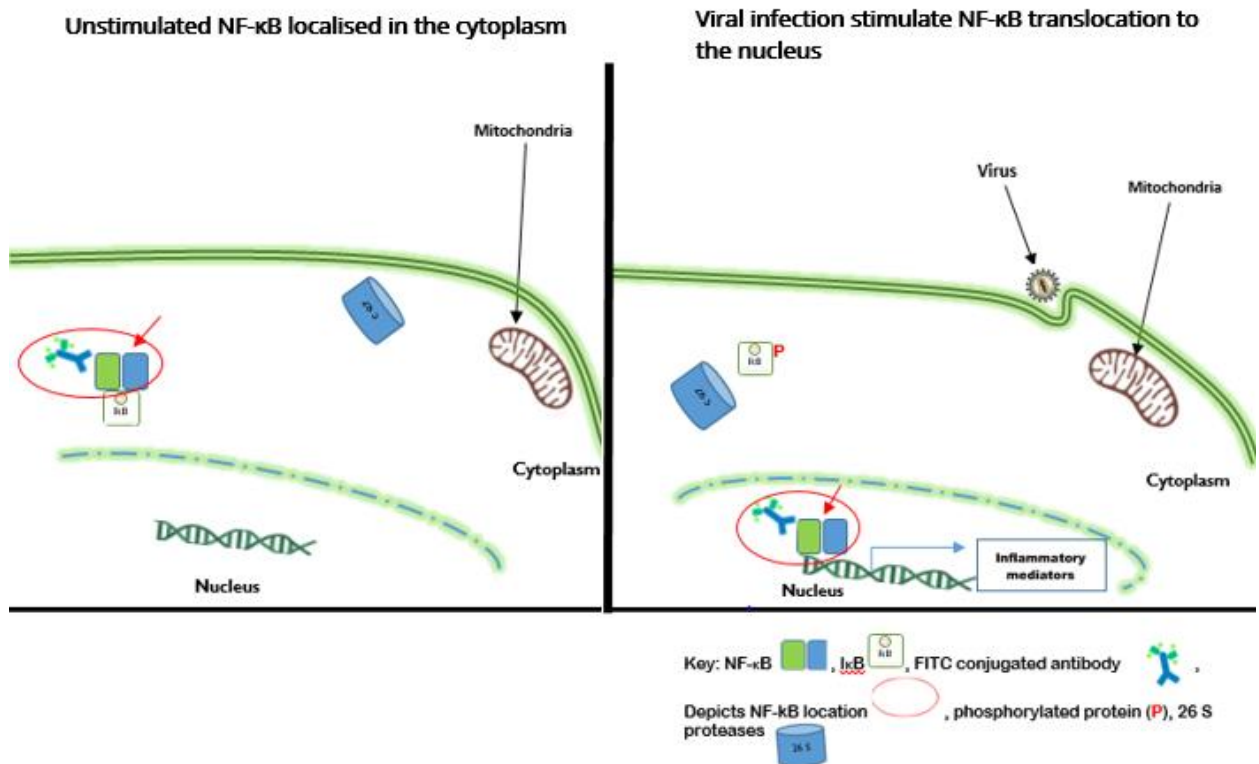


**Figure 3.1: Depiction of NF- $\kappa$ B location during viral activation and on a resting cells.** The NF- $\kappa$ B is targeted by a NF- $\kappa$ B specific antibody that is conjugated to a FITC (fluorescing green *Ex-Em* 495/519). The location of the NF- $\kappa$ B is then located by the green fluoresces on the cell in relation to the blue-nucleus labelling dye (DAPI).

Immunocytochemistry is the method to depict the molecular location of a protein in a cell with the use of specific fluorogenic antibodies. Raw 264.7 macrophage cells were cultured in 6 well plates on the slides at  $4 \times 10^5$  cells/well for 3hrs. This was followed by RVFV inoculation at  $1 \times 10^{4.8}$  titre/ml for 1 hr, and the excess virus was discarded. Cell treatment with lithium was executed as outlined in cell treatment and some wells were stimulated with LPS (5 mg/ml) for 24 hrs. The media was then aspirated after 24 hrs incubation and cells were fixated with 4% paraformaldehyde for 1 hr. Thereafter, cells were permeabilised with 0.1% Triton X-100, 1%BSA for 60 min and the nonspecific binding sites were blocked by adding 1% BSA for 1 hr, followed by 2 x wash with wash buffer. Cells were incubated for 60 min with rabbit anti-p65 antibody (1:500) (Santa Cruz, USA) followed by 3x wash with wash buffer. The cells were incubated with FITC-labelled goat anti-rabbit secondary anti-body for 60 min. After 5 min, the nuclear staining was done with DAPI, and then cells were mounted on slides

using 50% glycerol and analysed using the fluorescent inverted Nikon Ti-E microscope at 20x magnification.

#### *Examination of inflammatory protein expression using Western blotting assay*

In order to examine NF- $\kappa$ B related protein expression, the Raw 264.7 cells were seeded in T25 flasks for 3 hrs at a density of  $1 \times 10^6$  cell/ml and inoculation at  $1 \times 10^{4.8}$  titre/ml for 1 hr, and the excess virus was discarded. Cell treatment with lithium was executed as outlined in cell treatment section and stimulated with LPS (5 mg/ml) for 24 hrs. After 24 hrs treatment cells were washed once with 1x PBS, thereafter, cell lysis was accomplished with 500 $\mu$ L lysis buffer (10 mM Tris-HCl, pH 6.8, 1 % SDS, 100 mM sodium chloride, 1 mM EDTA, 1% NP 40, protease inhibitor), the cells were vortexed for 10 seconds and incubated on ice for 30 minutes. The supernatant was collected by centrifugation at 15 000 xg for 20 minutes at 4°C and then the protein concentration was determined using BCA protein assay at 562 nm. For SDS PAGE 50 $\mu$ g proteins were mixed with the sample buffer (1 mM Tris buffer pH 6.8, 20 % SDS, 20 % glycerol, 0.05 %  $\beta$ -mercaptoethanol, 0.002 % bromophenol blue) separated on 12 % SDS-PAGE and then transferred to a polyvinylidene fluoride (PVDF) membrane using a semi-dry blotting system (Bio-Rad).

The membranes were blocked with Tris buffered saline (TBS) [150 mM NaCl, 50 mM Tris, 0.1 % Tween, pH 7.5] containing 3 % fat-free dried milk. The membranes were washed with wash buffer [0.05 % TBS- Tween] and then incubated each time with 1:500 dilutions of anti- NF- $\kappa$ B-p65, I $\kappa$ B, HO-1, NOS-2 and  $\beta$ -actin primary antibodies for 1 hr at RT. After incubation, the membranes were washed 3 x with wash buffer and incubated with corresponding peroxidase-conjugated secondary antibodies at 1:10 000 dilutions for 1hr at RT. The membranes were washed with wash buffer and the immune-reactive proteins were detected using the super-signal west pico chemiluminescent substrate (Thermo Scientific, Rockford, USA). The protein bands were visualised and photographed using the ChemiDoc XRS+ (Bio-RAD, USA).

#### *Extraction of the cytoplasmic and nuclear proteins*

In order to extract both the cytosolic and nuclear NF- $\kappa$ B protein, the Raw 264.7 cells were seeded in T25 flasks for 3 hrs at a density of  $1 \times 10^6$  cell/ml. The cells were treated and inoculated as outlined above. Cells were then washed once with 1x PBS and then harvested. For assessment of cytoplasmic proteins, buffer A composed of (10 mM HEPES, 10 mM KCl, 1 mM MgCl<sub>2</sub>, 5% glycerol, 0.5 mM EDTA, 0.1 mM EGTA,



1X protease inhibitor solution, 2 mM PMSF and 0.5 mM DTT) was added and the cell pellets were incubated on ice for 15 min with an addition of 0.5 % NP-40. This was followed by vortexing for 10 sec and centrifugation at 12,000 xg for 1 min. For nuclear NF- $\kappa$ B protein extraction the centrifugation pellet was exposed to 500  $\mu$ l high salt buffer B (20 mM HEPES, 1% NP-40, 400 mM NaCl, 10 mM KCl, 1 mM MgCl<sub>2</sub>, 20% glycerol, 0.5 mM EDTA, 0.1 mM EGTA, 1x protease inhibitor solution, 2 mM PMSF and 0.5 mM DTT) for 1 hr on ice. The mixture was followed by vortexing for 15 sec and centrifuged at 12,000 xg for 1 min.

### *Statistical analyses*

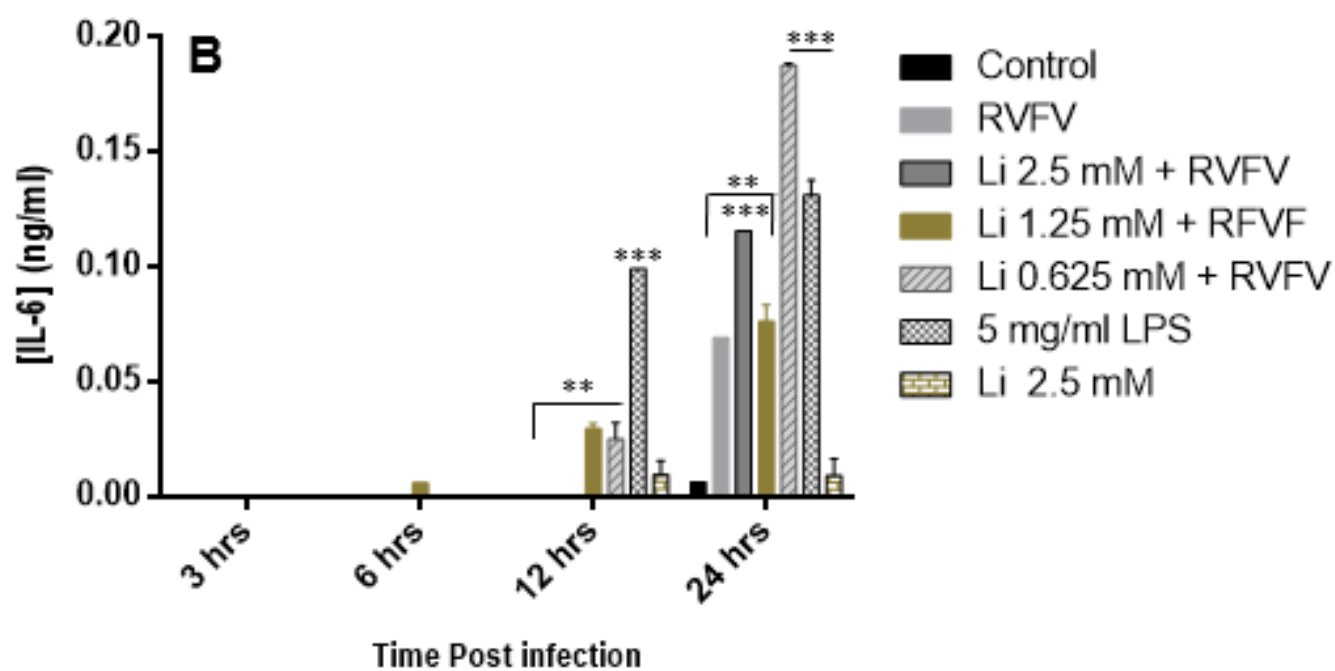
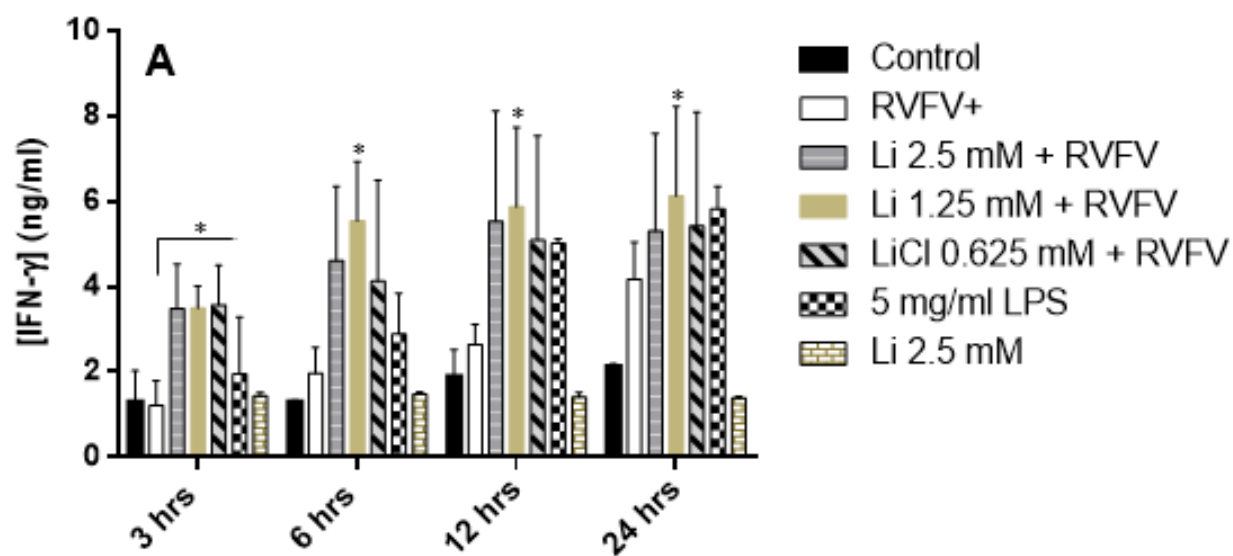
All assays were performed 3 times in duplicates or triplicates and the error bars represent the degree of variance. Graph-Pad Prism 6 software was used to plot the graphs and statistical analysis was performed using GraphPad InStat 3 software. Duncan's multiple comparison t-test was used to determine significant differences between the means of treated and untreated groups. Differences were considered significant at \*  $p \leq 0.05$ ; \*\*  $p \leq 0.01$ , \*\*\*  $p \leq 0.001$ .

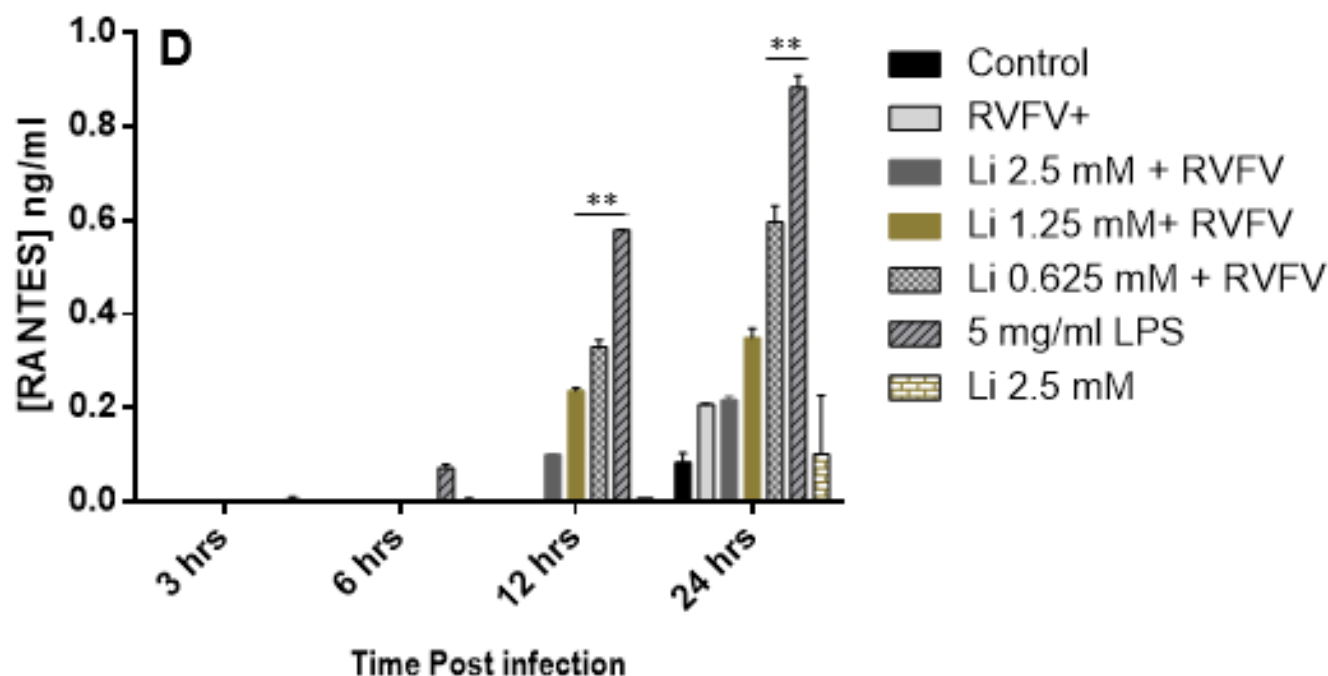
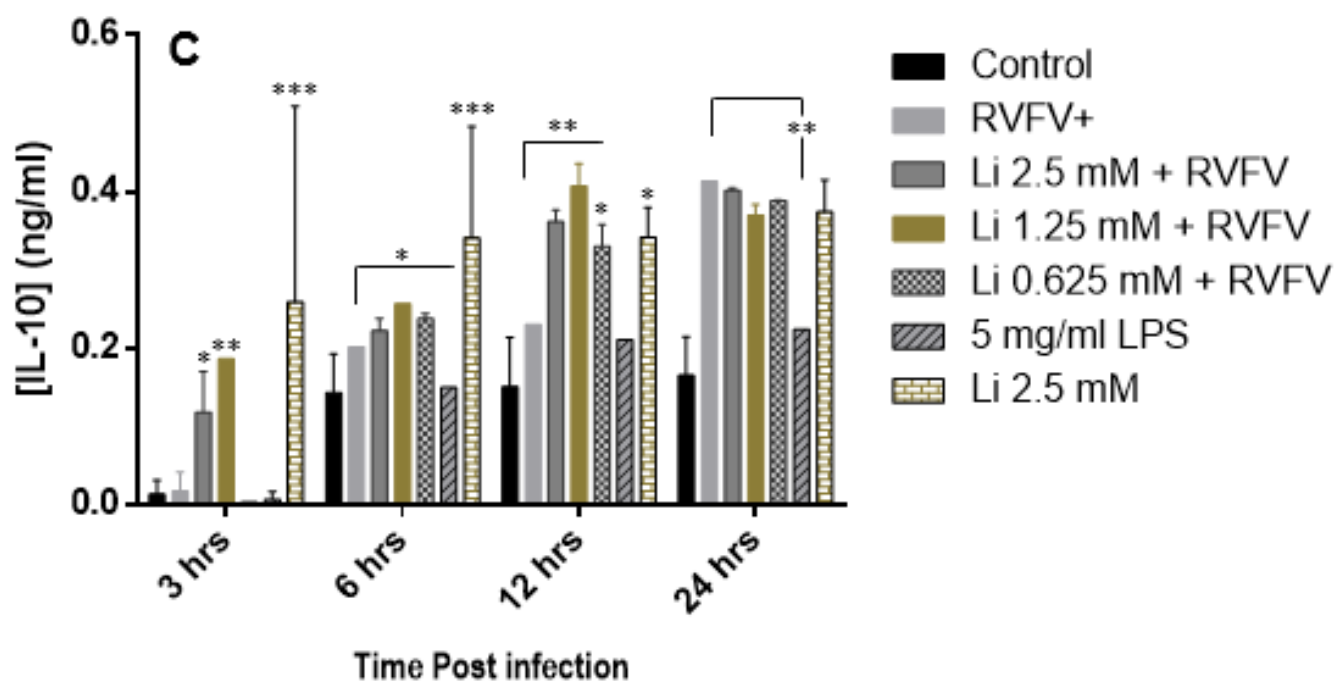
## **Results**

### *Influence of lithium on the production of the inflammatory pro and anti-inflammatory Cytokines; IFN- $\gamma$ , IL-6, IL-10, RANTES and TNF- $\alpha$ .*

This study examined the effects of lithium on cytokine and chemokines production in Raw 264.7 cells after RVFV inoculation. After treatment with lithium, the levels of TNF- $\alpha$ , IL-6, IL-10, IFN- $\gamma$  and RANTES were measured from supernatants of Raw 264.7 cells infected with RVFV. Results showed that lithium modulated production of several of these cytokines. Lithium stimulate increase in IFN- $\gamma$  production in the RVFV infected Raw 264.7 macrophage model system. Increase in lithium concentration was accompanied by a significant increase in IFN- $\gamma$  production in RVFV-infected cells compared to the lithium-free RVFV-infected control cells (Fig 3.2A). The increase in IFN- $\gamma$  production also increased proportionally with an increase in incubation time, however, uninfected lithium-treated cells did not stimulate IFN- $\gamma$  production. IFN- $\gamma$  production in lithium-treated RVFV-infected cells was even higher than LPS stimulated cells *albeit* reaching comparable levels at 24 hrs post inoculation (pi). Lithium at 1.25 mM induced the highest amount of IFN- $\gamma$  production compared to other concentrations in all the time points. Another prominent inflammatory cytokine, IL-6, was shown to be produced after 12 hrs pi (Fig 3.2 B). After 12 hrs pi, 0.625 mM lithium produced IL-6 almost 3-fold compared to lithium-free RVFV-infected cells and 1.5-fold compared to LPS stimulated cells.

Lithium was shown to stimulate IL-10 (anti-inflammatory cytokine) production in both RVFV-infected and uninfected cells (Fig 3.2 C), from 3 hrs pi, the production of IL-10 increased with incubation time. The IL-10 was production more by 1.25 mM LiCl compared to other concentrations and control RVFV showed improvement as from 6 hrs pi and reached production peak after 24 hrs pi (Fig 3.2 C). The chemokine (RANTES/CCL-5) showed similar increment profiles to those observed in IL-6. Lithium induced CCL-5 production 12 hrs pi, the low concentrations of lithium stimulated more of CCL-5 (Fig 3.2 D). Furthermore, lithium concentrations were shown to increase the production of the TNF- $\alpha$  compared to that of lithium-free RVFV-infected control cells as from 6 hrs pi (Fig 3.2 E). The increase in TNF- $\alpha$  production was also shown to be time-dependent. The level of TNF- $\alpha$  after treatment with lithium was shown to be above that of 5 mg/ml LPS positive control.





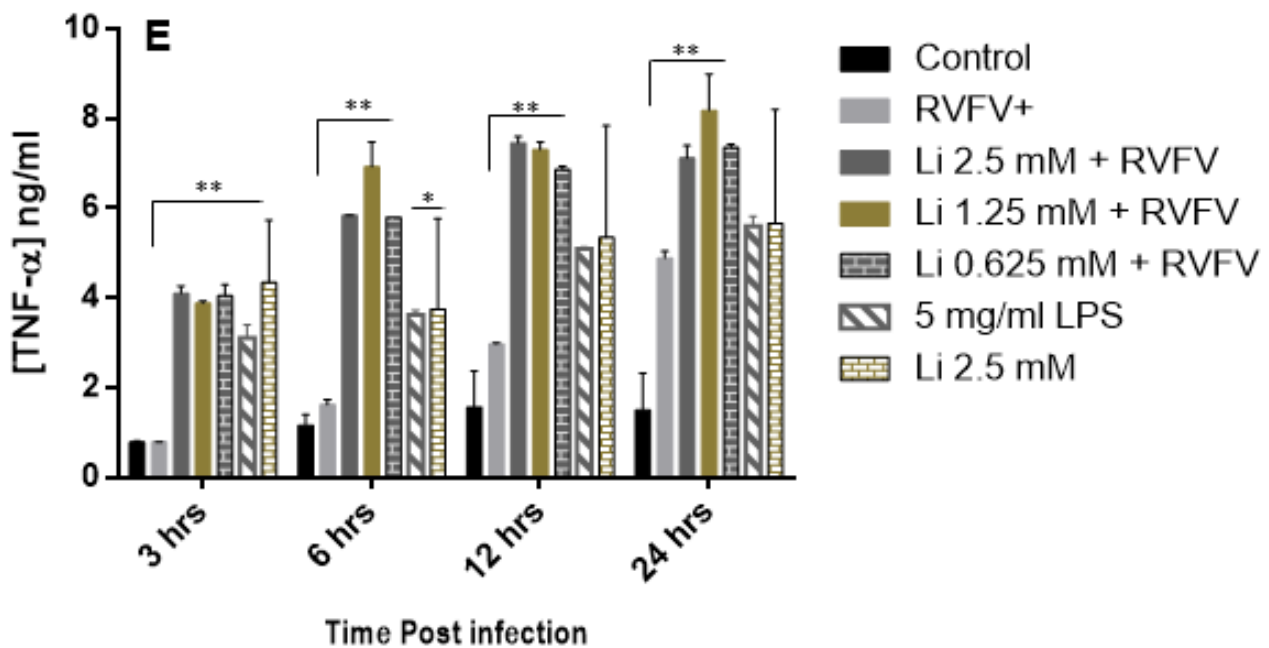
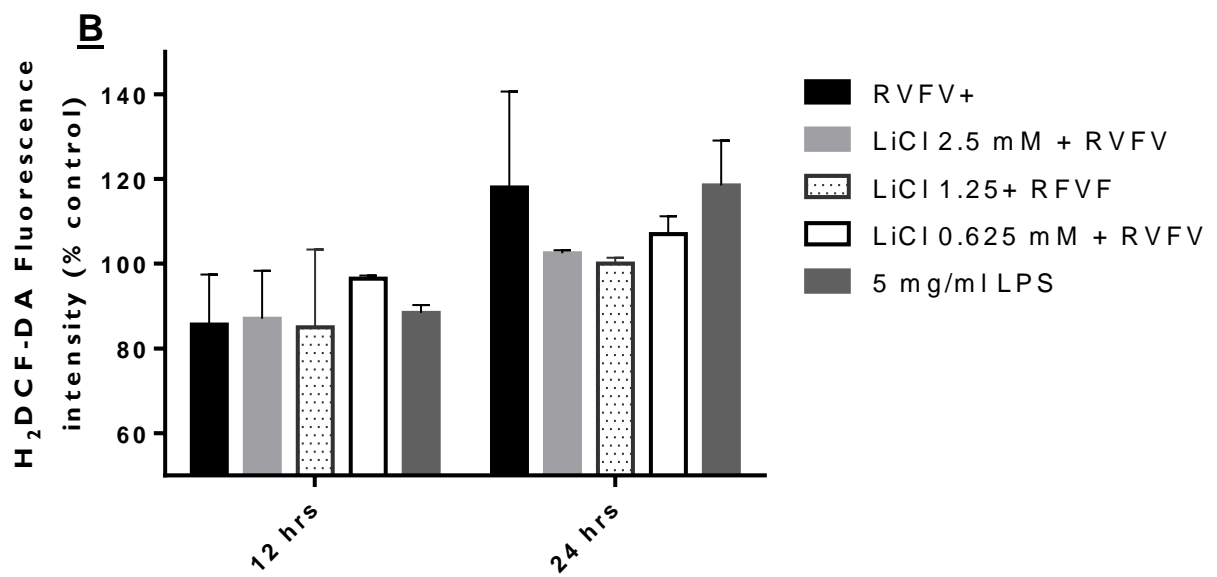
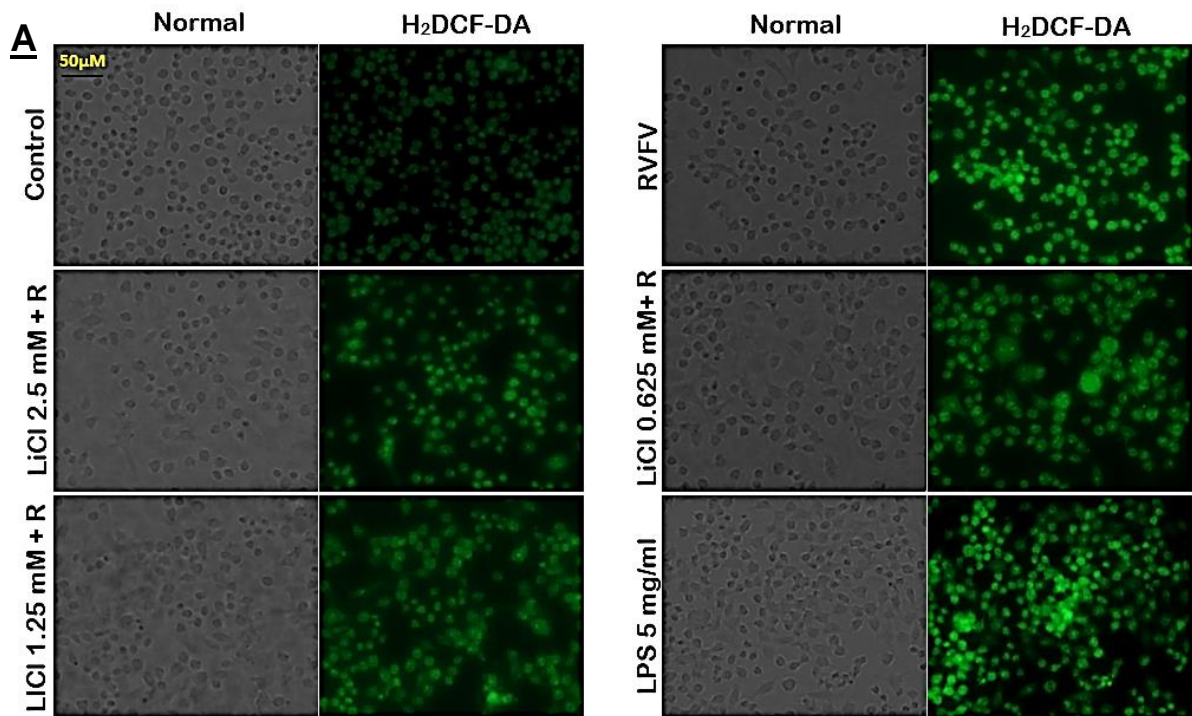


**Figure 3.2: Determination of the effects lithium on IFN- $\gamma$ , IL-6, IL-10, RANTES and TNF- $\alpha$  production after inoculation with the RVFV.** In order to measure effects of lithium on IFN- $\gamma$  (A), IL-6 (B), IL-10 (C), RANTES (D) and TNF- $\alpha$  (E) production, Raw 264.7 cells were seeded at the  $2.4 \times 10^6$  cells per T25 flask for 3 hrs inoculated with  $1 \times 10^{4.8}$  viral titre/ml for an hour. The excess virus was washed and the cells were treated with various concentration of lithium and then the supernatant was collected in 3, 6, 12 and 24 hrs time intervals. The Sandwich ELISA (PeproTech, USA) was executed to measure the amount of these cytokines from various time points. The data points represent the mean + standard deviation (error bar). The plot was developed with Graph-Pad Prism-6 software and GraphPad InStat-3 was used to establish the statistical analysis.

*Effects of lithium on production of reactive oxygen and nitrogen species after RVFV inoculation.*

Reactive oxygen species (ROS) are generated as metabolic by-products during mitochondrial respiration and excessively produced during inflammation (Reuter *et al.*, 2010). In this study, the two fluorescent probes, 2',7'-dichlorofluorescein diacetate (H<sub>2</sub>DCF-DA) and 4,5-diamino-fluorescein diacetate (DAF-2 DA), were used to determine the level of ROS and RNS production in RVFV-infected cells. Results displayed in Figure 3.3 A and 3.4 A represent the qualitative levels of ROS and RNS production in Raw 264.7 cells after treatment with lithium and infection with RVFV. Lithium concentrations are shown to downregulate the production of reactive molecules as the green fluorescence intensity is reduced in lithium-treated cells. Quantitative measurement of fluorescence intensity (Fig 3.3 B and 3.4 B) show that lithium lowered the production of ROS and RNS in a concentration-dependent manner. Highest inhibition of RNS production was observed in cells treated with lithium at 2.5 mM. These findings also showed that the production of ROS/RNS molecules only reached their highest production levels at 24 h pi. Moreover, lithium concentrations are shown to upregulate antioxidant enzyme Heme oxygenase-1 (HO-1) (Fig 3.3 C). Lithium is shown to induce HO-1 expression in a concentration dependent manner.

The determination of RNS production using DAF-2 showed that lithium inhibited RNS production in RVFV-infected Raw 264.7 cells. Treatment of cells with lithium notably reduced DAF-2 fluorescence intensity. These observations were accompanied by elevation of nitric oxide synthase-2 (NOS-2) expression as depicted in figure 3.4 C. The higher expression levels of the NOS-2 were elevated in control RVFV and LPS stimulated cells. Expression of NOS-2 was shown to be lowered by lithium in a concentration-dependent manner. NOS-2 is an enzyme that stimulates the production of the nitric oxide.



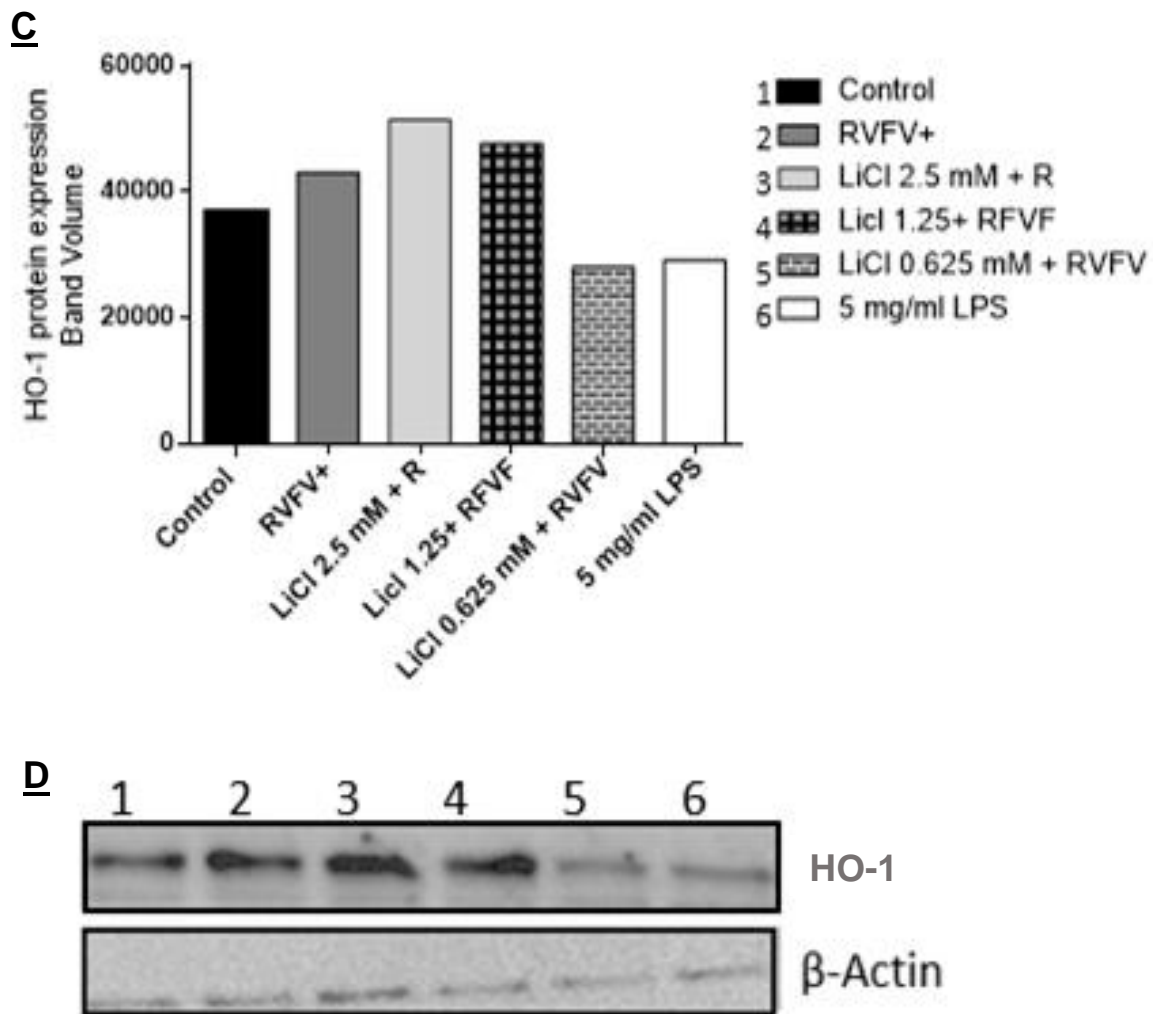
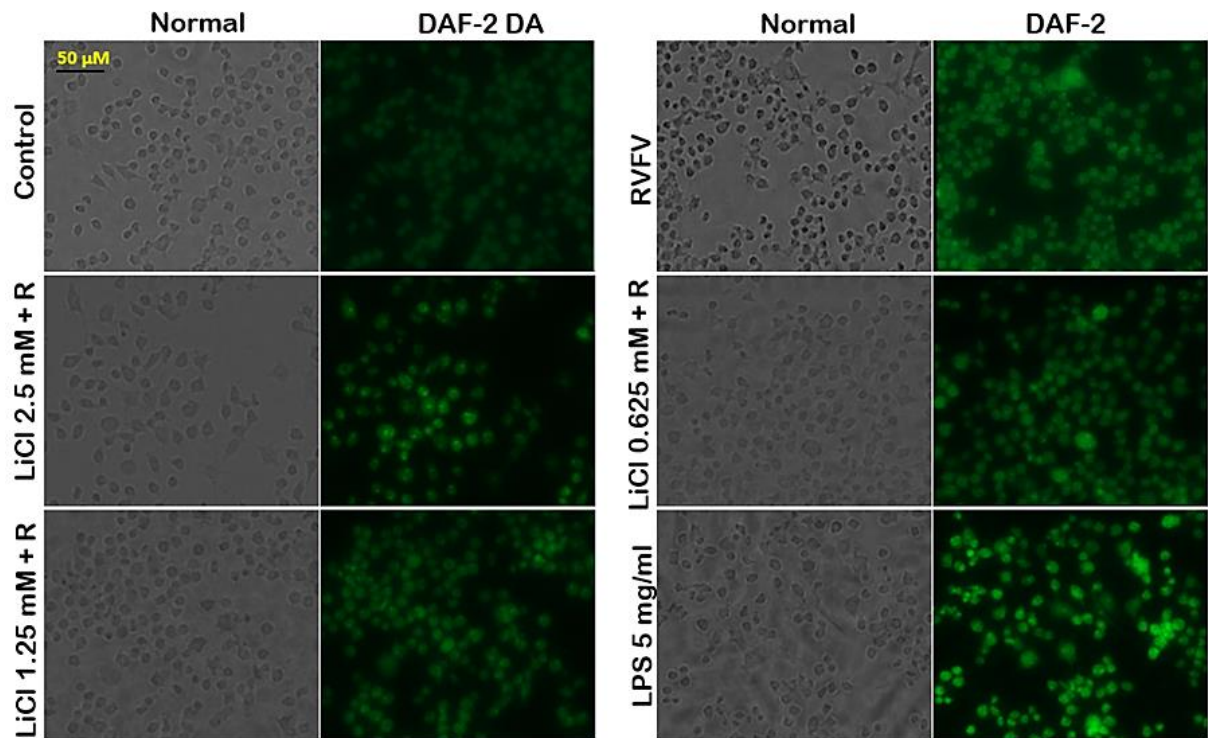


**Figure 3.3: Determination of the effects of lithium on oxidative burst after Raw 264.7 cell are challenged with RVFV and expression of levels of the antioxidant enzyme.** (A) Cells were seeded at  $4 \times 10^5$  cells/well in a 6-well plate for 3 hrs and then inoculated with  $1 \times 10^{4.8}$  viral titre/mL for an hour, the excess virus was substituted with fresh media and various lithium concentrations as well as 5 mg/ml LPS for 24 hrs. After 24 hrs of inoculation, cells were stained with  $H_2DCF$ -DA at RT for 30 min in the dark and then cell fixed with 3.7% paraformaldehyde for an hour. The pictures were captured with EVOS FL Colour imaging system (Life Technologies, USA) Ex: 495nm; Em: 515nm. (B) Cells were seeded at  $1 \times 10^6$  cells/well in a 96 well plate for 3 hrs and then inoculated with RVFV at  $10^{3.8}$  viral titer/100ul for an hr. The excess virus was then substituted with fresh media and lithium concentrations as well as 5 mg/ml LPS, this was incubated for 12 and 24 hrs. After the incubation hours the cells were stained with  $H_2DCF$ -DA for 30 min in the dark, and then the fluorescence intensity was measured with Fluoroskan Ascent FL (Thermo Fisher Scientific, USA) at ex (485 nm)-em (538 nm). The graphs were developed with Graph Pad Prism-6 software and GraphPad InStat-3 was used to establish the statistical analysis. (C) In order to determine the expression of HO-1 protein, Raw 264.7 cell were seeded at  $1 \times 10^6$  cell/ml for 3 and then inoculated with  $10^{4.8}$  viral titre/mL for 1 hr, and then the excess virus was substituted with a fresh media and lithium concentrations for 12 hrs. This was then followed by isolation of

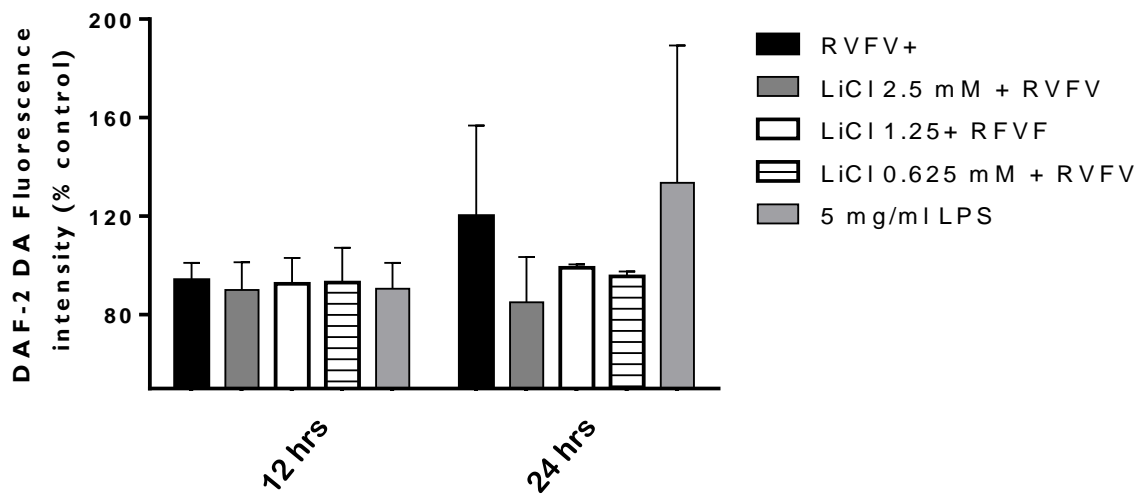


proteins and then western blotting assay(D). The pictures were captured with ChemiDoc XRS+ (Bio-RAD, USA).

**A**



**B**



C

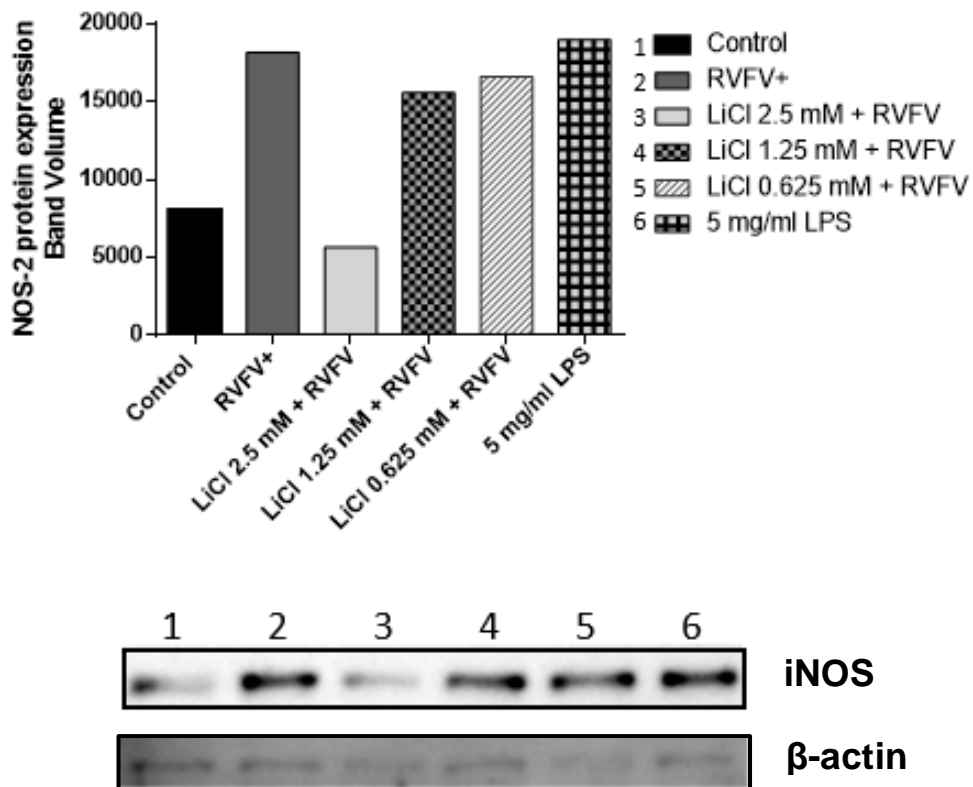


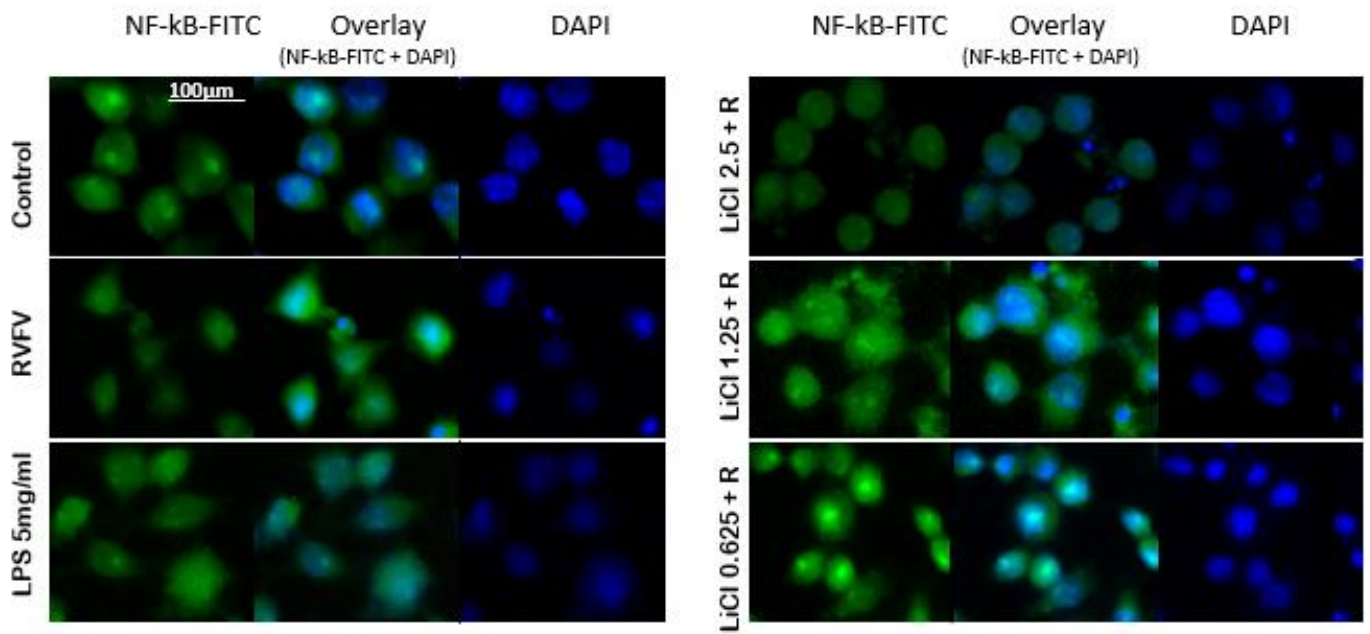
**Figure 3.4: Determination of the effects of lithium on the production of inflammatory reactive nitrogen species 24 hrs post RVFV inoculation and expression levels of the NOS enzyme.** (A) Cells were seeded at  $4 \times 10^5$  cells/well in a 6 well plate for 3 hrs and then inoculated with  $1 \times 10^{4.8}$  viral titre/mL for an hour, the excess virus was substituted with fresh media and various lithium concentrations as well as 5 mg/ml LPS for 24 hrs. After 24 hrs of inoculation, cells were staining with DAF-2 DA at RT for 30 min in the dark then cell were fixed with 3.7% paraformaldehyde for an hour. The pictures were captured with EVOS FL Colour imaging system (Life technologies, USA). (B) Cells were seeded at  $1 \times 10^6$  cells/well for 3 hrs and then inoculated with RVFV at  $10^{3.8}$  viral titter/100ul for an hr. The excess virus was then substituted with fresh media and lithium concentrations as well as 5 mg/ml LPS for 12 and 24 hrs. After the incubation hours the cells were stained with DAF-2 DA for 30 min in the dark, and then the fluorescence was measured with Fluoroskan Ascent FL (Thermo Fisher Scientific, USA) at ex (485 nm)-em (538 nm). The plots were developed with Graph Pad Prism-6 software and GraphPad InStat-3 was used to establish the statistical analysis. (C) In order to determine the expression of NOS-2 protein, Raw 264.7 cell were seeded at  $1 \times 10^6$  cell/ml for 3 hrs and then inoculated with  $10^{4.8}$  viral titre/mL for 1 hr, and then the excess virus was substituted with a fresh media and lithium concentrations for 12 hrs. This was then followed by isolation of proteins and then western blotting assay. The pictures were captured with ChemiDoc XRS+ (Bio-RAD, USA).

*Effects of lithium on nuclear translocation and expression of the NF- $\kappa$ B signalling pathway molecules*

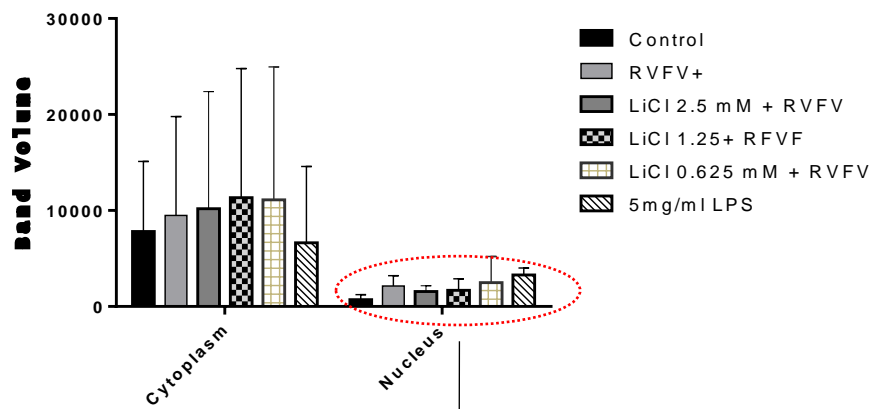
The molecular location of a transcription factor NF- $\kappa$ B is used as measure of inflammatory response. NF- $\kappa$ B binds to the kappa responsive element and induce expression of inflammatory mediators. Thus, the cellular location of the NF- $\kappa$ B molecule is an essential phenomenon in inflammatory studies. The molecular location of the NF- $\kappa$ B was examined using immunocytochemistry depicted in figure 3.5 A. Figure 3.5 A shows that NF- $\kappa$ B is located in both the nucleus and cytoplasm in lithium-treated cells, since green fluorescence is on both inside and outside of the nucleus. However, control untreated cells showed less of the green fluorescence in the nucleus and the image overlays showed an intense blue nuclear fluorescence, displaying that the two stains are not in the same location.

The positive control LPS (5 mg/ml) treatment shows the light blue nuclear fluorescence since all the green (NF- $\kappa$ B staining) and the blue (nucleus staining) are all in the same location in the nucleus. The control RVFV show similar patterns as control LPS, indicative of NF- $\kappa$ B nuclear translocation. On the other hand, figure 3.5 B and C shows that lithium inhibits translocation of NF- $\kappa$ B with LiCl 2.5 mM showing the most inhibitory effects, although in this assay the inhibition margin is narrow. The I $\kappa$ B- $\alpha$  expression 12 hrs pi (Fig 3.5 D) showed to be elevated in lithium-treated cells in a dose-dependent manner. I $\kappa$ B- $\alpha$  is the inhibitory molecule that keeps NF- $\kappa$ B in the cytoplasm and is known to regulate the activity of this transcription factor (Garcia *et al.*, 2009).

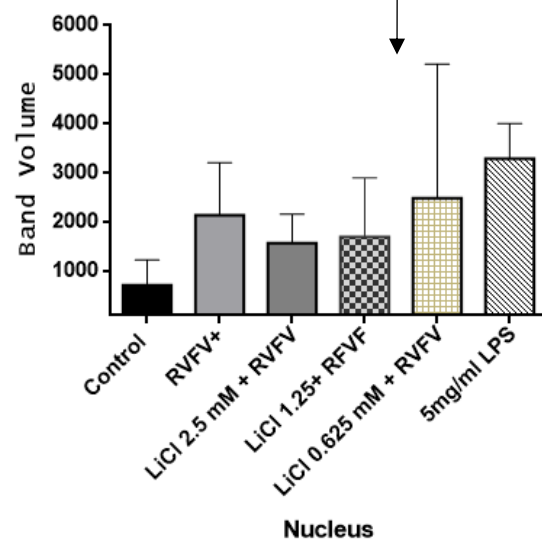
**A**



**B**



**C**



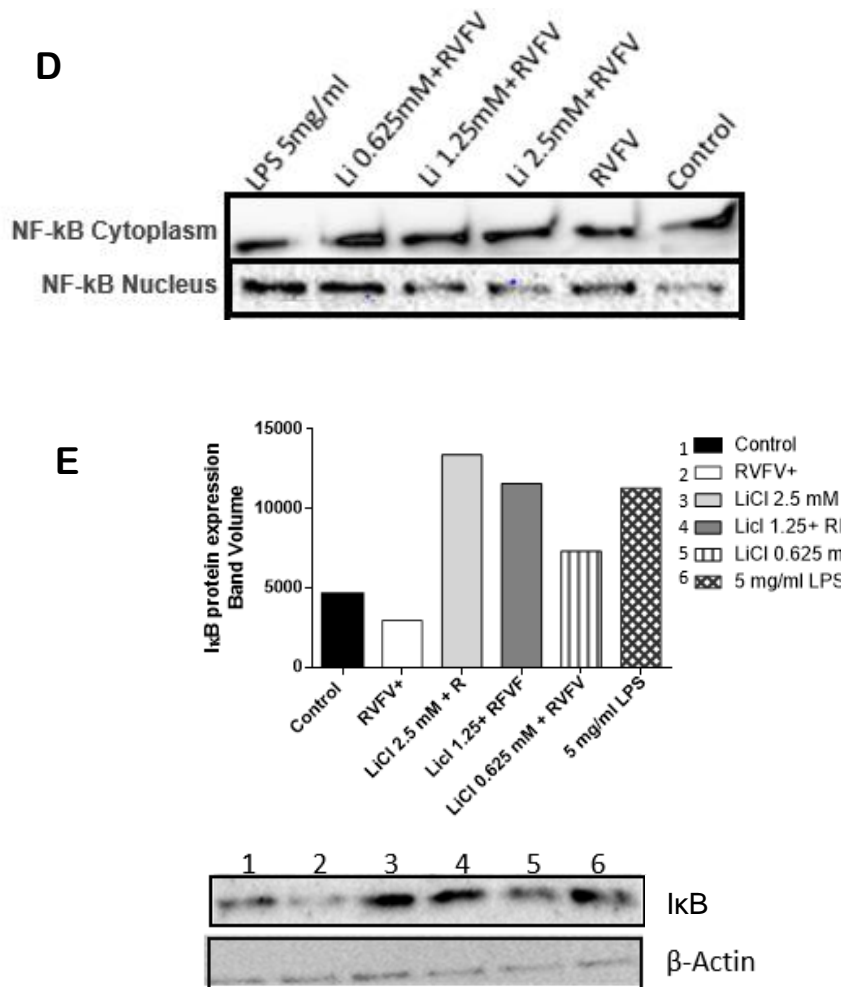


**Figure 3.5: Effects of lithium on translocation of NF- $\kappa$ B between the cytoplasm and nucleus, and expression levels of I $\kappa$ B.** (A) The cells were seeded at  $4 \times 10^5$  cells/well in a 6 well plate for 3 hrs and then inoculated with  $1 \times 10^{4.8}$  viral titre/ml for an hour, the excess virus was substituted with fresh media and various lithium concentrations as well as 5 mg/ml LPS for 24 hrs. After 24 hrs of inoculation, cells were fixed with 4% paraformaldehyde for an hour, and then permeabilised with (0.1% Triton X-100, 1%BSA) for 30 min. Permeabilised cells were incubated for 60 min with rabbit anti-p65 antibody (1:500). The primary antibody was followed by FITC-labelled goat anti-rabbit secondary Ab incubation for 60 min. Thereafter, nuclear staining with 25 $\mu$ g/ml DAPI was executed for 5min in the dark. Cells were mounted on slides using 50 % glycerol and pictures were captured with fluorescent inverted Nikon Ti-E microscope at 20x magnification. (B&C) In order to determine the translocation quantity of the NF- $\kappa$ B, Raw 264.7 cell were seeded at  $1 \times 10^6$  cell/ml for 3 hrs in the T25 cell culture flasks and then inoculated with  $1 \times 10^{4.8}$  viral titre/mL for an hour, the excess virus was substituted with fresh media and various lithium concentrations as well as 5 mg/ml LPS for 24 hrs. This was then followed by isolation of cytoplasmic proteins as well the nucleus proteins and then western blotting assay followed. The pictures were captured with ChemiDoc XRS+ (Bio-RAD, USA). The ChemiDoc XRS+ image lab 5.2.1 software was used to measure band volume (Bio-RAD, USA). The plot was developed with Graph pad prism-6 software and instat-3 was used to establish the statistical analysis. (C) Rescaling of plot details expression in the nucleus. (D) In order to determine the expression of I $\kappa$ B- $\alpha$  protein, Raw 264.7 cell were seeded at  $1 \times 10^6$  cell/ml for 3 hrs and then inoculated with  $10^{4.8}$  viral titre/mL for 1 hr, and then the excess virus was substituted with a fresh media and lithium concentrations for 12 hrs. This was then followed by isolation of proteins and then western blotting assay(E). The



ChemiDoc XRS+ image lab 5.2.1 software was used to capture pictures and measure band volume (Bio-RAD, USA).

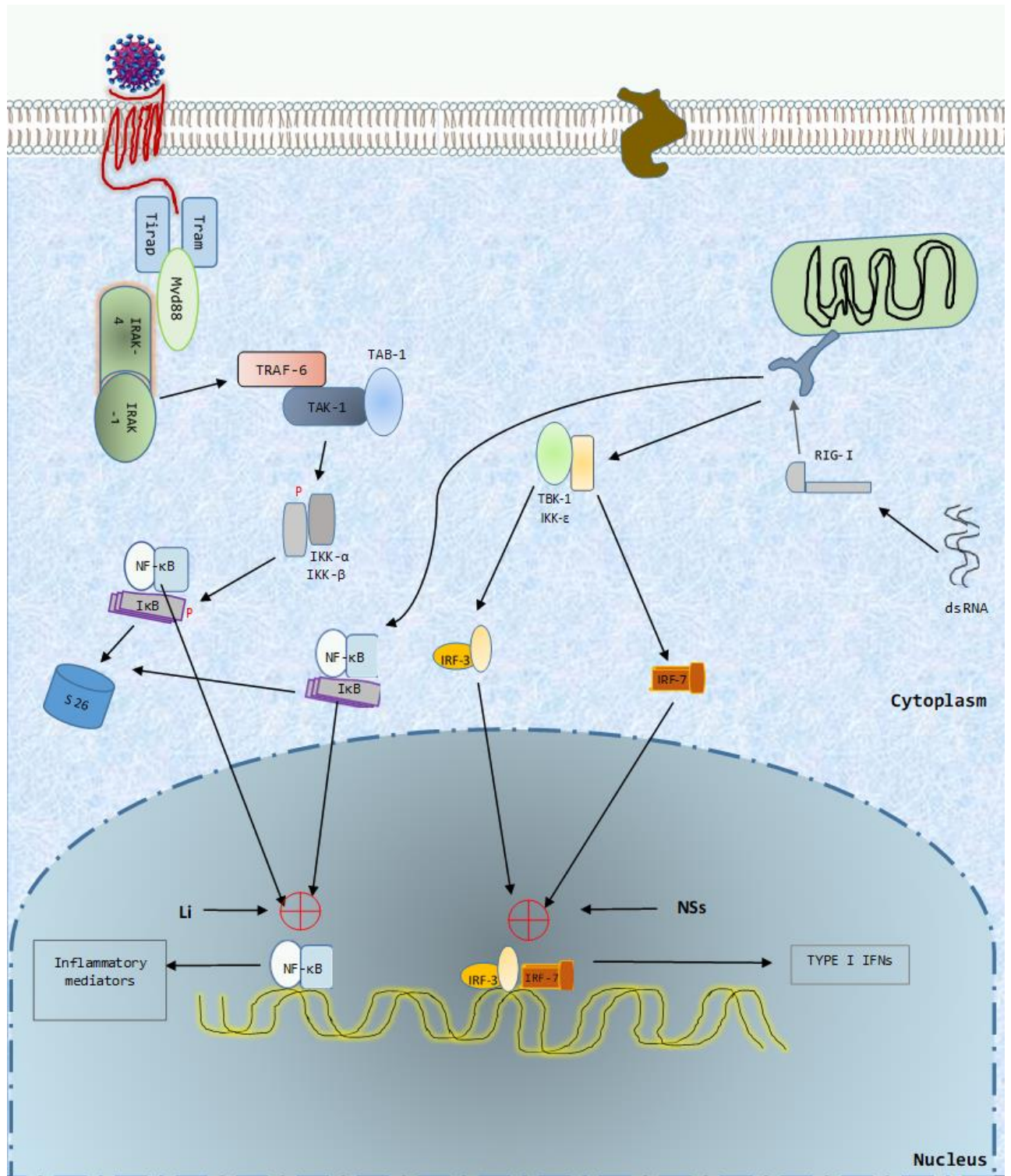


**Figure 3.6: Determination of the canonical NF- $\kappa$ B and IRF3/7 signalling pathways and the effects of lithium post RVFV infection.** TLR 2 and 4 are stimulated by the viral glycoproteins that in turn recruit adapter molecule Myd88 via tirap. The adapter molecules recruit Irak4 which phosphorylate recruit irak-1 which then associate with Traf-6. Traf-6 recruit Tak1 and Tab2. Tak1 phosphorylate IKK- $\beta$ , which then phosphorylate I $\kappa$ B which is then tagged for ubiquitination and then degradation by cytoplasmic proteases. This then allows translocation of NF- $\kappa$ B to the nucleus and inflammatory genes expression. The RIG-1 is known to be stimulated by dsRNA from replicating viral genome, which is said to be hidden from the TLR-3. This cytoplasmic receptor is shown to be essential for viral IFN expression. The RIG-1 is shown to associate with IPS-1 with its N-terminal card domain. The IPS-1 and RIG-1 association activate TBK1 and IKK- $\epsilon$  which phosphorylate IRF-3 and 7. The NSs is suggested to interfere with the IFN signalling at the transcription factor level since there is an expression of other inflammatory mediators except for IFNs. Since, the NSs inhibit the interferon production via IRF inhibition other transcription factors such NF- $\kappa$ B continue to produce inflammatory mediators, hence, elevated production of other inflammatory mediators except the IFN. This diagram suggests that NF- $\kappa$ B inhibition as a result of upregulated I $\kappa$ B could be the, mechanism in which lithium restore dysregulated inflammation after RVFV infection leading to haemorrhagic fever pathogenesis observed during this viral infection.

## **Discussion**

Most viruses have developed mechanisms to evade the immune system which favours viral replication and increase viral progeny. RVFV is not an exception to this type of virus-induced immune invasion mechanism. RVFV is known to inhibit the innate immune system, particularly the type I IFN cytokine production as its mechanism of invasion (Nfon *et al.*, 2012). Other studies (Caroline *et al.*, 2016; Jansen van Vuren *et al.*, 2015) outlined prolonged immune response as the primary detrimental factor in patients who suffer clinical symptoms of this viral infection.

The innate immune response plays a central role in the immune system as the first line of defense against foreign and infectious agents. Innate immunity, although non-specific, can orchestrate the humoral immune system through antigen presentation to the CD<sup>4</sup> T-cells (Xiao, 2017). It facilitates the first line of defense through inflammation; an ontogenetically old defense mechanism regulated by cytokines, products of the plasma enzyme systems, lipid mediators released from different cells, and vasoactive mediators released from mast cells, basophils, platelets and macrophages (Ross *et al.*, 2002). Macrophages are antigen presenter cells (APC) that produce cytokines as inflammatory mediators, which recruit other immune cells to the inflamed site and link the innate and adaptive immune response (McElroy and Nichol, 2012).

Despite the essential role played by inflammation, under-controlled inflammation leads to tissue damage and various adverse conditions that include neurodegeneration disorders, diabetes, cancer and endothelial leakage (Koriyama *et al.*, 2013; Jope *et al.*, 2007; Wang *et al.*, 2004). Viruses such as RVFV target macrophages to invade the innate immune system and use them as a vehicle to target tissues such as brain and liver (McElroy and Nichol, 2012). This virus is known to inhibit the production of the IFNs as targeted by the NSs. This is thought to be the mechanism in which RVFV circumvent the immune system in favour of viral replication (Nfon *et al.*, 2012). In addition to inhibited IFNs, NSs is shown to induce direct degradation and inhibition of the PKR involved in the translational arrest of both cellular and viral mRNA (Habjan *et al.*, 2009).

Weakened inflammatory responses by RVFV infection has been suggested to contribute to RVFV pathogenesis and fatality (Nfon *et al.*, 2012). Contrary to this hypothesis, a recent body of evidence (Caroline *et al.*, 2016; Jansen van Vuren *et al.*,



2015; Gray *et al.*, 2012) suggests that deregulation and prolonged inflammation correlate with viral pathogenesis and fatality. The combination of this contradicting inflammatory evidence and the IFNs inhibitory role of the NSs led to the hypothesis that unbalanced and deregulated inflammation could be central to the RVFV pathogenesis and lethality. Our work examined lithium as a potential drug to restore regulatory patterns of inflammation and innate immune system. In this study, lithium with and without the viral stimulant has shown to stimulate the production of the primary pro-inflammatory cytokine, TNF- $\alpha$ , in Raw 264.7 cells as early as 3 hrs pi.

Analogous with these findings, Kleinerman *et al.*, 1989 observed elevated TNF- $\alpha$  production in LPS-stimulated macrophages treated with lithium as early as 10 min post-stimulation, with the plateau reached within 12 hrs post-stimulation. Other studies hypothesised that lithium induced the production of TNF- $\alpha$  in macrophages subsequently this stimulate the production of the granulocyte-macrophage CSF (GM-CSF) from the endothelial cells. These observations can be associated with observed lithium-induced leukocytosis and granulocytosis as a result of GM-CSF (Merendino *et al.*, 1994; Kleinerman *et al.*, 1989). The secondary pro-inflammatory cytokine, IL-6, and a chemokine, RANTES, were shown to be produced during the late hours of infection 12 and 24 hrs with 1.25 mM LiCl being the most effective (Fig 3.2 B and D). These findings coincide with observations by Maes *et al.*, 1999 which showed that lithium did not induce significant production of the IL-6 in both stimulated and unstimulated cells.

Recent work published work from our laboratory reported inhibitory properties of lithium at 10 mM on RANTES production 24 hrs post stimulation with lipopolysaccharide (LPS) suggested to be GSK-independent. This could suggest that the ability of lithium to modulate IL-6 and RANTES production is dose-dependent and that this cytokine production is NF- $\kappa$ B dependent, a signalling pathway shown to be inhibited by lithium (Makola *et al.*, 2020). *In vitro* studies by Jansen van Vuren showed a 10 times elevated production of IL-6 in fatal cases as compared to non-fatal patients. This observation suggests that elevated production of this cytokine could be favouring virus survival as opposed to host defense (Jansen van Vuren *et al.*, 2015). Interestingly, lithium was shown to delay the elevated production of IL-6 pro-inflammatory cytokine in RVFV-infected cells. Another study showed that lithium enhances the production of another secondary pro-inflammatory cytokine IL-8 in both

LPS and phytohemagglutinin (PHA) stimulated and unstimulated cells (Maes *et al.*, 1999).

This current work demonstrated significant up-regulation of IFN- $\gamma$  by lithium on RVFV stimulated cells as from 3 hrs post infection (Fig 3.2, A), however, lithium alone did not show any modulatory effects on this cytokine production. This work shows that lithium stimulates the production of some pro-inflammation cytokines which is the most important inflammatory phenomenon since Nfon *et al.*, 2012 linked the weakened inflammation with pathogenesis and lethality. A review by Nassar and Azab, supports the findings from this current study as they are in agreement with previous reports. However, a general view from a review by Nassar and Azab showed inhibitory role of lithium on various cytokines production rather than stimulation (Nassar and Azab, 2014). Nfon *et al.*, 2012 have linked elevated levels of IFN- $\gamma$  to the survival of infected goats in animal experimental models. The IFN- $\gamma$  is suggested to inhibit viral replication and stimulate the cytotoxic activity of the NK cells since lowered viremia has been observed in surviving infected goats (Nfon *et al.*, 2012).

Elevated IFN- $\gamma$  levels could be another mechanism used by lithium to lower viral replication. In addition to pro-inflammatory cytokines, lithium stimulated the production of anti-inflammatory cytokine, IL-10 (Fig 3.2 C), in both viral stimulate and virus-free lithium-treated cells. Similar findings have been reported in other studies (Maes *et al.* 1999; Rapaport and Manji, 2001). These studies showed that lithium stimulates the expression of IL-10 and IL-1R anti-inflammatory molecules. This is suggested to be a regulatory mechanism as a result of the overwhelming production of inflammatory mediators known to have deleterious outcomes. Lithium has been shown to stimulate both the pro and anti-inflammatory cytokines in the current and previous studies (Nassar and Azab, 2014; Maes *et al.*, 1999).

It is hypothesised that lithium could be restoring the balance in the production of inflammatory cytokines, as pro-inflammatory molecules are later balanced by regulatory cytokines to limit over production of pro-inflammatory molecules. Besides the inflammatory properties of lithium observed in this study, lithium has been used for decades as a preferred treatment option for bipolar disorders despite the sparse and limited understanding of its mechanism of action (Nassar and Azab, 2014). Nonetheless, under-regulated inflammation has been linked to pathological processes behind manic depression and bipolar disorders. Hence, studies suggest

that lithium could be restoring inflammatory deregulation as the mechanism underlying its anti-depressant property (Nassar and Azab, 2014; Maes *et al.*, 1999).

Lithium-treated RVFV-infected cells show lowered production of the reactive oxygen and nitrogen species. The lowered production of these reactive molecules has been depicted in figure 3.3 A and 3.4 A, a qualitative assay. Quantitative findings (Fig 3.3 B and 3.4 B) show the same trend as in the qualitative assay figure 3.3 A and 3.4 A. As represented in Figure 3.2 B and 3.3 B, there is adequate production of these reactive species at 24 hrs pi. Previous work has shown lithium at 10 mM to reduce ROS production while 5 mM shown to be effective in reducing NO production in LPS-stimulated Raw 264.7 cells (Makola *et al.*, 2020). More interestingly, in the current study, lithium downregulated the expression of NOS-2 enzyme (Fig 3.4 C), which correlate with lowered NO production. In addition to the inhibited NOS-2, lithium stimulates HO-1 expression, an antioxidant enzyme (Fig 3.3 C). This work aligns inflammation regulatory properties of lithium with activation of the NF- $\kappa$ B transcription factor.

Lithium-treated RVFV-infected cells showed the presence of the NF- $\kappa$ B in both the cytoplasm and the nucleus, suggesting the reversal/ inhibition of the transcription factor from translocating to the nucleus (Fig 3.5 A). Molecular translocation of NF- $\kappa$ B into the nucleus is observed to be lowered by lithium-treated cells in a concentration dependent manner (Fig 3.5 B & C). Previous study (Narayanan *et al.*, 2014) has shown that RVFV stimulate NF- $\kappa$ B nuclear translocation, culminating in production of inflammatory mediators and resulting in oxidative stress (Narayanan *et al.*, 2014). Oxidative stress is a condition emanating from excessive production of oxidants and free radicals, leading to imbalance between oxidants and antioxidants. Studies (Christen, 2000; Reuter *et al.*, 2010; Narayanan *et al.*, 2014) have shown that oxidative stress conditions elicit biomolecules deformation that lead to altered cell function and then cell demise.

Narayanan *et al.*, 2014 hypothesised that the RVFV prevalent liver disease emanates from oxidative stress that leads to hepatic cell demise (Narayanan *et al.*, 2014). Inflammatory deregulation and oxidative stress have been linked with several pathogenic outcomes. This study suggests that lithium could ameliorate detrimental outcomes emanating from this viral infection. Figure 3.5 D, show that lithium concentrations upregulate the inhibitory molecules, I $\kappa$ B- $\alpha$ . I $\kappa$ B- $\alpha$  inhibit the translocation of the NF- $\kappa$ B by masking its nuclear translocation domain (Garcia *et al.*,

2009). Our previous work showed that high lithium doses (10 mM) express the NF- $\kappa$ B inhibitors such as I $\kappa$ B- $\alpha$ , TRAF3, Tollip and NF- $\kappa$ B1/p50 to be lithium inhibition biomarkers (Makola *et al.*, 2020). What remains profound about lithium is that in as much as it was shown to promote expression of some pro-inflammatory cytokines, it stimulates anti-inflammatory cytokines in an attempt to avoid oxidative stress and nonspecific damage to host cell biomolecules.

Previous studies demonstrated that NSs selectively tempers with the type I IFN signalling while sparing the other signalling pathways that produces inflammation mediators such as ROS, NOS and Pro/ anti-inflammation cytokines/chemokines. On a signalling level this could mean that NSs inhibit nuclear translocation of IRF3 and 7 transcription factors since they are central to type I IFNs production, or perhaps targeting the transcription of ISGs, leading to silencing of antiviral molecules as depicted in figure 3.6 (Ghaemi-Bafghi and Haghparast, 2013). Since NSs selectively inhibit IFNs which are linked to IRFs transcription factors, it then implies that other inflammatory mediators linked to other transcription factors such as AP-1 and NF- $\kappa$ B will continually be produced leading to elevated inflammatory mediators and then oxidative stress. Thus, this work links the regulatory mechanism of lithium with inhibition of the NF- $\kappa$ B signalling pathway.

The NF- $\kappa$ B signalling pathway is suggested to be stimulated by the glycoproteins detected by TLR-4 or ssRNA detected by TLR-7 or dsRNA detected by the RIG-I. All these PRRs are linked to the NF- $\kappa$ B signalling pathway in as much as others stimulate IRF signalling as well (Fig 3.6). The *in vitro* and *ex vivo* studies have shown cytokine and chemokines production excluding type I IFN during RVFV infection (Nfon *et al.*, 2012; Jansen van Vuren *et al.*, 2015). Therefore, the activated NF- $\kappa$ B pathway continue producing these inflammatory mediators that are suggested to participate in the RVFV pathogenesis. Therefore, lithium restores the production of excessive inflammatory mediators as it has been observed to limit NF- $\kappa$ B translocation through upregulation of the I $\kappa$ B molecule.

## **Conclusion**

The NF- $\kappa$ B transcription factor is shown to be the targeted molecule behind the anti-inflammation properties displayed during RVFV infection. Results from this work show that lithium inhibits NF- $\kappa$ B-activity, which may be linked to the observed inhibited inflammatory mediators. Although additional work is required to outline the

link between lithium and NSs. The current findings suggest that lithium could be used as an anti-haemorrhagic fever agent, since RVFV-induced oxidative stress, a suggested critical factor that lead to server symptoms such as haemorrhagic fever is shown to be reversed by lithium treatment. This study predicts that the RVFV virulence factor NSs inhibits the production of the type I IFN at a transcription factor level (IRF), since, the production of other inflammatory mediators such as RNS, ROS, cytokines and chemokines are observed except type I IFN. Lithium may potentially act as remedial agents for RVFV-induced by modulating NF- $\kappa$ B nuclear translocation in macrophages.

## CHAPTER 4

**EFFECTS OF LITHIUM-TREATED AND RVFV INOCULATED RAW 264.7  
MACROPHAGE CELLS SUPERNATANT ON ENDOTHELIAL MONOLAYER  
INTEGRITY CO-INOCULATION**

---

**Abstract**

Haemorrhagic fever is characterised by altered endothelial integrity from damaged endothelial cells that results in septic shock and multiple organs failure leading to death. Rift Valley fever virus (RVFV) belongs to the *Phenuiviridae* family and is one of the viruses that elicit viral haemorrhagic fevers. The exact RVFV pathogenesis that leads to haemorrhagic fever is still poorly understood. Therefore, this study hypothesises that oxidative stress leads to endothelial leakage which culminates into haemorrhagic fever. The Huvec endothelial monolayer was used to represent the blood vessels integrity model and the xCelligence system together with the Transwell assay were used to measure endothelial integrity. Results from the xCelligence system showed that endothelial cells exposed to supernatants from RVFV-infected and lithium-treated Raw 264.7 cells displayed a cell integrity index of above 4.0 as compared to control cells. The transwell assay results showed that supernatants from lithium (1.25 and 2.5 mM)-treated RVFV-infected Raw 264.7 cells demonstrated protective properties compared to RVFV-inoculated Raw 264.7 cells not treated with lithium. An RT-PCR Profiler Array system was employed to examine expression of cell-to-cell junction-associated genes. Supernatants from lithium-treated cells upregulated expression of cytoplasmic molecules such as  $\alpha$  and  $\beta$ -catenins, talins, zyxins, as well as vinculins. These molecules are responsible for attaching integrins to the extracellular matrix (ECM) and to other endothelial cells. Moreover, lithium has been observed to express transmembrane molecules such as E-cadherin, P-cadherin, R-cadherin and N-cadherin. The expression of VE-cadherins was, however, observed to be lower compared to expression induced by supernatants from control RVFV-infected Raw 264.7 cells. The endothelial integrity observed in the permeability assays can be correlated with the expression of the molecules involved in keeping the cell to cell junction intact. Thus, this study links the anti-inflammatory properties of lithium with preservation of endothelial integrity.

Key words. Lithium, endothelial integrity, inflammation, RVFV

## **Introduction**

RVFV is the causative agent of human and veterinary RVF diseases. This viral infection can elicit a broader spectrum of symptoms that correlate with disease severity and fatality rates. Those symptoms range from mild flu-like symptoms to more severe clinical symptoms that include: retinal vasculitis, meningoencephalitis, fatal hepatitis, encephalitis and hemorrhagic fever (Bird and McElroy, 2016) with a fatality rate between 0.5-1 %. However, the fatality rate in individuals with clinical symptoms that require medical attention is between 8 - 29 % (McElroy and Nichol, 2012 and Njenga *et al.*, 2009). Haemorrhagic fever clinical symptoms have been recognised in other viral infections that include: Marburg, Ebola, Crimean Congo virus, yellow fever and Dengue (Cobo, 2016).

Haemorrhagic fever is a consequence of damage to endothelial integrity and barrier function as influenced by the mentioned haemorrhagic fever viral infections. Endothelial cells form a thin protective layer of cells joined and held tight by structural organisation that constitute a regulatory blood-brain barrier (Niessen, 2007). Organelles are structural molecules that ensure endothelial integrity and selective barrier. Four junctional organelles are well defined, namely: Tight Junction (TJ), Gap Junction (GJ), Syndesmos Junctions and Adherence Junction (AJ) (Dejana *et al.*, 1995). These organelles are composed of a network of intracellular and transmembrane proteins which are permissible to rearrangement and passage of macromolecules or circulating leukocytes (Dejana *et al.*, 1995).

The degree of junctional complexity varies along the vascular tree depending on the requirements of a tissue. The junctional organisation in the blood-brain barrier is well organised with a number of TJs as opposed to organisation on the post-capillary venules which allow trafficking of circulating cells and plasma proteins (Bazzoni and Dejana, 2004). The AJs initiate and maintain cell-to-cell contact. In addition, AJs are known to regulate the actin cytoskeleton, intracellular signalling and transcriptional activities (Hartsock and Nelson, 2009). AJs are involved in the control of para-cellular permeability to circulating leukocytes and solutes. These junctional organelles play a distinctive role during organisation of new vessels (angiogenesis) (Bazzoni and Dejana, 2004).

Transmembrane molecules such as cadherins engaged in homophilic interactions that hold neighbouring cells together and they play a central role in diapedesis. These

adhesive glycoprotein molecules are linked by a catenin to the actin cytoskeleton (Bazzoni and Dejana, 2004; Niessen, 2007). The catenin proteins are composed of the armadillo repeats with triple  $\alpha$ -helices that bind the c-terminal of the cytosolic domain of cadherin molecules (Hartsock and Nelson, 2009). Beta-catenin and p120 interact directly with cadherin proteins via armadillo repeats while  $\alpha$ -catenin link this complex to the actin cytoskeleton (Niessen, 2007). Cadherins are composed of a conserved cytoplasmic entity and a  $\text{Ca}^{++}$  dependent extracellular domain involved in cell-to-cell adhesion (Bazzoni and Dejana, 2004).

Vascular endothelial cadherin (VE-cadherin) assembly at the cell border is tension dependent. The activated non-muscle myosin II molecules bind and slide the anti-parallel actin filaments thereby generating tension which enables  $\alpha$ -catenin to bind simultaneously to the  $\beta$ -catenin and actin cytoskeleton. Adherence junction induce tension and clustering of the VE-cadherin molecules and subsequent assembly at the cell border (Komarova *et al.*, 2017). VE-cadherin is an endothelial cell specific cadherin that is located at the intercellular junctions (Bazzoni and Dejana, 2004). VE-cadherins elicit critical primary adhesion events during vascular development (Komarova *et al.*, 2017).

Integrins are other essential receptor molecules involved in adhesion of the endothelial cells to the extracellular matrix (ECM) and other neighbouring cells. There are 24  $\alpha\beta$  heterodimeric integrins which support different forms of cell-ECM and cell-cell attachment (Gough and Goult, 2018). Integrins are small proteins with 40 to 60 amino acids and are linked by cytoplasmic-complex proteins that assemble and connect integrins to the actin cytoskeleton. Other studies infer that talin is at the centre of integrin adhesion (integrin-talin-actin) while vinculin is recruited to stabilise connection of talin to the actin cytoskeleton (Gough and Goult, 2018).

Endothelial integrity is regulated by a number of small molecules that include nitric oxide. In addition to protein signalling this molecule plays an important role in the regulation of neurotransmission and blood vessel tone on the endothelium (Soufli *et al.*, 2016). Nitric oxide molecules diffuse to the vessels and adjacent smooth muscles and induce vasodilation (Habib and Baig, 2007). Nitric oxide is produced from oxidation of L-arginine that result in NO and L-citrulline by either a calcium-dependent constitutively expressed endothelial nitric oxide synthase (eNOS) and neuronal nitric oxide synthase (nNOS) or by a calcium-independent inducible nitric oxide synthase (iNOS) (Clancy *et al.*, 1998).



Endothelial nitric oxide synthase (eNOS) produces adequate levels of nitric oxide (NO) involved in maintenance of endothelial integrity (Komarova *et al.*, 2016). The NO molecules have been shown to possess dual roles as anti- and pro-inflammatory mediators; a phenomenon known as the nitric oxide paradox. These NO molecules have been shown to yield contradictory outcomes, both protective and destructive. Soufli and colleagues have reported that the effects of NO are dependent on the production location, duration and concentration (Soufli *et al.*, 2016). Low NO produced by calcium-dependent constitutively expressed isoforms of eNOS have been shown to perform regulatory functions such as neurotransmission and regulation of vessel tone (Soufli *et al.*, 2016).

Low levels of NO benefit not only the endothelial cells, but was shown to stimulate lymphocyte activation and proliferation (Clancy *et al.*, 1998). Furthermore, inadequate levels of NO lead to endothelial damage and then atherosclerosis (Habib and Baig, 2007). The elevated levels of NO elicit protein S-nitrosylation, a covalent link between the NO group and cysteine thiol. S-nitrosylation of  $\beta$ -catenins occurs on the Cys619, p120-catenin on Cys579, Cys429, Cys450, Cys618 and Cys692 sites while that of VE-cadherins occur at Cys579. The S-nitrosylation lowers affinity of  $\alpha$ -catenin to  $\beta$ -catenin and p120-catenin, destabilising the catenin VE-cadherin complex and endothelial integrity (Komarova *et al.*, 2016).

Under-controlled inflammation leads to an oxidative stress condition which is observed when oxidants outweigh antioxidants (Makola *et al.*, 2020; Reuter *et al.*, 2010). This condition leads to diminished NO levels as a result of super oxides reacting to produce a very reactive molecule, peroxynitrite (Habib and Baig, 2007). Oxidative stress is linked to chronic ailments such as cancer, diabetes and atherosclerosis by oxidising LDL and inactivating eNOS and targeting endothelial cells (Habib and Baig, 2007). Activation of the iNOS enzyme leads to elevated levels of peroxynitrite, causing tissue damage which is perpetuated by the cytotoxicity of peroxynitrite (Habib and Baig, 2007). The NO molecules are involved in the maintenance of persistent inflammation observed in inflammatory bowel disease (IBD) (Soufli *et al.*, 2016).

Nitric oxide has been previously shown to trigger effective defensive activities against bacteria, viruses and parasites. It is well-known to be involved in the first line of defense; however, its cytotoxicity effects are not specific to the invading microbes (Clancy *et al.*, 1998). During innate immune activities, the elevated concentrations of

NO and RNS are stimulated by various factors such as infections. These factors trigger iNOS production, resulting in an increase in production of NO (Kathryn, 2007). Soufli *et al.* have shown the link between elevated production of NO and the disturbed balance among pro-inflammatory cytokines (TNF- $\alpha$ , IL-1 $\beta$ , IL-8 and IL-17A), anti-inflammatory cytokines (IL-4 and IL-13) and regulatory cytokines (IL-10 and transforming growth factor  $\beta$ ) (Soufli *et al.*, 2016).

In addition to the ROS and RNS, a high concentration of cytokines elicits endothelial dysfunction. Endothelial dysfunction then leads to leukocytes infiltration and smooth muscle infiltration that trigger development of atherosclerotic lesions. Hyperlipidaemia, hyperglycaemia and aging are some of the contributing factors promoting release of cytokines, reactive oxygen species and other inflammatory molecules from endothelial lining, vascular muscles and infiltrating leukocytes. These situations inactivate the endothelial-derived NO and therefore, perpetuate endothelial damage. Kathryn proposed the use of circulating endothelial progenitor to ameliorate the endothelial damage and atherosclerotic lesions (Kathryn, 2007)

Moreover, inflammatory mediators such as TNF- $\alpha$ , histamine and platelets activating factor (PAF) have been observed to alter VE-cadherin assembly to the AJ via phosphorylation of the VE-cadherin and p120-catenin resulting in phosphorylation of the  $\beta$ -catenin at Tyr654 and Tyr489 by c-Src. This phosphorylation lowers  $\beta$ -catenin affinity to the VE-cadherin and destabilises the AJ (Komarova *et al.*, 2016). Thus, this study links persistent inflammation to production of inflammatory mediators such as cytokine, chemokines, reactive oxygen species, reactive nitrogen species and endothelial malfunction leading to haemorrhagic fever.

## **Materials and Methods**

### *Cell Culture and Viral Propagation*

The RVFV AR 20368 strain was isolated in 1974 during the RVF outbreak in South Africa. The virus was propagated on Vero C1008 cells at a MOI of 0.2, followed by harvesting the monolayer after extensive CPE was observed. The supernatant was stored at -70°C after centrifugation at 3,000 xg for 30 minutes (Martín-Folgar *et al.*, 2010). The Raw 264.7 macrophage cells were obtained from Prof Lyndy McGraw (University of Pretoria). The cells were maintained in cell culture flasks at 37°C, in a humidified 95% air and 5% CO<sub>2</sub> atmosphere. Raw 264.7 cells were propagated in

Dulbecco Modified Eagle Medium (DMEM) supplemented with 10% Fetal Bovine Serum (FBS), 2 mM L-glutamine and 1x penicillin-streptomycin. Vero C1008 cells were purchased from ATCC and propagated in Minimum Essential Medium (MEM), supplemented with 10 % FBS, 2 mM L-glutamine and 1x penicillin-streptomycin (Lonza). Huvec primary cells lines were used at very low passage and maintained in EGM-2 endothelial cells media supplemented with hEGF 0.1%, Hydrocortisone 0.04%, GA-1000 (Gentamicin, Amphotericin-B) 0.1%, FBS (Fetal Bovine Serum) 5%, VEGF 0.1%, hFGF-B 0.1%, R3 -IGF-1 0.1%, Ascorbic Acid 0.1%, Heparin 0.1% (Lonza, USA). Trypan blue dye and haemocytometer were used to determine cell density (Matsebatlela *et al.*, 2012).

### *Cell treatment*

Lithium Chloride (LiCl) was purchased from Fluka (Chemika, Switzerland) and 500 mM stock was prepared and stored at -20°C. Sodium Chloride was purchased from Sigma-Aldrich (USA) and the stock was prepared at 500 mM NaCl stored at -20°C. The experiments were executed using the supernatant from Raw cells seeded at a density of  $2.4 \times 10^6$  cells/ml in the T25 flasks, after 3 hrs of cell adaptation, the cells were inoculated with  $10^{4.8}$  viral titre/mL for 1 hr and other cells were stimulated with LPS (5 mg/ml) for 24 hrs. The Raw cells supernatant was stored at -20°C after 24 hrs of incubation.

### *Determination of endothelial integrity using real time cell analyser system (RTCA) assay*

The electric impedance dependent real-time cell analyser system of the xCelligence measure the integrity of endothelial cells post exposure to the Raw 264.7 macrophage supernatant. This assay measures change in the cell morphology, cell number and cell adhesion of the endothelial cells as “cell index”. In order to measure the endothelial integrity of the endothelial cells, the cells were seeded in the 16-E plates at density of 20 000 cells/well for 24hrs. The E plates with cells were then connected to the equipment for 24 hrs and then the cells were exposed to the supernatant from lithium-treated and RVFV-infected Raw 264.7 for 72 hrs. The xcelligence software was set according to manufacturer’s protocol to take readings at 15 minutes intervals (Roche, USA).

### Determination of the huvec cell monolayer integrity using the trans-well (FITC-BSA)

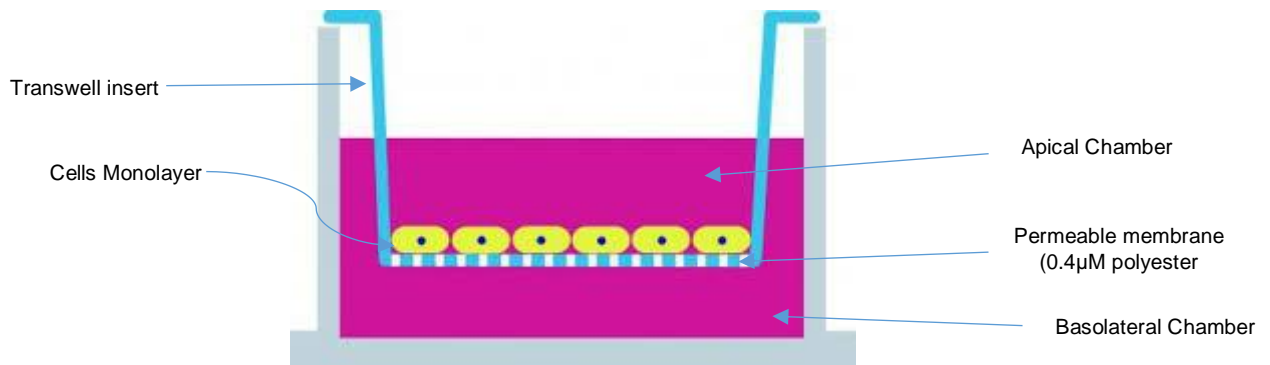


**Figure 4.1: Depiction of the transwell plate and mechanisms used by this assay to measure monolayer integrity.** Transwell plates are preferred tools to study monolayer integrity. The permeable membrane provides free access to both sides of the monolayer, thus providing a versatile tool to study transport and other metabolic activities *in vitro*.

Trans-well plates have the basolateral and apical chamber wherein the monolayer is established on the semi permeable membrane. The integrity of the monolayer is examined with the use of the fluorescent molecule, FITC, conjugated to BSA (FITC-BSA) on the basolateral chamber. Briefly, the Raw 264.7 cell were inoculated with RVFV at  $1 \times 10^{4.8}$  viral titer for 1 hr, then the excess virus was discarded followed by treated with lithium (as outlined in Cell treatment). The resulting supernatants were collected and used to treat Huvec monolayers so as to assess the endothelial integrity. Huvec cells were seeded on the permeable membrane (0.4 μm polyester) in the apical chamber of the trans-well plate at a density of 20 000 cell/well for 5 days to establish a monolayer. This was then followed by exposing the monolayer to Raw 264.7 cells supernatant for 12 and 24 hrs. The integrity detecting solution (50 μm FITC-BSA) was added and then 100 μl of the media was taken from the basolateral chamber in 0.5, 1, 3, 6, 12, 24 and 48 hrs. The media taken from the basolateral chamber was then measured for the presence of FITC-BSA with Glo-max multy plax plate reader (Promega, USA) at 490 nm/ 520 nm Ex/Em.

### Examination of the expression of the junctional genes using Profiler RT PCR

#### Total RNA extraction from Huvec endothelial cells

Cells were seeded at 100 000 cells /well in a 6 well plate for 5 days to establish a monolayer. The cells were then challenged with the lithium-treated RVFV-inoculated Raw 264.7 cells supernatant for 24 hrs. Cells were harvested by aspirate the medium,

and washing with 1x PBS and then cells were suspended with trypsin. The cells were then centrifuge at 300 x g for 5 minutes and then 350 µl RLT buffer was added and pipetted up and down to disrupt the cells. This was followed by pipetting the lysate directly into a QIAshredder spin column and centrifuge for 2 min at full speed. Thereafter, 350 µl of 70% ethanol was added to the homogenized lysate, and mixed by pipetting. Furthermore, 700 µl of ethanol and cell lysate solution was transferred to an RNeasy spin column placed in a 2 ml collection tube. This was then followed by centrifugation for 15 seconds at 8000 x g, the flow through was discarded. In order to wash the RNeasy spin column membrane, 700 µl of buffer RW1 was added to the RNeasy spin column membrane then centrifuged for 15 seconds at 8000 x g the flow-through was discard. Further washing of the RNeasy spin column membrane was executed by adding 500 µl Buffer RPE and then centrifuged for 15 seconds at 8000 x g and then the flow-through was discard. The above washing was repeated with long centrifugation to dry the membrane and this was centrifuged for 2 min at 8000 x g. In order to elute the membrane-bound RNA the RNeasy spin column was placed in a new 1.5 ml collection tube and then 50 µl RNase-free water directly added to the spin column membrane and centrifuged for 1 min at 8000 x g.

#### *cDNA synthesis from RT<sup>2</sup> First strand kit*

The genomic DNA elimination mix composed of 5 µg/ml total RNA, 2 µl Buffer GE and RNase-free water (various volume) to a total volume 10 µl for 5 min at 42°C, then place immediately on ice for 1 min. A volume of 10 µl of a reverse-transcription mix (4 µl 5x Buffer BC3, 1 µl Control P2 RE3, 2 µl Reverse Transcriptase Mix and 3 µl RNase-free water to a total volume of 10 µl) was added to each tube containing 10 µl genomic DNA elimination mix. The solution was the mixed gently by pipetting up and down. This was followed by Incubation at 42°C for exactly 15 min and then the reaction was ceased by incubating at the reaction at 95°C for 5 min. A volume of 91 µl RNase-free water was added in each reaction and mixed by pipetting the mixture up and down. The reaction was stored at - 20°C freezer for later use.

#### *Real Time Polymerase Chain Reaction using RT<sup>2</sup> profiler arrays*

For RT PCR the 1350 µl 2x RT2 SYBRR Green Mastermix, 102 µl cDNA synthesis reaction, 1248 µl RNase-free water to a total volume of 2700 µl were mixed and then

twenty five  $\mu$ l PCR components were added to each well of the RT2 Profiler PCR Array. The RT2 Profiler PCR Array was sealed with Optical Thin-Wall 8-Cap Strips, thereafter the plate was centrifuged for 1 min at 1000 g at RT to remove bubbles. Roche LightCycler 480 was used to execute the PCR cycles. 1 cycle for 10 min at 95°C and other 45 cycles for 15 seconds at 95°C and 1 min 60°C

Table 4.1 Adherence Junction gene table: Accession numbers of the gene primer used in the Profiler Real Time PCR array assay on Raw 264.7 macrophage cells lithium-treated and RVFV inoculated supernatant endothelial cells co-inoculation.

ADHERANCE JUNCTION ASSOCIATED GENE	Description	Unigene	GeneBank
1. ACTN2	Actinin, alpha 2	Hs.498178	NM_001103
2. ACTN3	Actinin, alpha 3	Hs.737862	NM_001104
3. CDH5	Cadherin 5, type 2 (vascular endothelium)	Hs.76206	NM_001795
4. CDH1	Cadherin 1, type 1, E-cadherin (epithelial)	Hs.461086	NM_004360
5. CDH2	Cadherin 2, type 1, N-cadherin (neuronal)	Hs.464829	NM_001792
6. CTNNA1	Catenin (cadherin-associated protein), alpha 1, 102kDa	Hs.656653	NM_001903
7. CTNNA2	Catenin (cadherin associated protein), alpha 2	Hs.167368	NM_004389
8. CTNNA3	Catenin (cadherin-associated protein), alpha 3	Hs.21375	NM_013266
9. TNNB1	Catenin (cadherin-associated protein), beta 1, 88kDa	Hs.712929	NM_001904
10. TLN1	Talin 1	Hs.471014	NM_006289
11. TLN2	Talin 2	Hs.569438	NM_015059
12. VCL	Vinculin	Hs.643896	NM_003373
13. VEZT	Vezatin, adherens junctions transmembrane protein	Hs.24135	NM_017599
14. ZYX	Zyxin	Hs.490415	NM_003461

## **Results**

### *Determination of the endothelial integrity using the xCelligence system*

The xCELLigence system provides monitoring of cellular integrity in real-time. The system measures the net adhesion of cells to high-density gold electrode networks printed on custom-designed E-plates. As cells proliferate and growth across the gold electrodes they impede voltage. The voltage-gated impedance values are converted by the software into the Cell Index (CI), which is then used as a measure of strength of adhesion. The strength of cellular adhesion is influenced by a wide variety of factors that include cell size, volume, shape, viability, growth, migration, spreading and proliferation. In the absence of cells, the CI will be zero, and as cells adhere to the array, the CI increases. Thus, the greater the CI values, the greater the level of adhesion.

The xCelligence real time cell analyser system was used to measure the changes in integrity of the endothelial monolayer after exposure to supernatant from lithium-treated RVFV-infected Raw 264.7 cells. The three graphs below show that lithium (2.5, 1.25 and 0.625 mM) treated and RVFV infected Raw 264.7 cells supernatant have less damaging effects on the endothelial monolayer compared to RVFV-infected Raw 264.7 cells supernatant. Huvec cells monolayer integrity exposed to lithium-treated and RVFV-infected Raw 264.7 supernatant scored a CI between 4 and 5, similar to untreated control. However, the RVFV, LPS and control curcumin monolayer integrity lay below 4 cell-index (Fig 4.2 A, B and C).

All the three lithium concentrations showed some level of monolayer protection, however, 1.25 and 2.5 mM lithium treatments displayed significantly higher CI levels compared to 0.625 which scored a CI value below 4 (Fig 4.2 C). Therefore, the Huvec monolayer protection after treatment with supernatants from RVFV-infected Raw 264.7 cells increased with concentration of lithium.

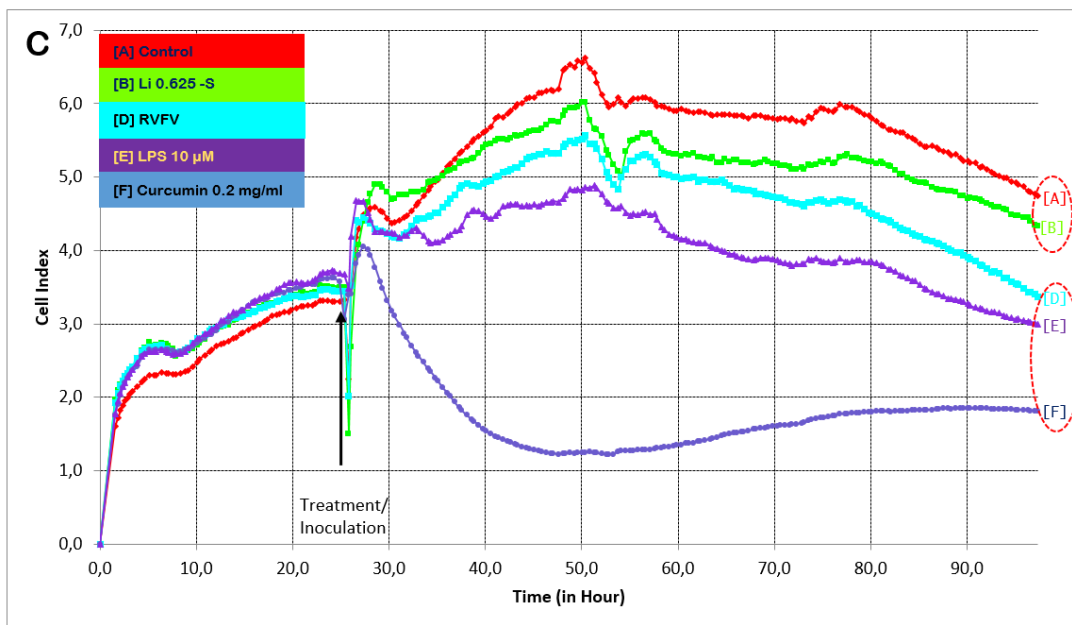
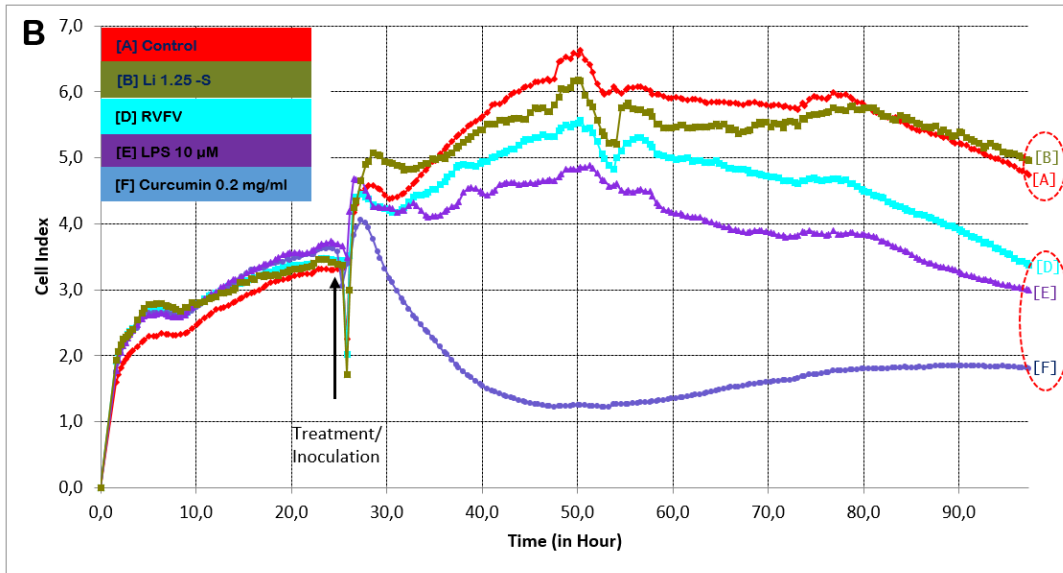
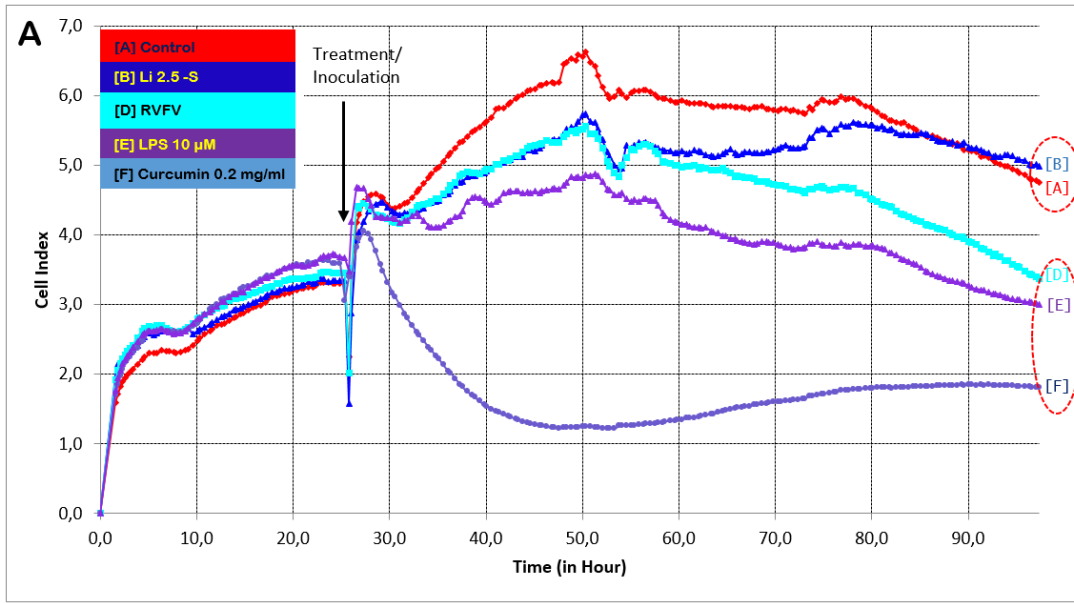




**Figure 4.2: Examination of the effects of macrophage supernatant on endothelial cell integrity and the influence of lithium.** Cells were seeded at 5 000 cell/well for 24 hrs and then connected with the xCelligence detection system for 24 hrs. This was followed by treatment with LiCl (2.5 mM (A), 1.25 (B) and 0.625 (C)) and challenged with Raw 264.7 macrophage cells supernatant that was treated with LiCl (0.625, 1.25 and 2.5 mM), 10  $\mu$ M LPS and inoculated with  $10^{4.8}$  viral titer/mL for 72 hrs. The endothelial cell integrity was measured on real time by the xCelligence real time analyser system according to manufacturer's protocol.

*Determination of the HUVEC cells monolayer integrity using the trans-well (FITC-BSA)*

The trans-well monolayer integrity determination assay, utilise the FITC-BSA to determine the level of monolayer integrity. The plots below show that lithium-treated RVFV-infected Raw 264.7 cells supernatant protects the endothelial monolayer integrity as compared to the lithium-free RVFV-infected Raw 264.7 cells supernatant. On the 12 hrs post exposure plot (Fig 4.3 A), 2.5 mM lithium-treated and RVFV-infected supernatant showed less FITC-BSA translocation through the endothelial monolayer compared to control RVFV supernatant. The RVFV supernatant show to be damaging to the monolayer from first to the third time interval and then the monolayer recovers, however this is postulated to be as a result of exhausted FITC-BSA monolayer detecting solution. Similar protection trend has been observed in the 24 hrs post exposure plot, the difference in endothelial integrity recovers after 12 hrs time point (Fig 4.3 B).

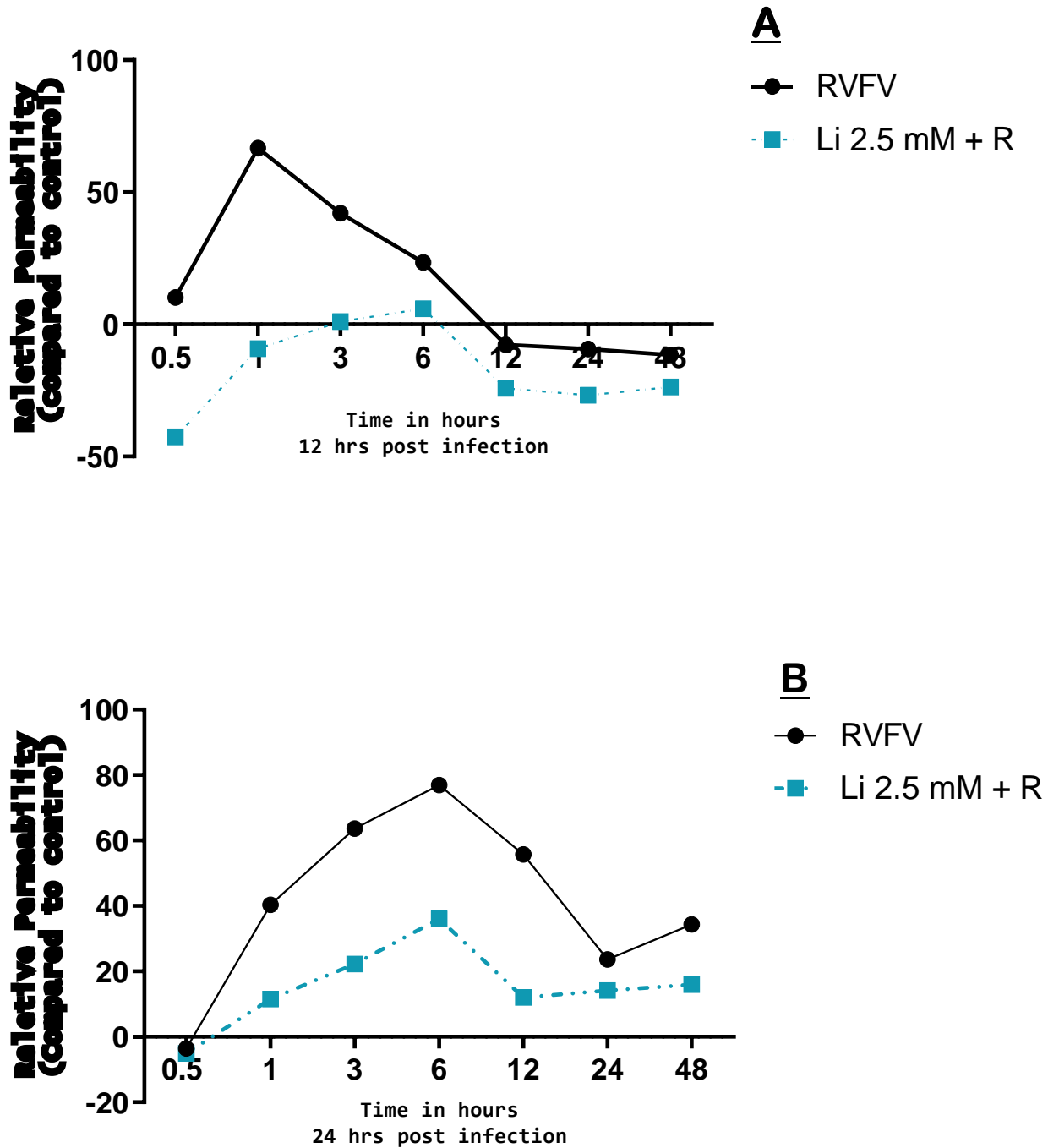


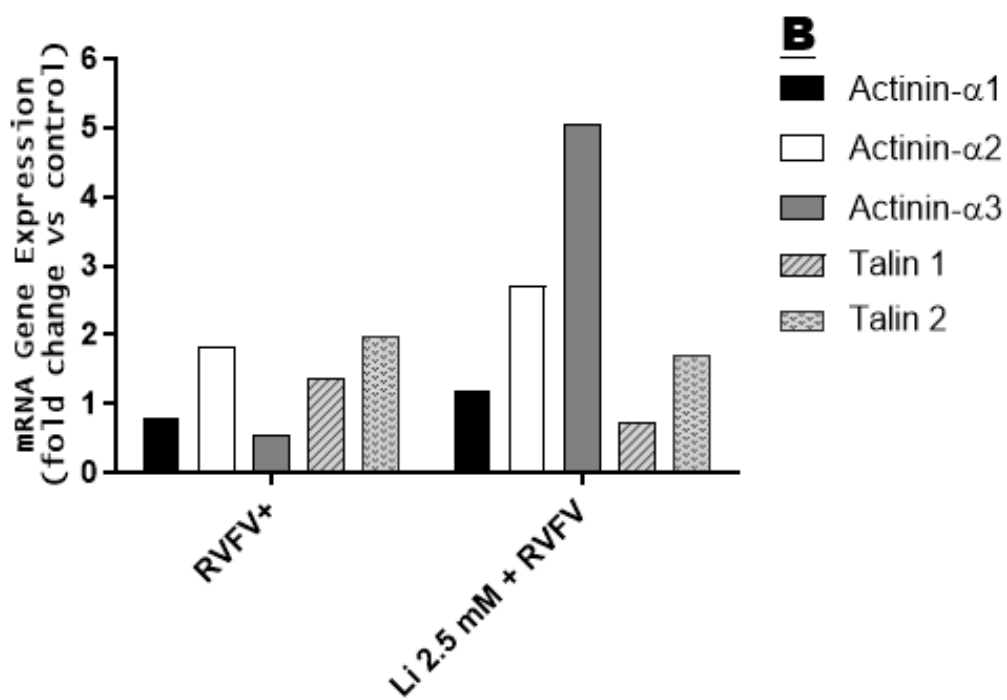
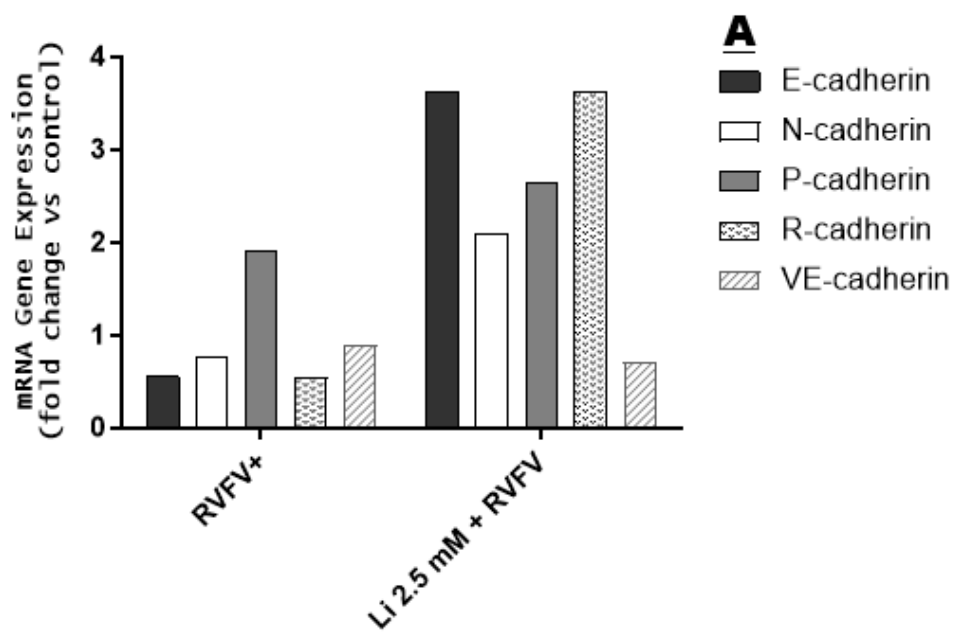
**Figure 4.3: The permeability effects of lithium on the endothelial cells (Huvec cells) after exposure to supernatant of pre-treated and pre-inoculated Raw 264.7 macrophage cells.** The endothelial Huvec cells were cultured 20 000 cell/well for 5 days to establish a monolayer on the upper chamber of the trans-well plates. Then the cells were exposed to the Raw 264.7 cells lithium-treated and RVFV-infected cells supernatant. The integrity of the monolayer was determined through examination the translocation of BSA-FITC fluorescent molecule from the upper through the monolayer to the lower chamber after 12 (A) and 24 (B) hrs post infection/exposure with the Raw 264.7 cells supernatant. The media on the lower chamber was collected in 3, 6, 12, 24 and 48 hrs time interval. The Glo-max multy plax plate reader (Promega, USA) was used to measure the quantity of the fluorescent BSA-FITC molecule. The plot was developed with Graph-Pad Prism-6 software.

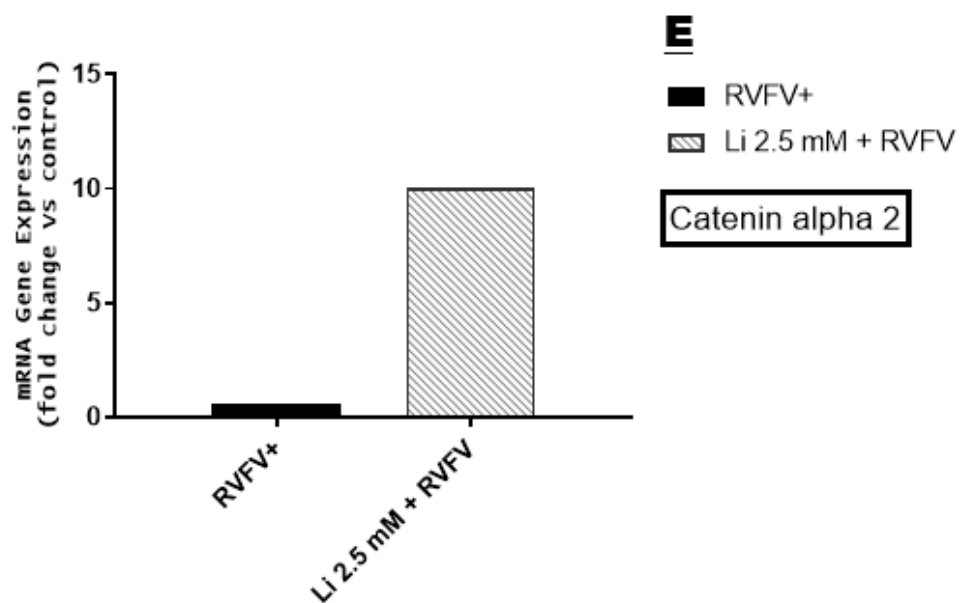
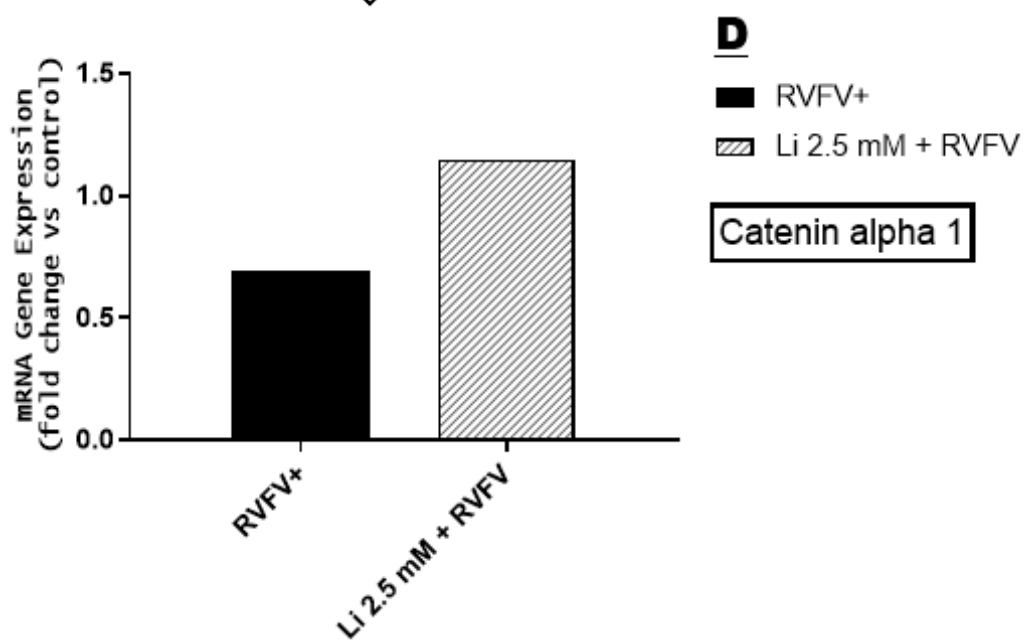
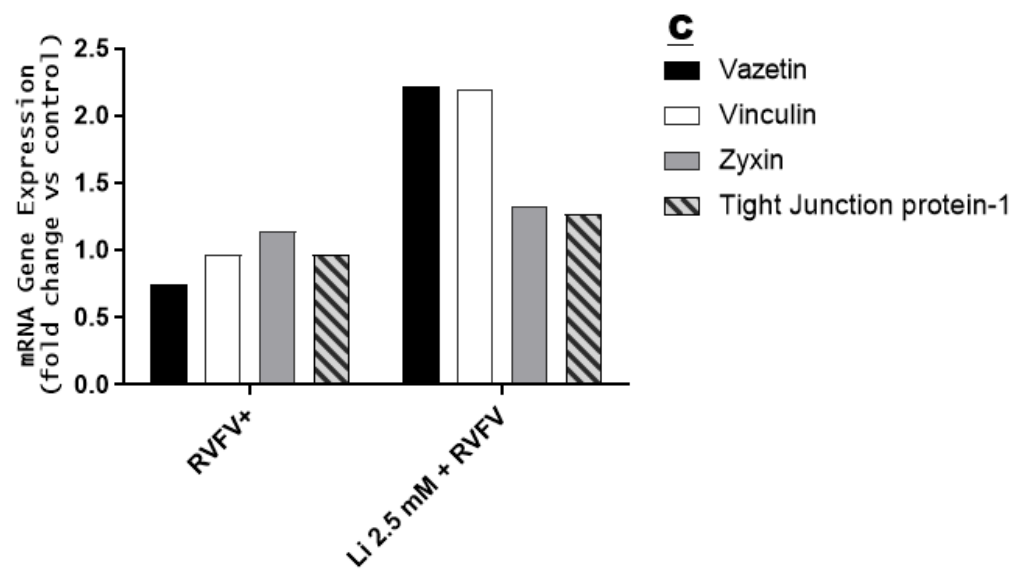
*The influence of lithium on Adherence junction gene expression profiles using RT<sup>2</sup> profiler PCR array*

Adherence junction proteins are important type of proteins known to initiate and maintain cell to cell as well as cell to extracellular matrix (ECM) adhesion and integrity. Figure 4.4 A below show that lithium upregulates expression of the E, N, P, and R-Cadherin excluding VE-Cadherin proteins. The cadherin molecules are shown to be expressed more in the endothelial cells monolayer exposed to lithium-treated and RVFV-infected supernatant compared to control RVFV. The E, N, P, R-cadherin are expressed 3.6, 2.1, 2.6, 3.6 and 0.7-fold in Li 2.5 mM +RVFV as compared to control +RVFV which expressed these proteins 0.6, 0.8, 2, 0.6 and 0.9-fold respectively (fig 4.4 A).

The other proteins such as actinin- $\alpha$ 1,  $\alpha$ 2,  $\alpha$ 3, Talin-1 and Talin-2 are expressed 1.2, 2.7, 5.1, 0.7 and 1.7-fold in lithium-treated RVFV-infected supernatant compared to 0.8, 1.8, 0.6, 1.4 and 2-fold in control RVFV respectively (Fig 4.4 B). Moreover, Vazetin, Vinculin, Zyxin and Tight Junction protein-1 are expressed 2.2, 2.2, 1.3 and 1.3-fold in 2.5 mM lithium-treated and RVFV-infected supernatant compared to 0.8, 1, 1.1 and 0.9-fold expression in RVFV-infected control (Fig 4.4 C) respectively.

On the other hand, the catenin- $\alpha$ 1 is expressed 1.15-fold in lithium-treated and RVFV-infected compared to 0.7-fold in RVFV-infected control (Fig 4.4 D). Catenin- $\alpha$ 2 is expressed 10 fold more in lithium-treated and RVFV-infected compared to 0.6-fold in RVFV-infected control (fig 4.4 E). Catenin- $\alpha$ 3 is expressed 10-fold in lithium-treated RVFV-infected supernatant compared to 0.6-fold in RVFV-infected control (fig 4.4 F). The catenin-beta-1 is expressed 1.2-fold in lithium-treated and RVFV-infected supernatant compared to 0.8-fold in RVFV-infected control (fig 4.4 G).





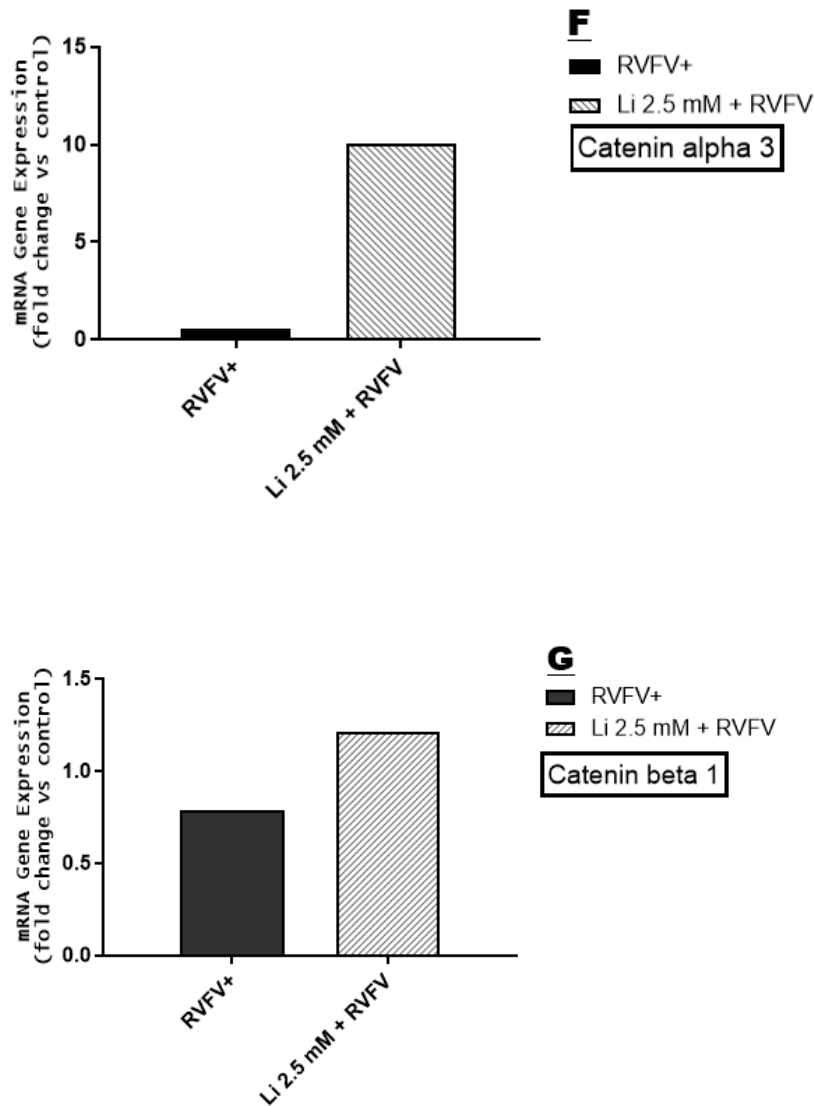


**Figure 4.4: Effects of lithium pre-treated Raw 264.7 macrophage cells supernatant on adherence junction gene expression profiles using HUVEC cells as the model for endothelial cells monolayer.** The endothelial Huvec cells were cultured at 100 000 cells/ml for 5 days to establish the monolayer in 6 well plates. Then the cells were exposed to the stored Raw 264.7 cells supernatant. The total RNA was isolated with qiagen total RNA isolation kit, then this was followed by cDNA synthesis then TR<sup>2</sup> PCR according to manufacturer's protocol. The qiagen data analysis website was used to calculate the gene expression. The calculated fold change values were used to plot the graphs, the Graph pad prism-6 software was then used to establish the plots.

## **Discussion**

Viruses such as Marburg, Ebola, Crimean Congo virus, yellow fever, Dengue and RVFV induce severe viral haemorrhagic fever. The internal haemorrhage condition remains the main pathologic outcome observed in these types of viral infections (Cobo, 2016). RVFV has been observed to elicit a variety of distinctive symptoms such as self-limiting febrile illness and severe symptoms that include encephalitis and haemorrhagic fever. The highest percentage of fatalities observed in RVFV infections emanated from severe symptoms displayed by patients (McElroy and Nichol, 2012 and Njenga *et al.*, 2009).

This study postulates that severe symptoms with high mortality rates observed in this viral infection is exacerbated by under-regulated inflammation as opposed to suppressed immune response since an *ex vivo* study by Jansen van Vuren showed that immune responses are mounted to the same degree in both survival and fatal cases (Jansen van Vuren *et al.*, 2015). This study was therefore designed to investigate the use of lithium as a potent haemorrhagic fever therapeutic agent which stabilises endothelial integrity through regulation of inflammatory responses. In order to understand the effects of inflammatory responses on endothelial cell monolayer integrity, co-inoculation was used in an attempt to understand the effects of inflammatory events on endothelial integrity.

Supernatants from lithium-treated RVFV-infected Raw 264.7 macrophage cells showed protective properties on the endothelial integrity as seen in figure 4.2 A, B and C. Using the RTCA xcelligence assay, a 4.0 cell-index was recorded in endothelial monolayers treated with supernatant from lithium-treated and RVFV-infected Raw 264.7 cells as displayed in figure 4.2. This cell index score falls within the range observed in untreated uninfected endothelial monolayers, demonstrating that lithium-treated and RVFV-infected supernatant protected monolayer integrity. However, treatment of endothelial cells with supernatants from lithium-free RVFV-infected Raw 264.7 cells supernatant showed a cell index below 4, demonstrating a compromised endothelial cell integrity.

The trans-well assay displayed similar protective findings displayed by lithium. Lithium displayed protective properties on endothelial cell integrity (Fig 4.3 A and B). In both the 12 and 24 hrs, endothelial cells exposed to lithium-treated and RVFV-infected supernatant induces less of the permeability as demonstrated using the

FITC-BSA translocation assay (fig 4.3 A and B). The RTCA xcelligence and transwell assay that measure monolayer integrity together displayed the protective properties of lithium on the endothelial monolayer integrity. Previous studies suggested that lithium stimulate neurovascular remodelling after stroke as it has been observed to upregulate expression of the VEGF expression through PI3-K/GSK-3 $\beta$ -dependent and independent pathways (Shuzhen *et al.*, 2009).

The *in vivo* study by Wang *et al* showed a lowered leukocyte infiltration as demonstrated using untreated vesicular stomatitis virus and Sendai virus-infected mouse model system (Wang *et al.*, 2013). Moreover, lithium was also used as treatment for sequelae after chemotherapy since most cancer patients die from delayed recovery from chemotherapy (Khasraw *et al.*, 2012).

Bosche *et al* have shown that lithium, at low doses (0.2 and 0.4 mM), elicits protection on the endothelial barrier. It is suggested that lithium stabilises the endothelial barrier by lowering phosphorylation of MLC which mediates vasodilation and endothelial contraction, leading to induction of hyper-permeability (Bosche *et al.*, 2016). Lithium inhibited inositol 3-phosphate (IP3), thereby blocking IP3-sensitive Ca<sup>2+</sup> release from endoplasmic reticulum (ER) leading to capping Ca<sup>2+</sup> cell influx which activate the MLC phosphorylation (Bosche *et al.*, 2013). Lithium treatment was shown to upregulate several essential adherence junction proteins that keep both cell to cell and cell to ECM intact.

Junctional proteins remain central to cellular integrity and play a crucial signalling role in controlling diapedesis and movement of molecules in and out of the blood to the tissues. The vinculin cytoplasmic adaptor proteins are involved in the focal adhesion complex that link the integrin adhesion proteins at the cell boarder to the actin cytoskeleton. Alteration of vinculin expression resulted in a weakened cell to cell and cell to extracellular matrix (ECM) adhesion, leading to elevated leukocyte invasion (Humphries *et al.*, 2007). Vinculin is a globular protein consisting of 5 helical domains (Birukova *et al.*, 2016). Vinculin, in its resting inactive state, has been shown to form hydrophobic interactions between the tail and the head domains (Izard *et al.*, 2006).

The head domain contains binding sites for talin,  $\alpha$ -actinin and  $\alpha$ -catenin while the tail domain contains binding sites for actin-cytoskeleton and paxillin (Birukova *et al.*, 2016). Vinculin is primarily targeted by the IpaA protein which mimic talins in binding the head domain and modulate activation of vinculin. IpaA-vinculin activate binding



of actin-cytoskeleton binding which form active-vinculin cub that aid in bacterial entry using the vinculin binding site (VBS) (Izard *et al.*, 2006). Lithium treatment was shown to upregulate expression of the vinculin protein compared to RVFV control (fig 4.4 A).

Since vinculin is one of the key molecules required in maintaining focal adhesion, this could explain reduced protection on endothelial integrity in monolayers treated with supernatants from lithium-free RVFV-infected Raw 264.7 control cells compared to those treated with 2.5 mM lithium as depicted in figure 4.2 and 4.3. Gough and Goult reported that vinculin is recruited to stabilise connection of talin to the actin cytoskeleton (Gough and Goult, 2018) while Humphries *et al* reported that vinculin interacts with this integrin via talins (Humphries *et al.*, 2007). The activator protein, talin, and  $\alpha$ -actinin that activate vinculin by binding its head domain were shown to be upregulated by lithium treatment as well (Birukova *et al.*, 2016).

In this study supernatants from RVFV-infected Raw 264.7 cells treated with 2.5 mM lithium induced expression of talin-1 0.7 folds compared to lithium-free controls which increased talin-1 expression 1.4 folds. Moreover, supernatants from lithium 2.5 mM-treated RVFV-infected Raw 264.7 cells induced talin-2 expression by 1.5 compared to the 2-fold increase induced by supernatants from lithium-free control cells (figure 4.4 E). Although the Talin-1 and 2 are expressed to a lesser extent in the lithium-treated RVFV-infected model compared to lithium-free RVFV-infected controls, the expression of the vinculin linker molecule was significantly more pronounced with lithium treatment. Nonetheless, Gough and Goult argue that talin, which is stabilised by vinculin, is the master of integrin adhesion (Gogh and Goult, 2018).

Lithium has been shown to upregulate expression of stabilising proteins, actinin- $\alpha$ 2 and actinin- $\alpha$ 3 (Figure 4.4 B). In addition to talins and actinins, another set of linker molecules, the catenin alpha 1, 2 and 3, is involved in integrin signalling and act as linkers of the VE-cadherin to the actin-cytoskeleton. These molecules were shown to be expressed more in cells exposed to lithium-treated and RVFV-infected supernatant compared to control RVFV-infected supernatant (Fig 4.4 B). The  $\beta$ -catenin molecules interact with the c-terminal of the VE-Cadherin in the cytoplasm with their conserved triple  $\alpha$ -helix of the armadillo repeats (Hartsock and Nelson, 2008), which is shown to be upregulated by 2.5 mM lithium treatment (fig 4.4 E, F and G).

The  $\alpha$ -catenin connects VE-cadherin to the actin cytoskeleton via  $\beta$ -catenin (Niessen, 2007). Expression of the most crucial transmembrane protein, VE-cadherin, is shown to be reduced by lithium (0.7 fold in Li 2.5 mM) compared to untreated RVFV-infected controls (0.9-fold expression). The VE-cadherin and focal adhesion proteins, such as vinculins, are highly expressed in cell treated with higher doses of lithium. These outcomes coincide with the preserved monolayer integrity observed with Li 2.5 mM compared to other lithium concentrations (Fig 4.2 and 4.3). Bosche and colleagues have shown lithium to be effective in maintaining endothelial integrity at therapeutic doses of 0.4 and 0.2 mM (Bosche *et al.*, 2013).

Zyxin is another cytoplasmic protein involved in focal adhesion which is suggested to interact with  $\alpha$ -catenin. Mutation of the zyxin  $\alpha$ -catenin binding site showed adverse outcomes such as lack of adhesion strength, wound healing speed and orientation response after cell stretch (Ngu *et al.*, 2009). Zyxin is said to be a marker of the intact focal adhesion on endothelial cell to cell border. Young and colleagues showed zyxin localisation on the cell border to be linked to endoglins. Zyxin is involved in signalling pathways that regulate clustering on integrins and cell morphology (Young *et al.*, 2015). This protein is expressed more in monolayer cells challenged with supernatants from Li 2.5 mM-treated and RVFV-infected Raw 264.7 cells. This expression pattern correlates well with preservation of endothelial integrity displayed in figure 4.2 and 4.3.

Vezatin is a key anchor molecule that has been suggested to be involved in initiation and maintenance of the adherence junction in the epithelial cell to cell interaction during embryonic development. Vezatin is shown to interact with the actin cytoskeleton in both the E-cadherin-catenin complex and myosin VIIA (Küssel-Andermann *et al.*, 2000). This work showed that lithium favours early clustering of the adaptor molecules such as vezatin that link E-cadherin-catenin complex to initiate cell to cell adhesion and embryonic development since lithium upregulated expression of vezatin (fig 4.4 C), as well as N and E-cadherins (fig 4.4 A). The anti-inflammatory properties of lithium are suggested to be central to the mechanism by which lithium lowers endothelial permeability

Endothelial leakage has been shown to be increased by ROS and RNS in both *in vivo* and *in vitro* models. This leakage is linked to  $\beta$ -catenin and  $\alpha$ -catenin phosphorylation leading to VE-cadherin junctional destabilisation (Aghajanian *et al.*, 2008). Results from this study and previous studies show that lithium lower production of

inflammatory mediators such as ROS, RNS and chemokines. Lithium has been shown to ameliorate multiple sclerosis-related Inflammation that has been linked to ailments involving neuronal demyelination as a result of leukocyte extravasation (De Sarno *et al.*, 2008).

The ROS and RNS inflammatory mediators are thought to be linked to altered endothelial signalling phosphorylation patterns and endothelial integrity. Elevated NO levels elicit S-nitrosylation of  $\beta$ -catenin which occurs on the Cys619 while VE-cadherin occurs at Cys579. The S-nitrosylation of this protein lowers affinity of  $\alpha$ -catenin to  $\beta$ -catenin, leading to destabilisation of the VE-cadherin complex and low endothelial integrity (Komarova *et al.*, 2016). Bosche *et al* suggested that lithium inactivates inositol 3-phosphate (IP<sub>3</sub>) which is thought to inhibit accumulation of Ca<sup>2+</sup> release from endoplasmic reticulum (ER). The accumulated Ca<sup>2+</sup> activates the actin-myosin fiber contraction and endothelial leakage (Bosche *et al.*, 2013). Phosphorylation of MLCK stimulate contraction of the actin-myosin fibers and endothelial permeability. The PI<sub>3</sub> molecule is known to sense decline in ATP production as a cell stress response mechanism and stimulate the accumulation of free cytoplasmic Ca<sup>2+</sup> that activate MLCK (Muller, 2013).

## **Conclusion**

Although more work is required to understand the molecular mechanism used by lithium to promote endothelial integrity, this drug has been shown to upregulate key regulatory genes that are important in initiating and maintaining the endothelial cell to cell as well as cell to ECM adhesion. Results from the permeability assays have shown lithium-treated immune cells supernatant to protect the endothelial integrity. This work hypothesises that RVFV-induced pathology is linked to under-controlled inflammation that leads to oxidative stress. Hence, the ability of lithium to regulate RVFV-induced inflammation and oxidative stress restores endothelial integrity.

## CHAPTER 5

### OVERALL CONCLUSION

Since identification of the RVFV in the 1930s, till to date, there is no treatment obtainable for human and animal use against this infection. The RVFV infection remains a world-wide public health concern due to its re-occurrence and transmission mechanism. Results from this work demonstrate the ability of lithium to inhibit RVFV replication. The postulated mechanism of action entails accelerated apoptosis of RVFV-infected and lithium-treated cells that leads to inhibition of replication. Lithium has been shown to stimulate expression of pro-apoptotic proteins while inhibiting expression of their anti-apoptotic counterparts as part of its mechanism of action. Lithium is observed to be a reliable non-toxic drug as it was shown to selectively induce cell death in infected cells while promoting cell proliferation in un-infected cells. Apoptosis was shown to be the mode of cell death induced by RVFV.

Haemorrhagic fever is one of the severe symptoms experienced by a small percentage of infected patients but with a huge mortality rate. Thus, previous work showed contradicting hypothesis in understanding the contributing factors that lead to this severe clinical symptom. This study postulates that under-controlled inflammation that leads to oxidative stress is central to RVFV- induced haemorrhagic fever pathogenesis. This study is the first to show inhibitory properties of lithium on the NF- $\kappa$ B activity in relation to the observed oxidative stress post RVFV infection. It also indicates that the haemorrhagic fever observed in RVFV patients could be as a results of under-controlled production of inflammatory mediators that lead to oxidative stress. In addition, results from this study suggest the putative mechanism of NSs in silencing the type I IFN and demonstrating the inhibitory role of lithium at the signalling level.

Lithium also demonstrated the protective properties on the endothelial cells monolayer. Lithium up-regulated important molecules involved in initiation and maintenance of junctional organelle and endothelial integrity. Although further work needs to be done, the combination of the regulatory properties of lithium on replication of the virus, restoration of control to inflammation and protective outcomes that accompany lithium treatment on endothelial cell permeability make lithium a candidate drug for consideration in the treatment of this viral haemorrhagic fever.

## FUTURE WORK

The future work will be focused on examining if the *in vitro* outcomes could hold in the *in vivo* studies. The compound in question, lithium has been already been used or tested in an *In vivo* setting for various other biological activity such as cytotoxicity and as an anti-depressant remedy. Thus, our future work will be examining its anti-inflammatory properties that are linked to amelioration of the haemorrhagic fever pathogenesis observed in clinical symptoms emanating from RVFV infection. Moreover, the proposed early apoptosis that is suggested to lower viral load will be examined.

## REFERENCES

1. Aghajanian A, Wittchen ES, Allingham MJ, Garrett TA, Burridge K (2008) Endothelial cell junctions and the regulation of vascular permeability and leukocyte transmigration. *Thromb Haemost.* 6: 1453–1460.
2. Akira S, Uematsu S, Takeuchi O (2006) Pathogen recognition and innate immunity. *J Cell.* 124:783–801.
3. Amitai M, Zivony A, Kronenberg S, Nagar L, Saar S, Sever J, Apter A, Shoval G, Golubchik P, Hermesh H, Weizman A and Zalsman G (2014) Short-term effects of lithium on white blood cell counts and on levels of serum thyroid-stimulating hormone and creatinine in adolescent inpatients: a retrospective naturalistic study. *J Child Adolesc Psychopharmacol.* 24:494-500.
4. Austin D, Baer A, Lundberg L, Shafagati N, Schoonmaker A (2012) p53 Activation following Rift Valley Fever Virus Infection Contributes to Cell, Death and Viral Production. *PLoS ONE.* 7: e36327.
5. Balenghien T, Cardinale E, Chevalier V, Elissa N, Failloux AB, Nipomichene TNJJ, Nicolas G, Rakotoharinome VM, Roger M, Zumbo B (2013) Towards a better understanding of Rift Valley fever epidemiology in the south-west of the Indian Ocean *Vet Res.* 44:78.
6. Barr RD, Galbraith PR (1983) Lithium and hematopoiesis. *J. Can Med Assoc,* 128: 123-126.
7. Barreiro, O. Ya´n˜ez-Mo´, M. Sala-Valde´s, M. Gutie´rrez-Lo´pez, M.D. Ovalle, S. Adrian Higginbottom, A. Monk, P.N. Caban˜as, C and Sa´nchez-Madrid, F (2005) Endothelial tetraspanin microdomains regulate leukocyte firm adhesion during extravasation. *Blood.* 105: 2852–2861.
8. Bazzoni G, Dejana E (2004) Endothelial cell-to-cell junctions: molecular organization and role in vascular homeostasis. *Physiol Rev.* 84(3):869-901
9. Bird BH, & McElroy AK (2016) Rift Valley fever virus: Unanswered questions. *Antiviral Res.* 132: 274–280.
10. Birukova AA, Shah AS, Tian Y, Gawlak G, Sarich N, Birukov KG (2016) Selective role of vinculin in contractile mechanisms of endothelial permeability. *Am J Respir Cell Mol Biol.* 55: 476–486.
11. Birukova AA, Shah AS, Tian Y, Gawlak G, Sarich N, Birukov KG (2016) Selective Role of Vinculin in Contractile Mechanisms of Endothelial Permeability. *Am J Respir Cell Mol Bio.* 55: 476–486.

12. Bosche B, Schäfer M, Graf R, Härtel FV, Ute Schäfer, Noll T (2013) Lithium prevents early cytosolic calcium increase and secondary injurious calcium overload in glycolytically inhibited endothelial cells. *Biochem Biophys Res Commun.* 434:268-272
13. Cade JFJ (1949) Lithium salts in the treatment of psychotic excitement. *Med J Aust.* 36: 349-352
14. Candé C, Cecconi F, Dessen P, Kroemer G (2002) Apoptosis-inducing factor (AIF): key to the conserved caspase-independent pathways of cell death? *J. Cell Science.* 115: 4727-4734.
15. Caroline AL, Kujawa MR, Oury TD, Reed DS, Hartman AL (2016) Inflammatory biomarker associated with Rift Valley Fever Encephalitis in the Lewis Rat Model. *Front. Microbiol.* 6:1509
16. Christen Y (2000) Oxidative stress and Alzheimer's disease. *Am J Clin Nutr.* 71: 621–629.
17. Clancy RM, Amin AR, Abramson SB (1998) The role of nitric oxide in inflammation and immunity. *Arthritis Rheum.* 41(7):1141-1151.
18. Cobo F (2016) viruses causing hemorrhagic fever. *Safety Laboratory Procedures. Open Virol J.* 10:1-9
19. Davies FG (2010) The historical and recent impact of Rift Valley fever in Africa. *Am. J. Trop. Med. Hyg.* 83: 73–74.
20. De Sarno P, Axtell RC, Raman C, Roth KA, Alessi DR, Jope RS (2008) Lithium prevents and ameliorates experimental autoimmune encephalomyelitis. *J Immunol.* 181: 338–345.
21. Dejana E, Corada M, Lampugnani MG (1995) Endothelial cell-to-cell junctions. *The FASEB J.* 9: 910-918.
22. Drosten C, Götting S, Schilling S, Asper M, Panning M, Herbert Schmitz, Günther S (2002) Rapid detection and quantification of RNA of Ebola and Marburg viruses, Lassa virus, Crimean-Congo hemorrhagic fever Virus, Rift Valley fever virus, Dengue virus, and Yellow fever virus by real-time reverse transcription-PCR. *J Clin Microbiol.* 40:2323-2330.
23. Elmore S (2007) Apoptosis: A review of programmed cell death. *Toxicol Pathol.* 35: 495–516.
24. Filone CM, Heise M, Doms RW, Bertolotti-Ciarlet A (2006) Development and characterization of a Rift Valley fever virus cell–cell fusion assay using alphavirus replicon vectors. *Virol.* 356:155-164.

25. Galluzzi L, Brenner C, Morselli E, Touat Z, Kroemer G (2008) Viral control of mitochondrial apoptosis. *PLoS Pathogens*. 13: e1000018.
26. Garcia MA, Gallego P, Campagna M, Gonzalez-Santamaria J, Martinez G (2009) Activation of NF- $\kappa$ B Pathway by Virus Infection Requires Rb Expression. *PLoS One*. 4: e6422.
27. Gaudreault NN, Indran SV, Bryant PK, Richt JA, Wilson WC (2015) Comparison of Rift Valley fever virus replication in North American livestock and wildlife cell lines. *Front Microbiol*. 6: 664.
28. Gavard J, Gutkind JS (2006) VEGF controls endothelial-cell permeability by promoting the beta-arrestin-dependent endocytosis of VE-cadherin. *Nat Cell Biol*. 8: 1223-1234.
29. Gewies A (2003) Introduction to apoptosis. *Apo Review*: 1–26.
30. Ghaemi-Bafghi M and Alireza Haghparast (2013) Viral evasion and subversion mechanisms of the host immune system. *ZJRMS*. 15: 6-1.
31. Gough RE, Goult BT (2018). The tale of two talins - two isoforms to fine-tune integrin signalling. *FEBS Lett*. 592: 2108-2125.
32. Gray KK, Worthy MN, Juelich TL, Agar SL, Poussard A (2012) Chemotactic and inflammatory responses in the liver and brain are associated with pathogenesis of Rift Valley fever virus infection in the mouse. *PLoS Negl Trop Dis*. 6: e1529.
33. Gupta M, Mahanty S, Ahmed R, Rollin PE (2001) Monocyte-derived human macrophages and peripheral blood mononuclear cells infected with ebola virus secrete MIP-1alpha and TNF-alpha and inhibit poly-IC-induced IFN-alpha in vitro. *Virology*. 284: 20-25.
34. Habib S, Baig F (2007) "Nitric oxide measurement from blood to lungs, is there a link?". *Pak J Physiol*. 3: 145-49.
35. Habjan M, Pichlmair A, Elliott R.M, Overby A.K, Glatter T, Gstaiger M, Superti-Furga G, Unger H, Weber F (2009) NSs protein of Rift Valley fever virus induces the specific degradation of the double-stranded RNA-dependent protein kinase. *J Virol*. 83: 4365-4375.
36. Harmon B, Benjamin R, Schudel, Dianna Maar, Carol Kozina, Tetsuro Ikegami, Chien-Te Kent Tseng, and Oscar A. Negrete (2012) Rift Valley fever virus strain MP-12 enters mammalian host cells via caveola-mediated endocytosis. *J Virol*. 86: 12954–12970.



37. Hartley CE, Buchan A, Randall S, Skinner G. R. B, Osborne M, Tomkins L. M (1993) The effects of lithium and potassium on macromolecular synthesis in herpes simplex virus-infected cells. *J Gen Virol.* 74: 1519-1525.
38. Hartsock A, Nelson WJ (2008) Adherens and tight junctions: structure, function and connections to the actin cytoskeleton. *Biochim Biophys Acta.* 1778: 660-669.
39. Hemler M.E (2008) Targeting of tetraspanin proteins — potential benefits and strategies. *Nat Rev Drug Discov.* 7: 747–758.
40. Humphries JD, Wang P, Streuli C, Geiger B, Humphries MJ, Ballestrem C. (2007) vinculin controls focal adhesion formation by direct interactions with talin and actin. *J Cell Biol.* 179: 1043-1057.
41. Hyenne V, Louvet-Vallée S, El-Amraoui A, Petit C, Maro B, Simmler M (2005) Vezatin, a protein associated to adherens junctions, is required for mouse blastocyst morphogenesis. *Dev Biol* 287: 180 – 191z.
42. Islam MK, Strand M, Saleeb M, Svensson R, Baranczewski P, Artursson, P, Evander M (2018) Anti-Rift Valley fever virus activity in vitro, pre-clinical pharmacokinetics and oral bioavailability of benzavir-2, a broad-acting antiviral compound. *Sci Rep.* 8: 1925.
43. Izard T, Tran Van Nhieu G, Bois PR (2006). Shigella applies molecular mimicry to subvert vinculin and invade host cells. *J Cell Biol.* 175: 465-475.
44. Jansen van Vuren PJ, Shalekoff S, Grobbelaar AA, Archer BN, Thomas J, Tiemessen CT, Paweska JT (2015) Serum levels of inflammatory cytokines in a Rift Valley fever patients are indicative of severe disease. *Virol J.* 12: 159.
45. Jope RS, Yuskaitis CJ, Beurel E (2007) Glycogen synthase kinase-3 (GSK3): Inflammation, diseases, and therapeutics. *Neurochem Res.* 32: 577–595.
46. Kalveram B, Lihoradova O, Ikegami T (2011) NSs protein of rift valley fever virus promotes posttranslational downregulation of the TFIIF subunit p62. *J Virol.* 85: 6234-6243.
47. Kamei M, Carman CV (2010) New observations on the trafficking and diapedesis of monocytes. *Curr Opin Hematol.* 17: 43-52.
48. Khasraw M, Ashley D, Wheeler G, and Berk M (2012) Using lithium as a neuroprotective agent in patients with cancer. *BMC Med.* 10: 131-137.
49. Khodapasand E, Jafarzadeh N, Farrokhi F, Kamalidehghan B, Houshmand, M (2015) Is Bax/Bcl-2 ratio considered as a prognostic marker with age and tumor location in colorectal cancer? *Iranian biomedical journal.* 19: 69–75.

50. Kleinerman ES, Knowles RD, Blick MB, Zwelling LA (1989) Lithium chloride stimulates human monocytes to secrete tumor necrosis factor/cachectin. *J Leukocyte Biol.* 46: 484–492.
51. Komarova YA, Kruse K, Mehta D, Malik AB (2017) Protein interactions at endothelial junctions and signaling mechanisms regulating endothelial permeability. *Circ Res.*120: 179-206.
52. Koriyama Y, Nakayama Y, Matsugo S, Sugitani K, Ogai K, Takadera T, Kato S (2013) Anti-inflammatory effects of lipoic acid through inhibition of GSK-3 $\beta$  in lipopolysaccharide-induced BV-2 microglial cells. *Neurosci Res.* 778: 7–96
53. Koyama AH, Irie H, Fukumori T, Hata S, Lida S, Akari H, Adachi A (1998) Role of virus-induced apoptosis in a host defence mechanism against virus infection. *J Med Inest.* 45: 37-45.
54. Küssel-Andermann P, El-Amraoui A, Safieddine S, Nouaille S, Perfettini I, Lecuit M, Cossart P, Wolfrum U, Petit C (2000). Vezatin, a novel transmembrane protein, bridges myosin VIIA to the cadherin-catenins complex. *The EMBO journal*,.19: 6020–6029.
55. Lamping K (2007) Endothelial progenitor cells: sowing the seeds for vascular repair. *Circ Res.* 100:1243-1245.
56. Lazo PA, Santos CR (2011) Interference with p53 functions in human viral infections, a target for novel antiviral strategies? *Reviews in Medical Virology.* 21: 285-300.
57. Le May N, Dubaele S, De Santis L.P, Billecocq A.S, le Bouloy M, Egly JM (2004) TFIIH transcription factor, a target for the Rift Valley hemorrhagic fever virus. *Cell Press.* 116: 541–550.
58. Lenox RH, Wang L (2003) Molecular basis of lithium action: integration of lithium-responsive signaling and gene expression networks. *Mol Psychiatry.* 8: 135–144.
59. Li, Q Li H, Roughton K, Wang X, Kroemer G, Blomgren K, Zhu C (2010) Lithium reduces apoptosis and autophagy after neonatal hypoxia-ischemia. *J Neurosci.* 10: 2041-4889.
60. Ly HJ, Ikegami T (2016) Rift Valley fever virus NSs protein functions and the similarity to other bunyavirus NSs proteins. *Virology.*13: 118.
61. Maes M, Song C, Lin A H, Pioli R, Kenis G, Kubera M, Bosmans E (1999) In vitro immunoregulatory effects of lithium in healthy volunteers. *Psychopharmacology (Berl).*143: 401-407.

62. Makola RT, Mbazima VG, Mokgotho MP, Gallicchio VS, Matsebatlela TM (2020) The effect of lithium on inflammation-associated genes in lipopolysaccharide-activated Raw 264.7 Macrophages. *International Journal of Inflammation*. 2020: 18.
63. Mansfield KL, Banyard AC, McElhinney L, Johnson N, Horton DL, Hernández-Triana LM, Fooks AR (2015) Rift Valley fever virus: A review of diagnosis and vaccination, and implications for emergence in Europe. *Vaccine*. 33(42):5520-5531.
64. Matsebatlela T, Gallicchio V, Becker R (2012) Lithium modulates cancer cell growth, apoptosis, gene expression and cytokine production in HL-60 promyelocytic leukaemia cells and their drug-resistant sub-clones. *Biol Trace Elem Res*. 149: 323–330.
65. McElroy AK, Erickson BR, Flietstra TD, Rollin PE, Nichol ST, Towner JS, Spiropoulou CF (2014) Biomarker correlates of survival in pediatric patients with Ebola Virus Disease. *Emerg Infect Dis*. 20: 1683-1690.
66. McElroy AK, Nichol ST, (2012) Rift Valley fever virus inhibits a pro-inflammatory response in experimentally infected human monocyte derived macrophages and a pro-inflammatory cytokine response may be associated with patient survival during natural infection. *Virology*. 422: 6-12.
67. Merendino RA, Mancuso G, Tomasello F, Gazzara D, Cusumano V, Chillemi S, Spadaro P, Mesiti M (1994) Effects of lithium carbonate on cytokine production in patients affected by breast cancer. *J. Biol. Regul. Homeostatic Agents*. 8: 88–91.
68. Mosomtai G, Evander M, Sandström P, Ahlm C, Sang R, Hassan OA, Affognon H, Landmann T (2016). Association of ecological factors with Rift Valley fever occurrence and mapping of risk zones in Kenya. *Int J Infect Dis*. 46: 49-55.
69. Muller W.A. (2013) Getting leukocytes to the site of inflammation. *Vet Pathol*. 50: 7-22.
70. Mydlikova Z, Gursky J, Pirsels M (2010) Transcription factor NF- $\kappa$ B – the protein complex with multiple functions. *Neoplasma*. 57: 287-290.
71. Narayanan A, Amaya M, Voss K, Chung M, Benedict A, Sampey G, Kehn-Hall K, Luchini A, Liotta L, Bailey C, Kumar A, Bavari S, Hakami RM, Kashanchi F (2014) Reactive oxygen species activate NF $\kappa$ B (p65) and p53 and induce apoptosis in RVFV infected liver cells. *Virology*. 449: 270–286.

72. Nassar A, Azab AN (2014) Effects of Lithium on inflammation. *ACS Chem Neurosci*. 5: 451–458.
73. Nedoszytko B, Sokołowska-Wojdyło M, Ruckemann-Dziurdzińska K, Roszkiewicz J, Nowicki RJ (2014) Chemokines and cytokines network in the pathogenesis of the inflammatory skin diseases: atopic dermatitis, psoriasis and skin mastocytosis. *Postep Derm Alergol*. 31: 84–91.
74. Nfon CK, Marszal P, Zhang S, Weingartl HM (2012) Innate Immune Response to Rift Valley Fever Virus in Goats. *PLoS Negl Trop Dis*. 6: e1623
75. Ngoshe YB, Avenant A, Rostal MK, Karesh WB, Paweska JT, Bagge W, van Vuren PJ, Kemp A, Cordel C, Msimang V, Thompson PN (2020) Patterns of Rift Valley fever virus seropositivity in domestic ruminants in central South Africa four years after a large outbreak. *Sci Rep*. 10: 5489.
76. Ngu H, Feng Y, Lu L, Oswald SJ, Longmore GD, Yin FC (2010) Effect of focal adhesion proteins on endothelial cell adhesion, motility and orientation response to cyclic strain. *Ann Biomed Eng*. 38: 208-222.
77. Niessen CM (2007) Tight junctions/adherens junctions: basic structure and function. *J Invest Dermatol*. 127: 2525-2532.
78. Njenga MK, Paweska J, Wanjala R, Rao CY, Weiner M, Omballa V, Luman TE, Mutonga D, Sharif S, Panning M, Drosten C, Feikin DR, Breiman RF (2009) Using a field quantitative real-time PCR test to rapidly identify highly viremic rift valley fever cases. *J Clin Microbiol*. 47: 1166-1171.
79. Paweska, JT and Jansen van Vuren, P (2014) Rift Valley Fever virus a virus with potential for global emergence. In Johnson, N (Eds), *The Role of Animals in Emerging Viral Diseases*. Academic Press is an Imprint of Elsevier. Chapter 8: 166-192.
80. Pietsch EC, Sykes SM, McMahon SB, Murphy ME (2008) The p53 family and programmed cell death. *Oncogene*. 27: 6507-6521.
81. Plotnikov EY, Silachev DN, Zorova LZ, Pevzner IB, Jankauskas SS, Zorovn SD, Babenko VA, Skulachev MV, Zorov DB (2014) Lithium Salts – Simple but Magic. *Biochemistry (Mosc)*. 79: 740-749.
82. Plowden J, Renshaw-Hoelscher M, Engleman C, Katz J, Sambhara S (2004) Innate immunity in aging: impact on macrophage function. *Aging Cell*. 3: 161-167.
83. Ramakrishnan MA (2016) Determination of 50% endpoint titer using a simple formula. *World J Virol*. 5: 85-86.

84. Rapaport MH, Manji HK (2001) The effects of lithium on ex vivo cytokine production. *Biol Psychiatry*. 50: 217-224.
85. Reed, L.J. Muench, H (1938) a simple method of estimating fifty per cent endpoints. *American Journal of Epidemiology*. 27: 493–497
86. Reuter S, Gupta SC, Chaturvedi MM, Aggarwal (2010) Oxidative stress, inflammation, and cancer: How are they linked? *J. Free Radical Bio Med*. 49: 1603–1616.
87. Roitt I, Brostoff J, Male D (1998) *Immunology*. Mosby International Ltd. Fifth Ed.157.
88. Ross JA, Auger MJ (2002) *The biology of the macrophage*. Burke B and Lewis CE, editors. Oxford: Medical Publications. 2nd ED.1–72.
89. Shuzhen G, Ken A, Monique FS, De-Maw C, Eng HL (2009) Lithium upregulates vascular endothelial growth factor in brain endothelial cells and astrocytes. *Stroke*. 40: 652-655.
90. Sinha D, Wang Z, Ruchalski KL, Levine JS, Krishnan S, Lieberthal W, Schwartz JH, Borkan SC (2004) Lithium activates the Wnt and phosphatidylinositol 3-kinase Akt signalling pathways to promote cell survival in the absence of soluble survival factors. *J. Physiol Renal Physiol*. 288: F703–F713.
91. Soufli I, Toumi R, Raza H, Touil-Boukoffa C (2016) Overview of cytokines and nitric oxide involvement in immuno-pathogenesis of inflammatory bowel diseases. *World J Gastrointest Pharmacol Ther*. 7: 353-360.
92. Strunecká A, Patočka J, Sárek M (2005) How does lithium mediate its therapeutic effects. *J. Appl. Biomed*. 3: 25-35.
93. Vogel DYS, Kooij G, Heijnen PDAM, Breur Peferoen, MLAN, van der Valk P, de Vries HE, Amor S, Dijkstra CD (2015) GM-CSF promotes migration of human monocytes across the blood brain barrier. *Eur. J. Immunol*. 45: 1808–1819.
94. Wahl-Jensen VM, Afanasieva TA, Seebach J, StrÖher U, Feldmann H, Schnittler HJ (2005) Effects of Ebola virus glycoproteins on endothelial cell activation and barrier function. *Viro J*. 79: 10442–10450.
95. Wang L, Zhang L, Zhao X, Zhang M, Zhao W, Gao C (2013) Lithium attenuates IFN- $\beta$  production and antiviral response via inhibition of TANK-Binding kinase 1 kinase activity. *J Immunol*. 191: 4392-4398.
96. Wang T, Town T, Alexopoulou L, Anderson JF, Fikrig E, Flavell RA (2004) Toll-like receptor 3 mediates West Nile virus entry into the brain causing lethal encephalitis. *Nat Med*. 10: 1366-1373.

97. Won S, Ikegami T, Peters CJ, Makino S (2007) NSm Protein of Rift Valley Fever virus suppresses virus-induced apoptosis. *Viro J.* 81: 13335–13345.
98. Wood ZA, Sabatini RS, Hajduk SL (2004) Targeting TFIIH to Inhibit basal transcription factor THIIH to induce shut-off of host cell transcription. *Mol Cell.* 13: 456-458.
99. Xiao TS (2017) Innate immunity and inflammation. *Cell & Mol Immunol.* 14: 1–3.
100. Yeste-Velasco M, Folch J, Jiménez A, Rimbau V, Pallàs M, Camins A (2008) GSK-3 $\beta$  inhibition and prevention of mitochondrial apoptosis inducing factor release are not involved in the antioxidant properties of SB-415286. *Eur J Pharmacol.* 588: 239-243.
101. Young K, Tweedie E, Conley B, Ames J, FitzSimons M, Brooks P, et al. (2015) BMP9 crosstalk with the hippo pathway regulates endothelial cell matricellular and chemokine responses. *PLoS ONE.* 10: e0122892.
102. Zachary A. Wood, Robert S. Sabatini, and Stephen L. Hajduk. (2004) Targeting TFIIH to Inhibit basal transcription factor THIIH to induce shut-off of host cell transcription. *Mol Cell.* 13: 456-458.
103. Zhang J and An J (2007) Cytokines, Inflammation and Pain. *Int Anesthesiol Clin.* 45: 27-37.